

THE STRUCTURE DETERMINATION OF
SOME CYCLIC PHOSPHONITRILIC COMPOUNDS

by

SIMON H. WHITLOW

B.Sc.(Hon.), University of British Columbia, 1965.

A THESIS SUBMITTED IN PARTIAL FULFILMENT OF
THE REQUIREMENTS FOR THE DEGREE OF
DOCTOR OF PHILOSOPHY

in the Department

of

Chemistry

We accept this thesis as conforming to the
required standard

THE UNIVERSITY OF BRITISH COLUMBIA

January, 1969

In presenting this thesis in partial fulfilment of the requirements for an advanced degree at the University of British Columbia, I agree that the Library shall make it freely available for reference and Study. I further agree that permission for extensive copying of this thesis for scholarly purposes may be granted by the Head of my Department or by his representatives. It is understood that copying or publication of this thesis for financial gain shall not be allowed without my written permission.

Department of Chemistry

The University of British Columbia
Vancouver 8, Canada

Date 13 March 1969

ABSTRACT

Supervisor: Professor James Trotter

The structures of four inorganic compounds have been determined by single-crystal X-ray diffraction methods. Three of the structures investigated were phosphonitrilic derivatives: octamethylcyclotetraphosphonitrilium trichlorocopper(II), $[\text{NPMe}_2]_4\text{H.CuCl}_3$, bis-(octamethylcyclotetraphosphonitrilium) tetrachlorocobaltate(II), $[(\text{NPMe}_2)_4\text{H}^+]_2\text{CoCl}_4^{2-}$, and hexadecamethoxycyclo-octaphosphonitrile, $[\text{NP}(\text{OMe})_2]_8$. The fourth analysis was a study of the ionic compound caesium difluorophosphate. For each structure determination the intensity measurements were collected on a diffractometer using a scintillation counter and Mo-K_{α} radiation.

The structure of $[\text{NPMe}_2]_4\text{H.CuCl}_3$ was determined from Patterson and Fourier summations. Refinement of positional and thermal parameters of the atoms was by least squares. The structure consists of discrete molecules in which the eight-member phosphonitrilic ring approximates the "tub" conformation with pairs of adjacent phosphorus and nitrogen atoms displaced alternately above and below the ring plane. A ring nitrogen atom is bonded to the copper atom ($\text{N-Cu} = 2.04 \text{ \AA}$) which has three chlorines arranged about it in a distorted square planar configuration. Across the ring from the N-Cu bond, there is a protonated nitrogen atom which is hydrogen-bonded to a neighbouring chlorine. The phosphorus-nitrogen bond lengths are not equal around the ring, but occur instead in four distinct pairs having lengths 1.63 \AA , 1.60 \AA ,

1.56 Å, and 1.67 Å. These varying bond distances are explainable in terms of π -bonding systems.

The structure of $[(\text{NPMe}_2)_4\text{H}^+]_2\text{CoCl}_4^{2-}$ has been determined by Patterson and Fourier methods and refined by least-squares. Most of the methyl hydrogen atoms were located in a final difference Fourier summation. The structure consists of tetrahedral CoCl_4^{2-} ions hydrogen-bonded to two protonated phosphonitrilic rings. The N-H...Cl distance in each case is 3.21 Å. The two independent rings have slightly different conformations. One approaches the "tub" shape and the other tends towards the "saddle" conformation. Protonation of the phosphonitrilic rings again results in non-equivalent P-N bond lengths. Averaged values for the two rings are 1.69 Å, 1.54 Å, 1.61 Å and 1.58 Å. Parameters which are unaffected by the addition of the proton agree with those found in related compounds when averaged values are considered.

$[\text{NP}(\text{OMe})_2]_8$ is a centrosymmetric sixteen-member phosphonitrile. Its structure was determined by Patterson, electron density, and least squares techniques. The phosphonitrilic ring consists of two approximately planar and parallel six-atom segments joined by a step. The P-N bond lengths are all equal within experimental error, their mean being 1.561 Å. The average P-O and O-C bond distances are 1.576 Å and 1.440 Å respectively. The methoxy groups cover the ring evenly, their arrangement being such that there is little conflict between steric and π -bonding requirements.

The structure of caesium difluorophosphate was determined by comparison with KPO_2F_2 and refined by least square methods. Caesium and rubidium difluorophosphate are isomorphous with the potassium salt; all have the barium sulfate structure. The mean P-F distance in CsPO_2F_2 is 1.58 Å, the P-O bond length, 1.48 Å. The lattice parameters and interionic distances increase with increasing radius of the alkali-metal cation.

TABLE OF CONTENTS

	PAGE
TITLE PAGE	i
ABSTRACT	ii
TABLE OF CONTENTS	v
LIST OF TABLES	vii
LIST OF FIGURES	ix
ACKNOWLEDGEMENTS	xi
GENERAL INTRODUCTION	1
PART I. THE STRUCTURE DETERMINATIONS OF OCTAMETHYLCYCLOTETRA- PHOSPHONITRILIUM TRICHLOROCOPPER(II) AND BIS-(OCTA- METHYLCYCLOTETRAPHOSPHONITRILIUM) TETRACHLORO- COBALTATE(II)	4
A. INTRODUCTION	5
B. THE STRUCTURE OF OCTAMETHYLCYCLOTETRAPHOSPHONITRILIUM TRICHLOROCOPPER(II)	16
Experimental	16
Structure Analysis	17
Discussion	25
C. THE STRUCTURE OF BIS-(OCTAMETHYLCYCLOTETRAPHOSPHONITRILIUM TETRACHLOROCOBALTATE(II)	36
Experimental	36
Structure Analysis	39
Discussion	52
PART II. THE STRUCTURE DETERMINATION OF HEXADECAMETHOXYCYCLO- OCTAPHOSPHONITRILE	62
A. INTRODUCTION	63

	PAGE
B. THE STRUCTURE OF HEXADECAMETHOXYCYCLO- OCTAPHOSPHONITRILE	66
Experimental	66
Structure Analysis	67
Discussion	76
PART III. THE STRUCTURE DETERMINATION OF CAESIUM DIFLUORO- PHOSPHATE	88
A. INTRODUCTION	89
B. THE STRUCTURE OF CAESIUM DIFLUORPHOSPHATE	94
Experimental	94
Structure Analysis	96
Discussion	99
APPENDIX. THE COMPUTER PROGRAMS <u>COFSYM</u> AND <u>CELDIM</u>	104
A. <u>COFSYM</u> PROGRAM FOR INDICATING A CENTRE OF SYMMETRY	105
B. <u>CELDIM</u> PROGRAM FOR CELL DIMENSION REFINEMENT	111
REFERENCES	129

LIST OF TABLES

TABLE		PAGE
I.	X-ray structure determinations of trimeric phosphonitriles	10
II.	X-ray structure determinations of tetrameric phosphonitriles	11
<u>Octamethylcyclotetraphosphonitrilium trichlorocopper(II)</u>		
III.	Comparison of elemental analyses, postulated composition, and actual composition of the compound	19
IV.	Measured and calculated structure factors	21
V.	Final positional and thermal parameters with standard deviations	24
VI.	Bond distances and valency angles	30
<u>Bis-(octamethylcyclotetraphosphonitrilium) tetra- chlorocobaltate(II)</u>		
VII.	Comparison of the postulated and actual composition of the compound with the chemical analysis	40
VIII.	Measured and calculated structure factors	45
IX.	Final positional and thermal parameters with standard deviations	49
X.	Hydrogen atom positions located on difference map . .	51
XI.	Bond lengths and valency angles	57

	PAGE	
XII.	X-ray structure determinations of the larger phosphonitriles	63
	<u>Hexadecamethoxycyclo-octaphosphonitrile</u>	
XIII.	Results of statistical tests to distinguish between centric and acentric distributions of intensities .	68
XIV.	Measured and calculated structure factors	71
XV.	Final positional and thermal parameters with standard deviations	74
XVI.	Bond lengths and angles	77
XVII.	Comparison of molecular parameters of $[\text{NP}(\text{OMe})_2]_4$ and $[\text{NP}(\text{OMe})_2]_8$	80
XVIII.	Bond lengths between tetrahedrally coordinated phosphorus and the first-row elements oxygen and fluorine . . .	89
	<u>Caesium difluorophosphate</u>	
XIX.	Crystal data for $\underline{\text{MPO}}_2\text{F}_2$	95
XX.	Measured and calculated structure factors	97
XXI.	Final positional and thermal parameters with standard deviations	98
XXII.	Interatomic distances and angles in $\underline{\text{MPO}}_2\text{F}_2$	100

LIST OF FIGURES

FIGURE		PAGE
1.	π -overlap systems in the phosphonitriles.	7
<u>Octamethylcyclotetraphosphonitrilium trichlorocopper(II)</u>		
2.	Sections of the three-dimensional electron density distribution and a drawing of the molecule	26
3.	Packing of the molecules in the unit cell viewed along the <u>c</u> -axis.	27
4.	Bond lengths and angles within the phosphonitrilic ring	29
<u>Bis-(octamethylcyclotetraphosphonitrilium) tetrachloro-</u> <u>cobaltate(II)</u>		
5.	Sections of the final electron density distribution. .	53
6.	A drawing of the structure viewed along the <u>c</u> *-axis. .	54
7.	Packing in the unit cell viewed down the <u>c</u> -axis. . . .	61
<u>Hexadecamethoxycyclo-octaphosphonitrile</u>		
8.	The N(Z) plot.	69
9.	Sections of the final electron density distribution . .	78
10.	A diagram of the structure viewed along the <u>a</u> '-axis of the orthogonal set <u>a</u> ', <u>b</u> , <u>c</u> *.	79
11.	The molecular packing viewed along the <u>c</u> -axis.	81

	PAGE
12. Idealized structures indicating the distortion of the phosphonitrilic ring from planarity.	83
13. Configurations about phosphorus	85
14. π -overlap between phosphorus <u>d</u> orbitals and ligands .	91
<u>Caesium difluorophosphate</u>	
15. The structure viewed along the <u>a</u> -axis.	101
16. The structure viewed along the <u>b</u> -axis.	102

ACKNOWLEDGEMENTS

I would like to thank Professor J. Trotter for his assistance and guidance throughout my research.

I am indebted to Professor N. Paddock for providing the crystal samples of the phosphonitriles and for much helpful discussion.

I wish to thank Mr. W. Reed and Dr. R.C. Thompson for supplying the samples of rubidium and caesium difluorophosphates.

I gratefully acknowledge financial support from the National Research Council of Canada.

GENERAL INTRODUCTION

From the first application of X-rays to determine the structure of zinc blende by W.L. Bragg¹ in 1912, X-ray diffraction has emerged as the most powerful way of investigating the solid state. Since the majority of compounds either exist or can be obtained in the solid form the method has wide applicability. With recent improvements in methods of data collection and in computing facilities crystal structures are being reported in unprecedented numbers. The basic principles of X-ray diffraction are by now well established as are the chief methods of structure elucidation. The Patterson, Fourier, and difference Fourier summations and the method of least squares refinement which were used in the present structural work have been discussed in a number of standard reference books²⁻⁵ and will therefore not be described here. Any symbol or crystallographic nomenclature occurring in the thesis has its conventional meaning described in the "International Tables for Crystallography".⁶

This thesis consists of an account of the X-ray structure determinations of several inorganic compounds with an attempt to interpret some of their main structural features. It is chiefly concerned with phosphonitrilic structures and is arranged in three main sections. In part I a summary of the bonding theory of the phosphonitriles is presented together with a review of the X-ray structural information available for the six- and eight-membered rings. The X-ray analyses of two tetrameric ring structures, octamethylcyclotetraphosphonitrilium trichlorocopper(II) and bis-(octamethylcyclotetraphosphonitrilium) tetrachlorocobaltate(II) are then described. Because of their lengthy

names, these will be referred to in the thesis by means of their more convenient chemical symbols, $[\text{NPMe}_2]_4\text{H}\cdot\text{CuCl}_3$ and $[(\text{NPMe}_2)_4\text{H}^+]_2\text{CoCl}_4^{2-}$, respectively. Part II contains an account of the structure determination of hexadecamethoxycyclo-octaphosponitrile, $[\text{NP}(\text{OMe})_2]_8$, a sixteen-member phosphonitrilic ring compound. Part III consists of the X-ray analysis of caesium difluorophosphate, CsPO_2F_2 .

The appendix contains a description and source deck listing of two computer programs written during the course of this work. The first was intended for a particular analysis and consists of an application of the $N(Z)$ test to detect a centric distribution of intensities. The second, of more general use, is a least squares refinement procedure designed to give accurate unit cell parameters from diffractometer measurements.

PART I

THE STRUCTURE DETERMINATIONS OF

OCTAMETHYLCYCLOTETRAPHOSPHONITRILIUM TRICHLOROCOPPER(II)

AND

BIS- (OCTAMETHYLCYCLOTETRAPHOSPHONITRILIUM) TETRACHLOROCOBALTATE(II)

A. INTRODUCTION

The first chemical reaction leading to the formation of a cyclic phosphonitrile, the reaction between phosphorus pentachloride and ammonia, was reported simultaneously by Rose,⁷ and Liebig and Wöhler⁸ in 1834. Stokes⁹ proposed a cyclic structure for the product, $[\text{NPCl}_2]_3$, which later X-ray diffraction work was to confirm. Since this early work much structural and chemical information has been gathered by various methods about the phosphonitriles and these findings are accumulated in a number of comprehensive reviews.¹⁰⁻¹⁹ To introduce the phosphonitrilic structure determinations in this chapter it is first necessary to review the essential features of phosphonitrilic bonding theory. Then it would seem appropriate to summarize the X-ray structure determinations which have been carried out on six- and eight-membered phosphonitrilic rings to the present time. Such a review and summary should not only serve to indicate the successes of the bonding theory in explaining experimental results, but should also provide a basis for discussing the results of the structure analyses both in this section and the next.

The system of bonding for the phosphonitriles has been largely developed by Craig and Paddock²⁰⁻²² so it is convenient to use their conventions with respect to nomenclature and axial labelling. Although Molecular Orbital theory is required for a complete analysis of the chemical bonding, the Valence Bond approach provides an intuitive explanation and goes far in rationalizing the observed structural

features found in the phosphonitriles. Single (σ) bonds are formed by the overlap of bonding orbitals on phosphorus and nitrogen atoms having the proper symmetry. Sp^3 hybridization at phosphorus is often suggested to account for the four tetrahedrally arranged bonds, and orbitals at nitrogen having s and p character, likely sp^2 hybrids, seem appropriate for the σ -bonds. The secondary or π -system of bonding must involve the d orbitals on phosphorus since all the p orbitals have been utilized in the σ -bonding. Overlap between phosphorus 3d and nitrogen 2p orbitals is feasible particularly where the phosphorus atoms have electronegative substituents attached to them.²³

The orientation of the phosphorus d orbitals with respect to the phosphonitrilic ring is shown in Figure 1. The z-direction is chosen perpendicular to the local NPN plane, the y-axis is in the plane and bisect the N-P-N angle, and the x-direction is orthogonal with respect to the other two. π -overlap occurring between the d_{xz} and d_{yz} lobes of phosphorus and the singly occupied p_z orbital on nitrogen is designated π_a (this type of overlap is antisymmetric with respect to reflexion in the NPN plane). A secondary π -system which lies in the ring plane and is designated π_s , can occur between the phosphorus $d_{x^2-y^2}$ and d_{xy} orbitals and the nitrogen sp_y hybrid which contains the nitrogen lone pair electrons. These two systems of orbital overlap are illustrated in Figure 1. A third type of overlap is also recognized which may permit π -bonding to exocyclic ligands on phosphorus. In this, the principal orbital on phosphorus involved is the d_{z^2} orbital (with the d_{xz} and d_{yz} participating to a lesser extent).

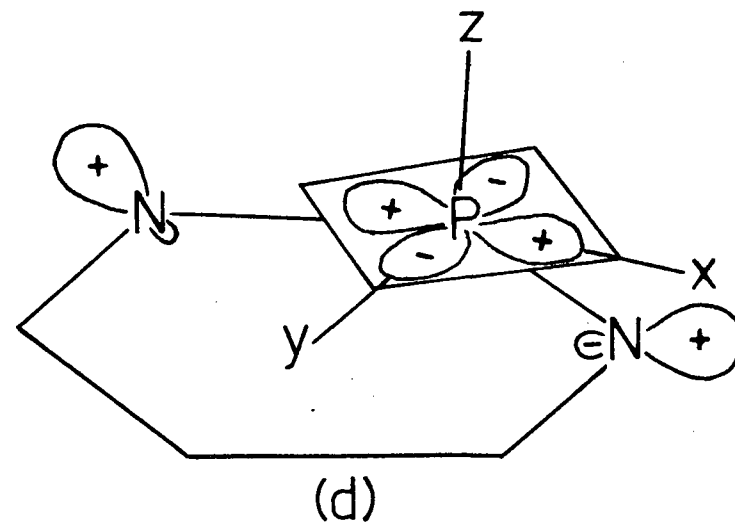
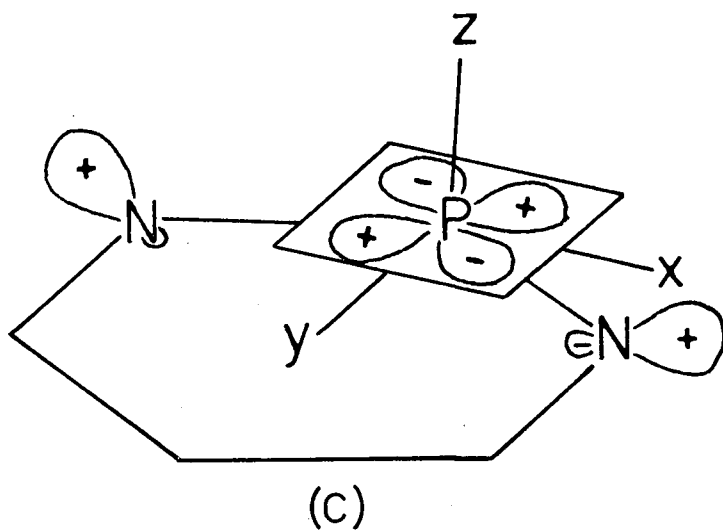
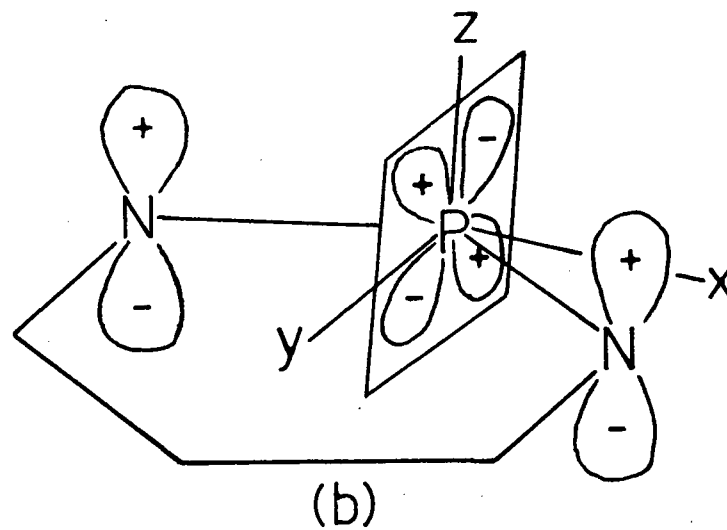
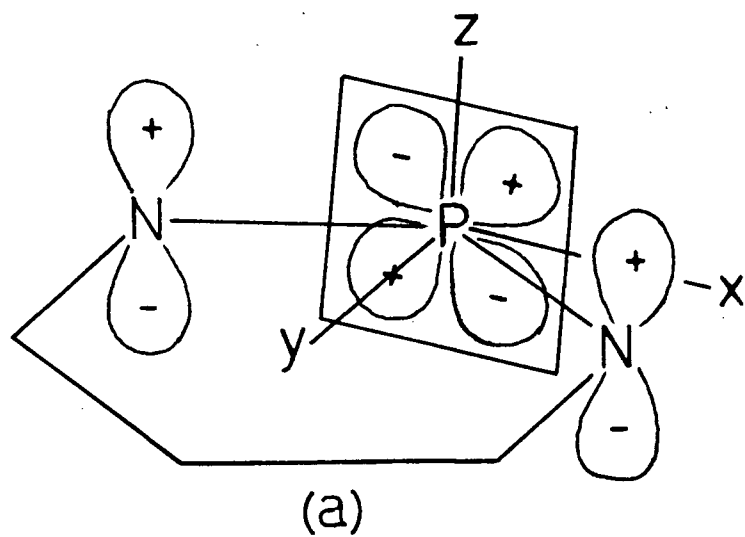


Figure 1. π -overlap systems in the phosphonitriles : (a) d_{xz} and (b) d_{yz} are used for π_a -bonding, (c) d_{xy} and (d) $d_{x^2-y^2}$ for π_s -bonding. (After Paddock¹⁴)

The π_a and π_s -systems are not equivalent nor do the \underline{d} orbitals involved in them interact equally. The π_a -system in the ring is the predominant one and overlap integrals suggest that in this the \underline{d}_{xz} orbital is the more strongly involved.²² A treatment proposed by Dewar et.al.,²⁴ however, is based on an equal participation of the \underline{d}_{xz} and \underline{d}_{yz} orbitals at phosphorus. In this approach a pair of linear combinations is constructed from these two orbitals which interact separately with adjacent nitrogen π -type orbitals to form a system of three-centre π -bonds. These "islands of electron density" which encompass P-N-P segments do not permit delocalization around the whole ring. In any case, the nature of the delocalization in the phosphonitriles differs from the π -systems of unsaturated hydrocarbons such as benzene chiefly because of the character of the \underline{d} orbitals and because of the bond polarity caused by electronegativity differences between phosphorus and nitrogen. In particular, Molecular Orbital calculations for the phosphonitriles show that the uppermost occupied orbital is always non-degenerate (it is doubly degenerate for hydrocarbons). This result predicts an aromatic nature for all cyclic phosphonitriles whether they have $4n$ or $4n + 2$ π -electrons.²⁰

After this introductory account of the bonding theory for phosphonitriles it is appropriate to comment on the significant structural features of the series which have been determined by X-ray analyses. Molecular structures of trimers and tetramers will be reviewed here; a discussion of the larger cyclic phosphonitriles will be deferred until the Introduction to Part II.

The most accurate of the crystal structure determinations which have been carried out on trimeric phosphonitriles are summarized in Table I. (References in brackets refer to other X-ray work on the same compound but of less reliability.) The trimeric halides are all nearly planar, have equal P-N bonds within the ring, and have approximately constant ring angles. From these structures it is evident that the π -systems extend over the whole ring for there is no indication of alternating single and double bonds. The structures of the diphenyl- and tetraphenyl-substituted trimers, however, do show inequalities in the observed bond lengths and angles. The P-N bond length is found to be dependent upon the electronegativity of the substituents on phosphorus. Thus when the electronegative chlorine atoms are attached to phosphorus, the P-N bond is shorter than when the ligands are phenyl groups. Presumably the chlorine atoms when attached to a phosphorus atom enhance the transfer of electron density from the adjacent nitrogen atoms into a π -bonding system with the phosphorus causing a stronger and shorter bond. The structure determination of a protonated phosphonitrilic trimer shows a pair of long P-N bonds (1.67 Å) involving the protonated nitrogen atom. Here the nitrogen lone pair electrons are required for bonding the hydrogen atom and do not participate in the π -bonding.

In Table II the results of X-ray structure analyses of tetrameric phosphonitriles are compiled. As will be noticed, in these eight-member rings more geometrical freedom is permitted and a planar configuration is only found in the fluoride. Deviations from planarity are

Table I. X-ray structure determinations of trimeric phosphonitriles.

<u>Compound</u>	<u>P-N(Å)</u>	<u>Angle PNP(°)</u>	<u>Angle NPN(°)</u>	<u>Ring Shape</u>	<u>Reference</u>
$[\text{NPCl}_2]_3$	1.59(.02)	119.4	119.6	chair, <u>m</u>	25(26-28)
$[\text{NPBr}_2]_3$	1.53(.20)	116.5	124.0	chair, <u>m</u>	29(30)
$[\text{NPF}_2]_3$	1.56(.01)	120.4	119.4	planar, <u>m m</u>	31(32)
$\text{N}_3\text{P}_3\text{Cl}_4(\text{C}_6\text{H}_5)_2$	1.615(.005) 1.555 1.578	122.0 119.2	115.2 119.7	chair	33
$\text{N}_3\text{P}_3\text{Cl}_2(\text{C}_6\text{H}_5)_4$	1.556(.008) 1.609 1.578	121.0 124.9	120.7 115.5	boat	34
$\text{N}_3\text{P}_3\text{Cl}_2(\text{NHP}^i)_4, \text{HCl}$	1.67(.005) 1.58 1.56	132 125.5	120 107.5	distorted boat	35

Table II. X-ray structure determinations of tetrameric phosphonitriles.

<u>Compound</u>	<u>P-N (Å)</u>	<u>Angle PNP (°)</u>	<u>Angle NPN (°)</u>	<u>Ring Shape</u>	<u>Reference</u>
$[\text{NPCl}_2]_4$ (K)	1.57 (.01)	131.3	121.2	tub, $\bar{4}$	36 (37)
$[\text{NPCl}_2]_4$ (T)	1.56 (.012)	133.6 137.6	120.5	chair, $\bar{1}$	38
$[\text{NPF}_2]_4$	1.507 (.017)	147.2	122.7	planar, $4/\bar{m}\bar{m}\bar{m}$	39 (32)
$[\text{NPMe}_2]_4$	1.596 (.003)	131.9	119.8	tub, $\bar{4}$	40
$[\text{NP}(\text{NMe}_2)_2]_4$	1.578 (.010) 1.68 (exo.)	133.0	120.1	tub, $\bar{4}$	41
$[\text{NP}(\text{OMe})_2]_4$	1.57	132	122	saddle, $\bar{4}$	42

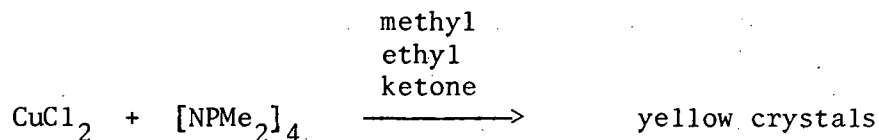
compatible with the theory of \underline{d}_{π} - \underline{p}_{π} bonding because of the shapes and diffuseness of the \underline{d} orbitals. Steric interactions between exocyclic groups and competition between π_a and π_s -bonding within the ring seem to account for the adopted conformations.¹⁷ The structural studies suggest that tetrameric ring configurations usually approximate one of three types. In the most common "tub" shape the ring atoms occur in pairs alternately above and below the ring plane. This shape has $\bar{4}$ symmetry and is reminiscent of the "boat" configuration found in six-membered rings. In this form the exocyclic atoms on successive phosphorus atoms have stable staggered positions and local environments favoring π_a or π_s -bonding occur around the ring. In the "saddle" arrangement the ring also has $\bar{4}$ symmetry (ideally $\bar{4}2m$ (D_{2d})). The phosphorus atoms are planar and the nitrogen atoms alternate above and below the plane. Overlap between successive π -orbitals is equal which tends to strengthen π_a -bonding as a whole. The "chair" shape with $\bar{1}$ symmetry, has larger dihedral angles between adjacent ring atoms. In this case the π_a system is expected to be less strong than π_s -bonding. It is important to appreciate, though, that the two systems of π -bonding complement each other since their planes of maximum overlap are perpendicular. Thus decreased overlap of the π_a -system due to a misalignment of the \underline{z} -axes on neighbouring atoms results in an increased participation in π_s -bonding. In addition to these π -systems within the ring the structure of the tetrameric dimethylamide indicates that π -bonding can also occur between the ring and its ligands. Here, not only are the exocyclic P-N bonds shorter than a pure single bond, but

one dimethylamido-group on each phosphorus is orientated so as to have good overlap with the phosphorus d_{z^2} orbital, the other with the phosphorus d_{xz} or d_{yz} orbitals. Tetrameric structures can largely be explained in terms of a compromise between steric requirements and conformations enhancing some type of π -bonding.

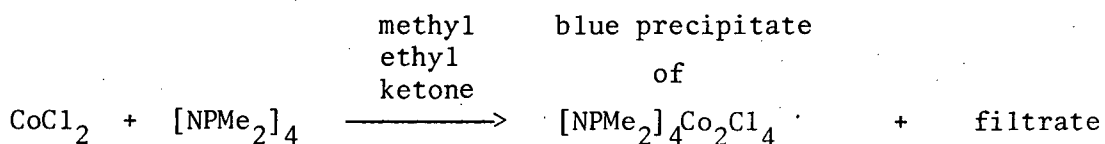
As can be seen by this review of trimeric and tetrameric structures, the bonding theory is able to explain many of the observed features. Most of the X-ray work to date has been done on compounds with just one type of ligand on the ring. Until the present analyses no phosphonitrilic structure has been reported in which the bonding of a metal atom to the ring was possible. In both the copper and cobalt compounds of tetrameric rings investigated here, the positions of the metal with respect to the phosphonitrilic ring and the interactions between them should be of interest. The metal atom could be bonded covalently to the ring or held by electrostatic forces. An exciting possibility is a type of organometallic bond between the metal and the aromatic ring. Bonding of this kind is found between organic aromatics and cobalt in $(\pi\text{-C}_5\text{H}_5\text{.Co.C}_5\text{H}_4\text{.C}_6\text{H}_5)$, for example.⁴³ The system of π -bonds in the phosphonitrilic ring might permit an analogous situation in which the metal atom is bonded either to a particular double bond or to the ring as a whole. This would probably not be as likely as a bond between a ring nitrogen atom and the metal, however, because of the polar character of the P-N bond. It is also possible that the ring might change its conformation so as to better accommodate the metal atom. Of equal interest is the effect the metal atom will have on the bonding

within the ring itself. Changes in bond order should be indicated by variations in bond lengths and valency angles. In the protonated trimer,³⁵ the addition of a hydrogen atom to a nitrogen atom within the ring caused a significant lengthening of two P-N bonds. The present analyses may indicate similar changes in tetrameric rings.

The two compounds investigated in this section were prepared by J. Dyson in a similar manner.⁴⁴ To make the copper compound, anhydrous copper chloride was reacted with the methyl phosphonitrile.



Analogously, anhydrous cobalt chloride was reacted with the phosphonitrile to give the cobalt compound.



Upon standing, small pale blue crystals were formed in the filtrate. Some of these crystals were used for the X-ray analysis.

The products were identified upon the basis of a (partial) chemical analysis. The yellow copper crystals were thought to be $[\text{NMe}_2]_4 \frac{4}{3} \text{CuCl}_2$ and the pale blue crystals from the filtrate of the cobalt compound to be $[\text{NMe}_2]_4\text{CoCl}_2$. Although these formulae are certainly plausible and are suggested by the chemical analyses, the

X-ray work to be described shows that neither compound has the formula assigned to it. Correctly formulated the compounds are $[\text{NMe}_2]_4\text{H}\cdot\text{CuCl}_3$ and $[(\text{NMe}_2)_4\text{H}^+]_2\text{CoCl}_4^{2-}$. Although a structure determination is rarely undertaken solely for the purpose of determining chemical composition, after an X-ray structure analysis the chemical composition of a compound is seldom in doubt.

B. THE STRUCTURE OF OCTAMETHYLCYCLOTETRAPHOSPHONITRILIUM
TRICHLOROCOPPER(II)

Experimental

Crystals of $[\text{NPMe}_2]_4\text{H.CuCl}_3$ are yellow needles elongated along a. Crystallographic data were obtained from various oscillation, Weissenberg and precession photographs and the unit cell parameters were refined by a least squares treatment of diffractometer measurements of 2θ values (see Appendix).

Crystal Data (λ , $\text{Cu-K}_{\alpha} = 1.5418 \text{ \AA}$; λ , $\text{Mo-K}_{\alpha} = 0.7107 \text{ \AA}$)

$[\text{NP}(\text{CH}_3)_2]_4\text{H.CuCl}_3$, $\underline{M} = 471.11$.

Orthorhombic, $\underline{a} = 15.70$, $\underline{b} = 17.72_8$, $\underline{c} = 14.52_6 \text{ \AA}$ (for all $\sigma = 0.01 \text{ \AA}$).

$\underline{U} = 4043.3 \text{ \AA}^3$, $\underline{D}_m = 1.54 \text{ g.cm.}^{-3}$ (flotation), $\underline{Z} = 8$, $\underline{D}_c = 1.55 \text{ g.cm.}^{-3}$, $\underline{F}(000) = 1928$.

Absorption coefficients, $\mu(\text{Cu-K}_{\alpha}) = 81.0 \text{ cm.}^{-1}$, $\mu(\text{Mo-K}_{\alpha}) = 18.2 \text{ cm.}^{-1}$.

Absent reflexions : $0k\ell$ when $k = 2n+1$, $h0\ell$ when $\ell = 2n+1$, and $hk0$ when $h = 2n+1$. Space group Pbca .

Intensity measurements were collected on a card-automated General Electric XRD-6 Spectrogoniometer with a scintillation counter, Mo-K_{α} radiation (zirconium filter and pulse height analyser) and a θ - 2θ scan. The scan width in 2θ was $(1.80 + 0.86 \tan \theta)$ degrees to allow for the increased width of reflexions at higher angles. Background counts were taken on either side of every scan so that the local background could be subtracted from the scan count for each

reflexion. Lorentz and polarization factors were applied and the structure amplitudes were derived as usual. Of the 2038 non-systematically absent reflexions with $2\theta \leq 40^\circ$ (minimum interplanar spacing 1.0 \AA) 1670 or 82% had intensities above the background level. The unobserved reflexions were assigned a value of $|F_o| = 0.6 F(\text{threshold})$ and were included in the analysis (but not in the residual calculation). The crystal used for the intensity measurements was mounted with the a-axis parallel to the ϕ axis of the goniostat and had a length of 0.25 mm. and a cross-section of 0.20 mm. by 0.15 mm.

Structure Analysis

The compound was initially thought to be a 3:4 combination of $[\text{N}_4\text{P}_4(\text{Me}_2)_4]$ and $[\text{CuCl}_2]$ units.⁴⁴ However, using the measured cell dimensions and density of 1.54 g.cm.^{-3} a satisfactory ratio of phosphonitrilic rings to copper chloride groups could not be found which would give a whole number of molecules per unit cell. The best variations were the 1:1 adduct for which $Z = 8$ and $\underline{D_c} = 1.44 \text{ g.cm.}^{-3}$ and the 2:3 combination where $\underline{Z} = 4$ and $\underline{D_c} = 1.66 \text{ g.cm.}^{-3}$. Neither of these appeared likely. A different ratio of phosphonitrile to copper groups, another chemical composition, or some form of disordered compound were considered possibilities. In an attempt to clarify this problem the sample was submitted for a chemical analysis. The results of this were similar to the original analysis so the compound appeared not to have decomposed since its preparation. The analytical results and the initially suggested composition are

tabulated in Table III together with the constitution of the actual structure determined by the X-ray analysis. The analyses tended to support the initial 3:4 model even though it was unlikely from the X-ray information.

From the three-dimensional Patterson function the coordinates of one copper and two chlorine atoms were derived. Uncertainty about the structure made it difficult to interpret further Patterson vectors. These three atoms were used to calculate phases for a starting Fourier summation, the initial R being 0.69. The scattering factors used were the usual forms given in the International Tables, volume III, and all atoms were assigned an initial isotropic temperature factor of 4.0 \AA^2 . This calculated electron density distribution then indicated clearly the positions of the phosphorus atoms of a phosphonitrilic ring. Successive Fouriers incorporating newly-found atomic positions revealed not only the ring nitrogen atoms and the methyl carbons but also an unexpected peak adjacent to the copper position. To identify this atom in an unbiased manner an atom was not immediately placed in this position. With one copper atom, two chlorine atoms, four phosphorus atoms, four nitrogen atoms and seven carbon atoms the residual factor was 0.30. At this stage a difference Fourier was calculated to locate the final methyl carbon and to identify the unexpected peak. Both atoms were prominent on the difference map, and the relative peak heights were very indicative: the unexplained peak was three times as strong as the carbon peak suggesting that about eighteen electrons were associated

Table III. Comparison of elemental analyses, postulated composition, and actual composition of the compound.

<u>ELEMENT</u>	<u>MICRO-ANALYSIS (%)</u>	
	Original*	Present ⁺ ($\pm .3\%$)
P	26.38	
N	11.87	12.03
C	20.74	20.21
H	5.87	5.0
Cu		
Cl	20.01	21.4

<u>ELEMENT</u>	<u>THEORETICAL COMPOSITION (%)</u>	
	Postulated $[P_4N_4(CH_3)_8]_3[CuCl_2]_4$	Actual $[P_4N_4(CH_3)_8]H[CuCl_3]$
P	25.84	26.30
N	11.69	11.89
C	20.04	20.40
H	5.05	5.35
Cu	17.67	13.49
Cl	19.72	22.58

* J. Dyson. Ph.D. Thesis, Victoria University of Manchester, 1964.

⁺ P. Borda. Chemistry Department, University of British Columbia.

with it. This information together with a bond distance of 2.24 Å to the copper, identified the anomalous peak as a chlorine atom. The difference map did not show any other prominent peaks.

With the inclusion of the chlorine and final carbon atom the R factor was reduced to 0.21. At this stage block-diagonal least squares refinement of all the positional and thermal parameters was begun. In minimizing $\sum w(F_o - F_c)^2$ a weighting scheme was used which kept $w\Delta^2$ approximately constant over ranges of F_o . The scheme used consisted of setting $\sqrt{w} = |F_o|/75$ when $|F_o| < 75$ and $\sqrt{w} = 75/|F_o|$ when $|F_o| \geq 75$. Unobserved reflexions were assigned $\sqrt{w} = 0.90$. After several cycles of isotropic refinement R was 0.11. Refinement was continued for two further cycles with anisotropic temperature parameters for the copper and chlorine atoms giving a final R of 0.097 for the 1670 observed reflexions. At this point the shifts in parameters were all less than the corresponding standard deviations. A final difference map did suggest several possible hydrogen positions with peaks of 0.5 to 1.0 electrons per cubic angstrom around some of the methyl carbons, but no attempt was made to accurately locate these since spurious fluctuations of $\pm 0.8 \text{ e.}\text{\AA}^{-3}$ were also present.

Measured and calculated structure factors are listed in Table IV. Sections of the three-dimensional electron density distribution are shown with a drawing of the molecule in Figure 2. The final positional and thermal parameters and their standard deviations are given in Table V, and a packing diagram looking down the c -axis is shown in Figure 3.

Table IV. Measured and calculated structure factors. Unobserved reflexions have $|F_0| = 0.6 F(\text{threshold})$ and are indicated by a negative sign.

Table with 5 columns of data, each containing two sub-columns (H K L and Fobs Fcalc). The columns represent different sets of structure factor measurements and calculations. The data points are organized in rows, with some rows having multiple entries for the same H K L values.

Table IV (continued).

H	K	L	FORS	FCAL	H	K	L	FORS	FCAL	H	K	L	FORS	FCAL	H	K	L	FORS	FCAL
4 0 8	30.3	30.9			4 11 0	122.8	-130.4			6 4 6	36.0	39.1			7 1 11	64.8	70.1		
4 0 10	105.3	99.6			4 11 1	137.3	140.1			6 4 7	33.2	26.4			7 1 12	-11.6	6.7		
4 0 12	48.4	45.6			4 11 2	94.4	-50.7			6 4 8	27.1	14.0			7 2 1	96.7	-99.9		
4 1 0	166.5	-159.3			4 11 3	175.8	182.8			6 4 9	27.3	67.1			7 2 2	2.2	23.5		
4 1 1	72.3	71.6			4 11 4	43.5	50.3			6 4 10	23.5	-35.7			7 2 3	4.0	-37.8		
4 1 2	33.9	-96.8			4 11 5	-9.8	2.3			6 4 11	11.9	-14.8			7 2 4	38.5	-34.2		
4 1 3	35.8	31.9			4 11 6	17.6	-6.1			6 4 12	27.5	-34.8			7 2 5	42.0	-40.3		
4 1 4	19.0	-23.4			4 11 7	18.9	-26.1			6 5 0	144.8	-147.9			7 2 6	6.0	-6.0		
4 1 5	24.3	-30.2			4 11 8	-10.8	2.7			6 5 1	39.5	34.5			7 2 7	25.0	-6.1		
4 1 6	33.9	83.0			4 11 9	51.9	-40.3			6 5 2	76.0	-27.4			7 2 8	-9.8	-18.0		
4 1 7	-8.4	9.8			4 11 10	-19.5				6 5 3	37.8	-61.1			7 2 9	39.1	37.3		
4 1 8	21.0	-16.3			4 12 0	126.0	-123.7			6 5 4	63.0	65.9			7 2 10	59.3	-65.5		
4 1 9	81.6	78.6			4 12 1	33.3	-28.9			6 5 5	118.1	-118.5			7 2 11	-11.2	6.6		
4 1 10	45.0	-42.9			4 12 2	109.5	-113.1			6 5 6	79.2	75.4			7 2 12	-11.7	-1.0		
4 1 11	40.7	33.1			4 12 3	3.9	-17.0			6 5 7	23.9	16.3			7 3 1	27.0	-6.2		
4 1 12	33.3	-36.1			4 12 4	6.2	-67.6			6 5 8	87.2	86.7			7 3 2	155.9	-153.4		
4 1 13	19.2	-15.5			4 12 5	37.1	31.6			6 5 9	176.1	174.9			7 3 3	3.8	7.7		
4 2 0	140.3	152.6			4 12 6	19.4	17.2			6 5 10	33.8	35.8			7 3 4	43.1	-67.9		
4 2 1	50.2	-41.8			4 12 7	39.5	-37.6			6 5 11	33.7	33.4			7 3 5	64.9	-60.7		
4 2 2	99.9	43.8			4 12 8	52.0	63.1			6 5 12	-11.7	-10.8			7 3 6	109.6	120.8		
4 2 3	10.3	-10.9			4 12 9	55.1	-56.3			6 6 0	91.7	93.9			7 3 7	94.2	-55.6		
4 2 4	-7.0	3.8			4 13 0	52.9	49.5			6 6 1	27.5	18.1			7 3 8	58.3	13.2		
4 2 5	-7.5	35.3			4 13 1	39.5	-44.3			6 6 2	-8.0	6.8			7 3 9	25.1	-25.8		
4 2 6	37.0	-31.3			4 13 2	70.2	73.0			6 6 3	47.5	61.8			7 3 10	-10.8	-9.5		
4 2 7	94.3	83.1			4 13 3	72.2	-70.1			6 6 4	84.5	-87.7			7 3 11	37.9	-34.5		
4 2 8	51.4	-56.3			4 13 4	-10.3	9.9			6 6 5	72.7	47.7			7 3 12	-11.7	-17.5		
4 2 9	-9.5	3.6			4 13 5	-10.5	21.9			6 6 6	20.1	-16.0			7 4 1	127.7	117.6		
4 2 10	29.9	-7.7			4 13 6	29.0	-30.7			6 6 7	91.1	86.6			7 4 2	27.0	-82.4		
4 2 11	20.2	0.5			4 13 7	39.7	44.1			6 6 8	21.0	-11.2			7 4 3	4.2	67.0		
4 2 12	70.1	-13.6			4 13 8	54.8	-66.8			6 6 9	45.4	-44.1			7 4 4	90.8	-94.2		
4 2 13	72.7	27.3			4 14 0	49.5	45.5			6 6 10	24.1	-11.6			7 4 5	18.7	-18.4		
4 3 0	179.8	-114.0			4 14 1	102.2	74.9			6 6 11	2.0	-43.3			7 4 6	10.1	18.2		
4 3 1	78.6	-75.3			4 14 2	30.6	-30.7			6 6 12	11.8	28.3			7 4 7	-9.4	3.3		
4 3 2	-6.3	-9.4			4 14 3	36.8	41.4			6 7 0	-8.0	18.2			7 4 8	37.9	65.3		
4 3 3	18.8	87.1			4 14 4	-47.2	-52.2			6 7 1	62.2	53.9			7 4 9	33.9	-28.1		
4 3 4	-7.0	6.6			4 14 5	-10.9	20.1			6 7 2	139.3	137.5			7 4 10	-10.1	18.2		
4 3 5	57.5	50.6			4 14 6	6.4	45.4			6 7 3	143.0	148.5			7 4 11	-11.4	-5.0		
4 3 6	122.5	-111.5			4 14 7	31.8	36.1			6 7 4	150.7	142.8			7 4 12	-11.8	16.3		
4 3 7	129.8	-125.5			4 14 8	44.4	-48.4			6 7 5	62.6	68.4			7 5 1	2.0	-25.1		
4 3 8	156.7	-152.3			4 15 0	1.1	-22.7			6 7 6	71.1	-77.1			7 5 2	139.4	-134.2		
4 3 9	105.9	-103.7			4 15 1	28.2	7.1			6 7 7	26.2	-30.7			7 5 3	131.5	-124.5		
4 4 0	-37.0	-31.3			4 15 2	37.4	25.1			6 7 8	143.2	-135.5			7 5 4	33.5	33.0		
4 4 1	44.2	40.3			4 15 3	44.0	41.4			6 7 9	28.8	-24.4			7 5 5	15.2	73.0		
4 4 2	76.5	73.7			4 15 4	71.9	65.7			6 7 10	-10.9	3.6			7 5 6	60.1	-61.7		
4 4 3	25.5	27.0			4 15 5	37.6	35.3			6 7 11	-11.3	-2.1			7 5 7	44.3	44.1		
4 4 4	117.8	113.3			4 15 6	54.4	50.7			6 8 0	2.0	-38.1			7 5 8	62.8	-64.6		
4 4 5	-6.3	-18.6			4 16 0	33.4	37.4			6 8 1	64.6	-62.0			7 5 9	1.1	1.1		
4 4 6	-6.6	1.4			4 16 1	52.4	40.9			6 8 2	65.8	71.6			7 5 10	60.3	-64.0		
4 4 7	19.8	-21.3			4 16 2	53.9	61.4			6 8 3	28.8	-24.4			7 5 11	51.9	-47.5		
4 4 8	88.1	-90.2			4 16 3	47.0	42.9			6 8 4	4.3	84.4			7 5 12	2.6	84.4		
4 4 9	38.6	-29.1			5 0 0	2.1	71.0			6 8 5	-9.3	9.8			7 6 1	-8.1	7.7		
4 4 10	87.6	-71.2			5 0 1	162.6	-155.5			6 8 6	-9.6	-16.0			7 6 2	-8.3	10.5		
4 4 11	28.7	2.1			5 0 2	154.5	140.7			6 8 7	2.7	55.7			7 6 3	22.9	8.4		
4 4 12	58.9	-50.8			5 0 3	136.3	140.7			6 8 8	10.2	-4.1			7 6 4	6.0	79.8		
4 4 13	-9.7	-11.7			5 0 4	88.8	80.9			6 8 9	26.2	-25.0			7 6 5	76.6	71.7		
4 4 14	110.4	-107.9			5 0 5	12.1	0.6			6 8 10	-11.1	12.9			7 6 6	5.8	94.1		
4 4 15	31.0	29.0			5 0 6	195.5	197.5			6 8 11	25.5	-18.4			7 6 7	17.8	12.2		
4 4 16	43.0	-41.1			5 0 7	208.8	181.0			6 8 12	67.7	-67.2			7 6 8	60.3	-56.7		
4 4 17	32.5	-53.2			5 1 0	3.4	12.5			6 9 0	151.2	-157.5			7 6 9	58.3	55.9		
4 4 18	40.3	-55.2			5 1 1	118.5	106.4			6 9 1	38.4	-44.4			7 6 10	19.4	73.0		
4 4 19	66.0	-78.1			5 1 2	-7.8	-2.0			6 9 2	193.5	-197.3			7 6 11	24.0	-21.7		
4 4 20	24.4	-22.3			5 1 3	6.4	79.9			6 9 3	-9.3	21.5			7 6 12	52.0	49.1		
4 5 0	212.7	-207.7			5 1 4	86.2	85.9			6 9 4	5.2	-20.0			7 7 1	23.3	33.2		
4 5 1	52.3	61.1			5 1 5	71.8	-71.3			6 9 5	23.3	-22.6			7 7 2	8.3	-22.6		
4 5 2	85.4	-84.3			5 1 6	24.1	14.3			6 9 6	24.9	19.7			7 7 3	-9.1	7.3		
4 5 3	28.3	17.0			5 1 7	29.3	37.8			6 9 7	54.0	-51.2			7 7 4	34.7	-36.9		
4 5 4	118.9	-116.8			5 1 8	76.8	-69.8			6 9 8	2.7	16.7			7 7 5	8.0	7.0		
4 5 5	70.0	76.7			5 1 9	-11.2	11.8			6 9 9	15.0	-33.8			7 7 6	31.1	-35.9		
4 5 6	37.9	43.8			5 1 10	27.2	5.4			6 10 0	75.6	74.9			7 7 7	49.0	47.7		
4 5 7	11.3	10.0			5 2 0	220.1	-212.2			6 10 1	43.2	-43.6			7 7 8	27.1	75.8		
4 5 8	-11.4	-23.5			5 2 1	34.0	45.2			6 10 2	7.7	25.8			7 7 9	11.0	-11.0		
4 5 9	-11.9	7.3			5 2 2	137.6	-124.6			6 10 3	57.4	52.7			7 7 10	47.0	34.0		
4 6 0	159.7	-145.1			5 2 3	211.2	200.8			6 10 4	-9.6	6.6			7 7 11	35.7	-29.6		
4 6 1	12.6	-2.0			5 2 4	94.7	-94.1			6 10 5	27.1	28.5			7 7 12	53.6	46.2		
4 6 2	68.9	-68.7			5 2 5	124.9	-118.9			6 10 6	23.9	-21.2			7 8 1	3.8	-9.1		
4 6 3	58.0	-83.5			5 2 6	27.3	6.4			6 10 7	48.6	39.8			7 8 2	33.7	-24.0		
4 6 4	15.1	-32.3			5 2 7	74.0	-64.6			6 10 8	7.6	7.8			7 8 3	49.0	-51.1		
4 6 5	125.4	-117.5			5 2 8	9.7	-7.4			6 10 9	28.2	-28.8			7 8 4	6.0	9.3		
4 6 6	13.6	10.4			5 2 9	10.8	-70.0			6 10 10	-11.4	-6.7			7 8 5	10.2	-7.7		
4 6 7	46.8	36.8			5 2 10	-10.7	12.5			6 11 0	42.4	-41.6			7 8 6	63.0	65.8		
4 6 8	96.0	94.3			5 2 11	35.3	-40.4			6 11 1	107.5	-112.9		</					

Table IV (continued).

H	K	L	F055	FCAL	H	K	L	F055	FCAL	H	K	L	F055	FCAL	H	K	L	F055	FCAL	H	K	L	F055	FCAL	
8 0 0	6	108.0	117.1		8 12 6	44.4	-53.0		9 14 1	32.4	30.1		11 1 8	494.4	-44.9		12 6 6	62.7	50.4						
8 0 0	8	38.9	-50.8		8 12 7	36.8	30.7		9 14 2	-11.4	17.3		11 1 9	26.8	22.5		12 6 7	56.7	69.1						
8 0 0	10	108.1	-114.0		8 13 0	17.1	-19.1		10 0 0	118.4	-132.3		11 1 10	23.9	-28.1		12 7 0	23.3	2.1						
8 1 0	167.5	-164.7		8 13 1	43.9	28.0		10 0 1	27.1	-58.9		11 2 1	56.3	54.9		12 7 1	-10.7	-7.2							
8 1 1	76.8	-67.0		8 13 2	-10.9	-0.2		10 0 2	6.2	95.5	95.4		11 2 2	142.0	-144.8		12 7 2	-19.8	-27.0						
8 1 2	104.5	-96.9		8 13 3	51.0	46.9		10 0 3	120.5	119.7		11 2 3	4.0	-10.1	-17.8		12 7 3	30.8	35.9						
8 1 3	66.5	-62.1		8 13 4	5.3	-3.9		10 0 4	10.7	-12.9		11 2 4	98.3	-97.1		12 7 4	21.2	21.3							
8 1 4	41.7	36.9		8 13 5	-11.6	-74.9		10 0 5	113.1	-113.1		11 2 5	24.2	-5.4		12 7 5	62.4	62.3							
8 1 5	52.2	-49.7		8 14 0	91.5	-80.7		10 1 1	67.1	68.7		11 2 6	35.6	77.7		12 7 6	56.7	57.6							
8 1 6	11.1	12.9		8 14 1	20.4	-10.3		10 1 2	61.9	-39.4		11 2 7	21.4	-10.0		12 7 7	8.1	-64.4							
8 1 7	45.1	-46.2		8 14 2	31.3	-29.8		10 1 3	109.3	107.0		11 2 8	3.2	-26.3		12 7 8	1.7	16.0							
8 1 8	-10.1	12.5		8 14 3	77.5	6.2		10 1 4	-9.6	4.7		11 2 9	1.5	56.5	-57.7		12 7 9	-10.7	-16.0						
8 1 9	-10.5	-1.2		8 14 4	22.2	28.1		10 1 5	-9.9	-10.7		11 3 1	2.4	-4.1	47.9		12 8 0	30.4	-16.9						
8 1 10	29.1	-14.2		8 14 5	51.8	41.8		10 1 6	4.0	-39.0		11 3 2	102.8	-97.5		12 8 1	6.1	33.3							
8 1 11	56.2	62.8		8 14 6	77.6	71.4		10 1 7	7.0	-10.5	2.7		11 3 3	4.0	-10.0	-0.3		12 8 2	5.0	-15.3					
8 1 12	29.4	-19.6		8 14 7	63.0	68.4		10 1 8	57.1	-59.2		11 3 4	24.9	-13.5		12 8 3	27.9	-20.7							
8 2 0	191.6	170.3		8 14 8	26.9	70.7		10 1 9	30.9	33.3		11 3 5	27.3	-35.3		12 8 4	51.7	-57.3							
8 2 1	31.6	25.4		8 14 9	42.9	42.6		10 1 10	-11.6	-0.6		11 3 6	1.7	-11.0	0.7		12 8 5	33.0	34.3						
8 2 2	55.6	61.6		8 14 10	25.3	-14.5		10 2 0	103.8	107.5		11 3 7	30.7	30.1		12 8 6	21.2	-27.4							
8 2 3	26.3	18.9		8 14 11	112.9	115.4		10 2 1	112.3	115.1		11 3 8	62.6	61.8		12 8 7	80.0	77.6							
8 2 4	102.2	-98.0		8 14 12	74.3	74.7		10 2 2	2.2	70.2	70.9		11 3 9	4.0	61.3	-63.8		12 8 8	-11.3	-68.0					
8 2 5	50.8	-52.3		8 14 13	4.0	68.4		10 2 3	113.7	105.4		11 3 10	2.4	74.8	63.2		12 8 9	27.7	27.1						
8 2 6	134.9	-135.4		8 14 14	22.8	-15.7		10 2 4	87.6	-74.1		11 3 11	4.3	41.2	-34.5		12 8 10	46.3	-34.9						
8 2 7	25.2	-20.5		8 14 15	6.0	-9.8	-9.1	10 2 5	24.9	-12.3		11 3 12	4.0	25.5	18.5		12 8 11	42.3	32.1						
8 2 8	56.4	-58.5		8 14 16	17.2	-83.3		10 2 6	25.6	-24.7		11 3 13	4.0	48.3	46.5		12 8 12	31.1	23.4						
8 2 9	27.1	-28.6		8 14 17	78.4	-84.1		10 2 7	7.0	18.2	-2.3		11 3 14	6.0	61.4	-52.5		12 8 13	36.7	49.6					
8 2 10	11.1	12.9		8 14 18	10.9	4.7		10 2 8	-10.9	4.7		11 3 15	8.0	86.6	83.4		12 8 14	11.4	-27.4						
8 2 11	23.6	-23.2		8 14 19	74.9	-80.3		10 2 9	29.7	27.1		11 3 16	4.0	-11.8	-0.5		12 8 15	27.4	74.1						
8 2 12	78.4	79.3		8 14 20	-11.7	13.7		10 2 10	-11.7	2.6		11 3 17	4.0	-11.8	29.4		12 8 16	74.8	74.1						
8 3 0	18.9	-1.9		8 14 21	3.0	-10.7		10 3 0	70.7	-75.1		11 3 18	1.0	60.8	-54.9		12 8 17	4.0	34.4	44.9					
8 3 1	13.2	11.1		8 14 22	62.7	64.3		10 3 1	4.2	62.2	64.3		11 3 19	4.0	102.8	-97.5		12 8 18	2.0	26.3	26.3				
8 3 2	60.9	-56.0		8 14 23	14.1	-9.0		10 3 2	14.1	-23.4		11 3 20	4.0	25.2	33.2		12 8 19	1.0	37.1	16.6					
8 3 3	13.2	-13.3		8 14 24	40.5	37.8		10 3 3	-9.3	-17.2		11 3 21	5.0	4.0	117.1	114.5		12 8 20	47.9	-37.7					
8 3 4	56.2	-52.2		8 14 25	74.1	-71.2		10 3 4	14.2	-9.4		11 3 22	5.0	2.0	10.2	-9.4		12 8 21	-10.1	-14.9					
8 3 5	52.7	-42.7		8 14 26	26.9	-27.0		10 3 5	97.4	90.6		11 3 23	5.0	6.0	45.0	47.4		12 8 22	4.0	-14.9					
8 3 6	-7.4	-12.3		8 14 27	103.3	-96.9		10 3 6	98.9	-90.5		11 3 24	7.0	-11.0	-5.1		12 8 23	5.0	-11.4	-25.7					
8 3 7	20.3	18.0		8 14 28	24.0	-19.6		10 3 7	-10.8	-7.1		11 3 25	8.0	-11.3	-6.5		12 8 24	3.0	33.3	13.7					
8 3 8	-10.2	-1.7		8 14 29	72.5	-72.7		10 3 8	8.0	-80.8	-80.8		11 3 26	1.0	77.8	76.3		12 8 25	1.0	56.9	56.9				
8 3 9	16.7	20.7		8 14 30	-11.3	-8.1		10 3 9	-11.3	-2.8		11 3 27	6.0	42.9	101.5		12 8 26	-1.0	17.6	17.6					
8 3 10	-11.1	-11.7		8 14 31	32.5	-34.2		10 3 10	28.7	9.8		11 3 28	6.0	2.0	10.2	-9.4		12 8 27	1.0	16.6	16.6				
8 3 11	20.3	-33.7		8 14 32	157.2	-151.3		10 3 11	12.3	-117.3		11 3 29	6.0	4.0	62.5	61.5		12 8 28	1.0	16.6	16.6				
8 3 12	25.6	14.2		8 14 33	2.0	-145.5		10 3 12	-9.1	-16.6		11 3 30	6.0	5.0	57.5	-58.1		12 8 29	4.0	44.4	-46.4				
8 3 13	181.6	-184.7		8 14 34	57.1	-54.2		10 3 13	30.2	-24.6		11 3 31	6.0	5.0	22.1	0.4		12 8 30	5.0	57.5	-58.1				
8 3 14	62.8	-62.5		8 14 35	150.8	-141.3		10 3 14	4.0	-62.6	-62.6		11 3 32	6.0	6.0	63.1	-72.2		12 8 31	2.0	20.1	-17.6			
8 3 15	106.4	-101.9		8 14 36	55.5	-60.8		10 3 15	4.0	6.0	6.0		11 3 33	6.0	7.0	74.4		12 8 32	1.0	16.6	16.6				
8 3 16	97.9	-98.1		8 14 37	19.0	20.2		10 3 16	5.0	76.9	-71.2		11 3 34	6.0	58.3	57.5		12 8 33	1.0	16.6	16.6				
8 3 17	84.6	84.6		8 14 38	39.0	-38.6		10 3 17	6.0	58.5	56.7		11 3 35	6.0	91.4	90.5		12 8 34	1.0	16.6	16.6				
8 3 18	9.1	-4.1		8 14 39	62.7	55.1		10 3 18	7.0	64.4	64.4		11 3 36	6.0	91.4	90.5		12 8 35	1.0	16.6	16.6				
8 3 19	107.0	133.6		8 14 40	69.4	-74.2		10 3 19	8.0	28.0	-23.5		11 3 37	6.0	33.2	32.7		12 8 36	1.0	16.6	16.6				
8 3 20	45.4	48.2		8 14 41	64.9	65.2		10 3 20	4.0	53.3	47.2		11 3 38	6.0	16.9	-27.0		12 8 37	1.0	16.6	16.6				
8 4 0	31.7	33.4		8 14 42	1.0	-34.2		10 3 21	11.0	-11.8	-7.1		11 3 39	6.0	16.9	15.8		12 8 38	1.0	16.6	16.6				
8 4 1	27.4	-32.1		8 14 43	90.5	-85.4		10 3 22	9.0	-2.0	-3.9		11 3 40	6.0	83.4	-82.5		12 8 39	1.0	16.6	16.6				
8 4 2	11.3	0.6		8 14 44	3.0	0.6		10 3 23	10.0	10.0		11 3 41	6.0	10.0	10.0		12 8 40	1.0	16.6	16.6					
8 4 3	19.7	15.6		8 14 45	38.5	-47.6		10 3 24	3.0	-9.7	-10.1		11 3 42	6.0	8.0	82.6	-92.3		12 8 41	1.0	16.6	16.6			
8 4 4	26.1	-37.4		8 14 46	44.3	35.7		10 3 25	4.0	82.6	68.0		11 3 43	6.0	17.0	21.1		12 8 42	1.0	16.6	16.6				
8 4 5	31.7	33.4		8 14 47	-9.8	1.5		10 3 26	5.0	34.5	27.0		11 3 44	6.0	3.0	51.1	44.1		12 8 43	1.0	16.6	16.6			
8 4 6	27.4	-32.1		8 14 48	33.7	-21.1		10 3 27	6.0	33.7	-21.1		11 3 45	6.0	4.0	66.0	61.0		12 8 44	1.0	16.6	16.6			
8 4 7	11.3	0.6		8 14 49	-13.6	13.6		10 3 28	7.0	-10.5	-16.7		11 3 46	6.0	5.0	117.3	113.7		12 8 45	1.0	16.6	16.6			
8 4 8	35.0	26.7		8 14 50	20.3	-2.6		10 3 29	8.0	-6.7	-63.8		11 3 47	6.0	5.0	55.4	56.9		12 8 46	1.0	16.6	16.6			
8 4 9	9.1	16.5		8 14 51	12.0	28.6		10 3 30	9.0	27.9	28.6		11 3 48	6.0	6.0	66.0	61.0		12 8 47	1.0	16.6	16.6			
8 4 10	26.1	-37.4		8 14 52	27.4	31.0		10 3 31	10.0	26.2	-23.1		11 3 49	6.0	7.0	58.2	-52.5		12 8 48	1.0	16.6	16.6			
8 4 11	20.3	-33.7		8 14 53	51.7	-59.7		10 3 32	11.0	60.3	-56.7		11 3 50	6.0	8.0	25.1	-19.5		12 8 49	1.0	16.6	16.6			
8 4 12	10.7	1																							

Table V. Final positional parameters (fractional) with mean standard deviations (\AA), and thermal parameters and standard deviations (B in \AA^2 , U_{ij} in $\text{\AA}^2 \times 10^2$).

ATOM	\underline{x}	\underline{y}	\underline{z}	mean σ	\underline{B} (\AA^2)	$\sigma(B)$
P(1)	0.1201	0.3906	0.1366	0.0066	1.81	0.12
P(2)	0.1352	0.3397	-0.0507	0.0067	1.90	0.12
P(3)	0.2656	0.4525	-0.0628	0.0073	2.59	0.14
P(4)	0.3047	0.4068	0.1307	0.0072	2.35	0.13
N(1)	0.1148	0.3248	0.0584	0.020	2.21	0.40
N(2)	0.1733	0.4215	-0.0693	0.021	2.44	0.42
N(3)	0.3253	0.4121	0.0181	0.022	2.70	0.44
N(4)	0.2108	0.4298	0.1528	0.020	2.09	0.40
C(1)	0.0848	0.3494	0.2406	0.028	2.97	0.55
C(2)	0.0486	0.4674	0.1110	0.028	3.02	0.56
C(3)	0.2018	0.2649	-0.0884	0.027	2.58	0.52
C(4)	0.0386	0.3311	-0.1132	0.028	3.06	0.56
C(5)	0.3297	0.4389	-0.1626	0.034	4.38	0.69
C(6)	0.2600	0.5511	-0.0433	0.033	4.34	0.67
C(7)	0.3767	0.4674	0.1863	0.031	3.76	0.62
C(8)	0.3363	0.3110	0.1616	0.031	3.72	0.62
Cu	0.0572	0.2235	0.0830	0.0033		
Cl(1)	-0.0740	0.2681	0.0990	0.0088		
Cl(2)	0.1646	0.1722	0.1597	0.0079		
Cl(3)	0.0248	0.1228	-0.0058	0.0080		

ATOM	\underline{U}_{11}	\underline{U}_{12}	\underline{U}_{13}	\underline{U}_{22}	\underline{U}_{23}	\underline{U}_{33}	mean $\sigma(U)$
Cu	3.10	-0.68	0.17	3.41	0.16	3.54	0.17
Cl(1)	2.55	-0.59	0.80	7.26	-0.89	7.94	0.47
Cl(2)	5.21	0.29	-1.09	4.31	0.45	4.70	0.41
Cl(3)	3.35	-0.54	0.61	4.92	-1.77	6.58	0.42

Discussion

The eight-member phosphonitrilic ring has the "tub" shape with pairs of adjacent phosphorus and nitrogen atoms alternately up and down. This is the conformation of the parent compound, $[\text{NPMe}_2]_4$,⁴⁰ although in the present structure the molecular $\bar{4}$ symmetry is destroyed by the CuCl_3 adduct and by non-equivalent bond lengths. In common with other tetrameric phosphonitrilic compounds^{17,42} the nitrogen atoms are displaced slightly more from the best plane through all the ring atoms (0.55 \AA) than are the phosphorus atoms (0.48 \AA). The methyl groups lie on either side of the ring and those on neighbouring phosphorus atoms tend to be staggered. The CPC planes are approximately perpendicular to the local ring (NPN) plane, the average angle being 86.5° . The CuCl_3 adduct bonded to nitrogen (1) has an unusual distorted configuration. Although the majority of Cu(II) complexes have octahedral environments, in the present case the arrangement of atoms about the metal atom is between the tetrahedral and square planar forms.

Recent crystallographic evidence for the effect of the protonation of a trimeric phosphonitrile has been given for $\text{N}_3\text{P}_3\text{Cl}_2(\text{NHPr}^i)_4, \text{HCl}$.³⁵ In this structure the hydrogen has been definitely located on one of the ring nitrogen atoms and long P-N bond lengths of 1.67 \AA are observed to this protonated nitrogen. Ring bonds are reported of $1.67, 1.58$ and 1.56 \AA , although the two latter lengths may be influenced by the different character of the substituents on the phosphorus atoms. The present study demonstrates that in the case of a tetrameric phosphonitrile as well, the formation of chemical bonds

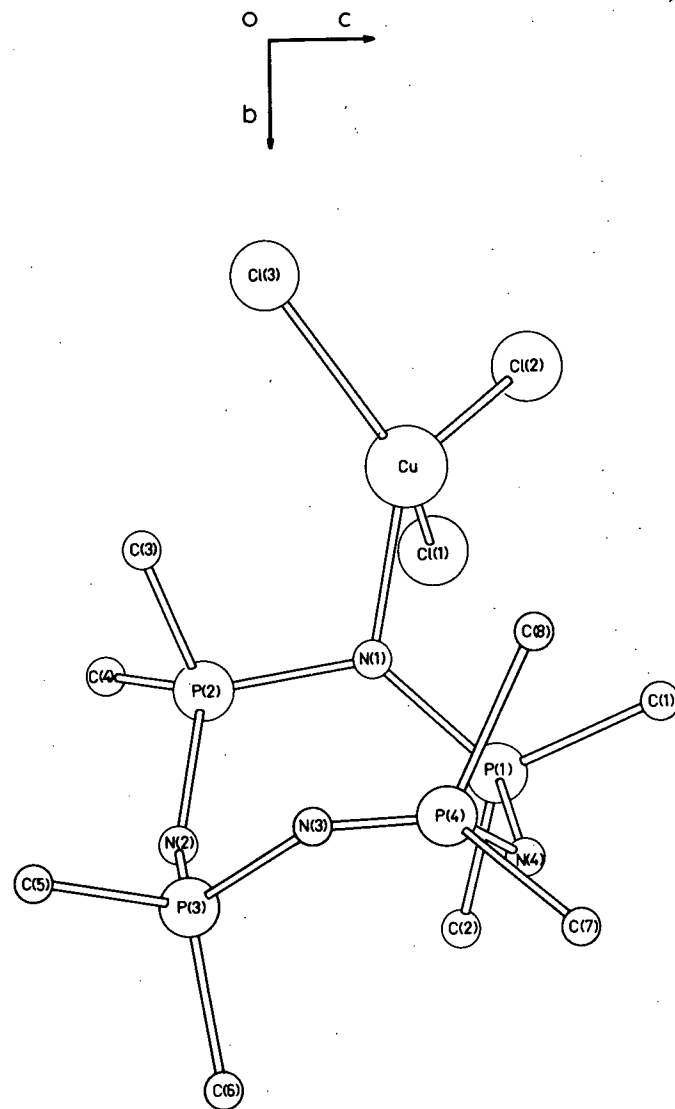
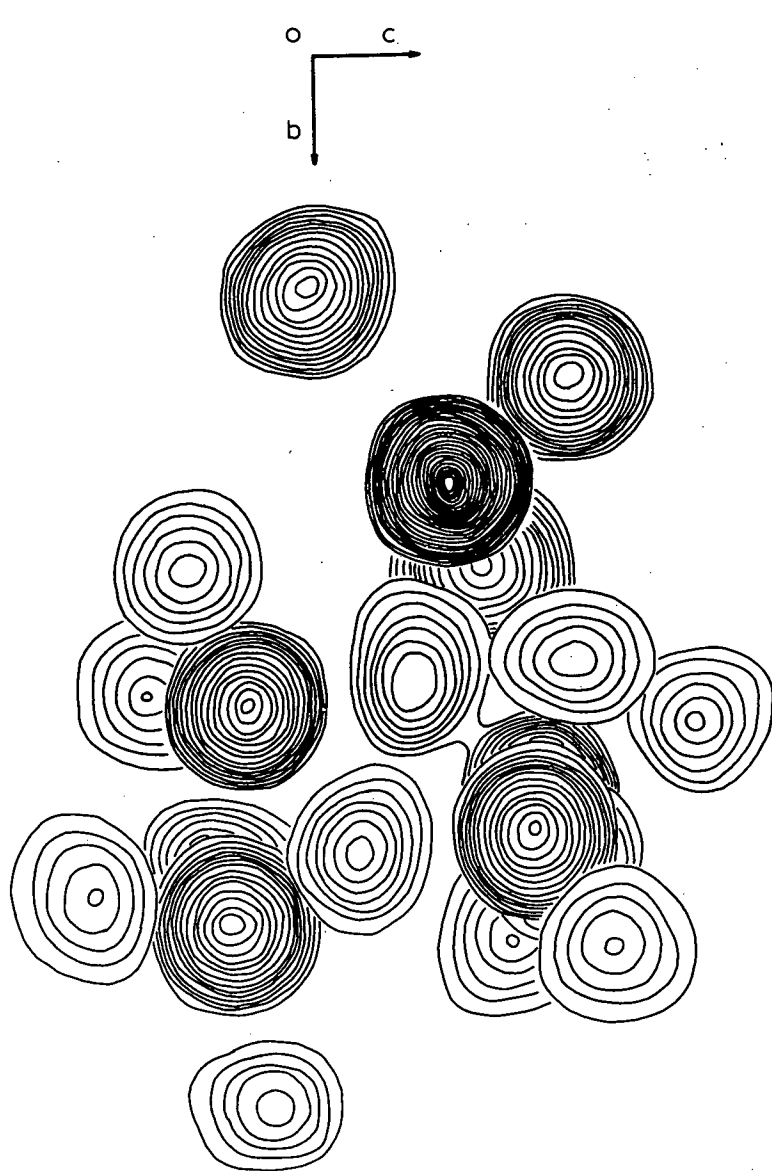


Figure 2. Sections of the electron density distribution and a drawing of the molecule. Contours are drawn at one electron intervals beginning with $1 \text{ e.}\text{\AA}^{-3}$. In the drawing, P(4) is displaced towards N(3) for clarity.

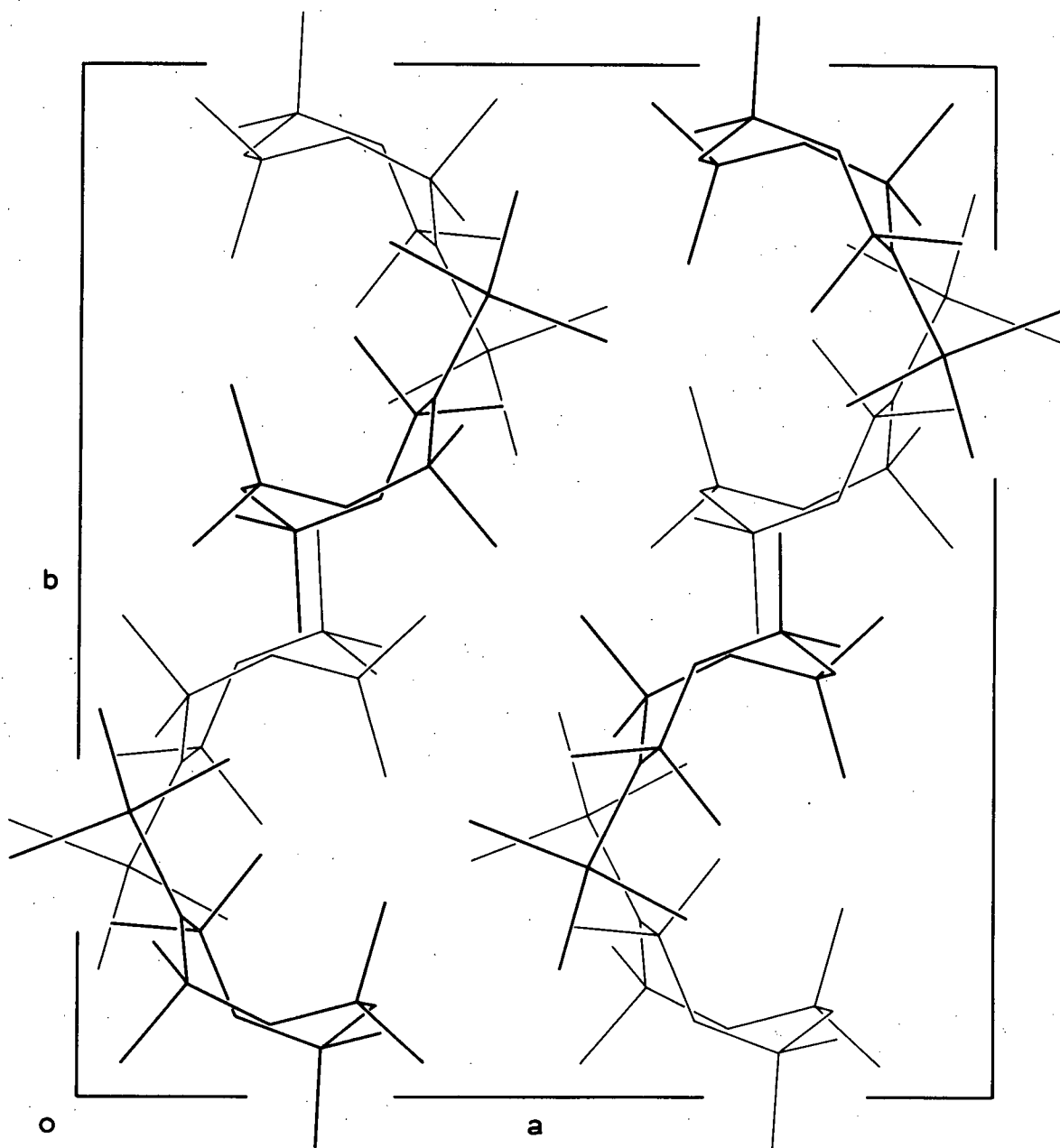


Figure 3. Packing of the molecules in the unit cell viewed along the c -axis.

to the nitrogen atoms markedly influence the detailed structure of the phosphonitrilic ring. Bond lengths and angles pertaining to the ring are shown on a diagrammatic representation in Figure 4, while the complete intramolecular bond distances and angles are given in Table VI. In all reported structures of cyclic phosphonitriles with similar substituents on the phosphorus atoms, the P-N ring bonds have been found to be equal. Bond lengths vary from 1.51 Å in $[\text{NPF}_2]_4$ ³⁹ to 1.60 in $[\text{NPM}_2]_4$ ⁴⁰ depending upon the electronegativity of the substituents. In the present structure the addition of the CuCl_3 group to a nitrogen atom (with the corresponding protonation of the ring) has broken the equality of the ring bonds. There appear to be four distinct P-N bond lengths : 1.63 Å, 1.60 Å, 1.56 Å and 1.67 Å, ($\sigma = 0.01$ Å).

These differences in bond length can be interpreted in terms of the π -bonding theory of Craig and Paddock for phosphonitriles.²² The π_a and π_s -notation (for overlap involving phosphorus \underline{d}_{xz} or \underline{d}_{yz} and $\underline{d}_{x^2-y^2}$ or \underline{d}_{xy} orbitals respectively) and the axial convention has already been described in the Introduction.

The pairs of distinct P-N bonds are symmetrically arranged so as to imply that the protonation takes place on N(3) where the longest P-N bonds of 1.67 Å occur. The nitrogen lone pair electrons are required for bonding the proton and are thus localized (presumably in an sp^2 hybrid orbital). The double bond character of the P-N bonds is decreased by this localization of the lone pair which now cannot be utilized for donation into the π_s -bonding system. Some π_a -bonding

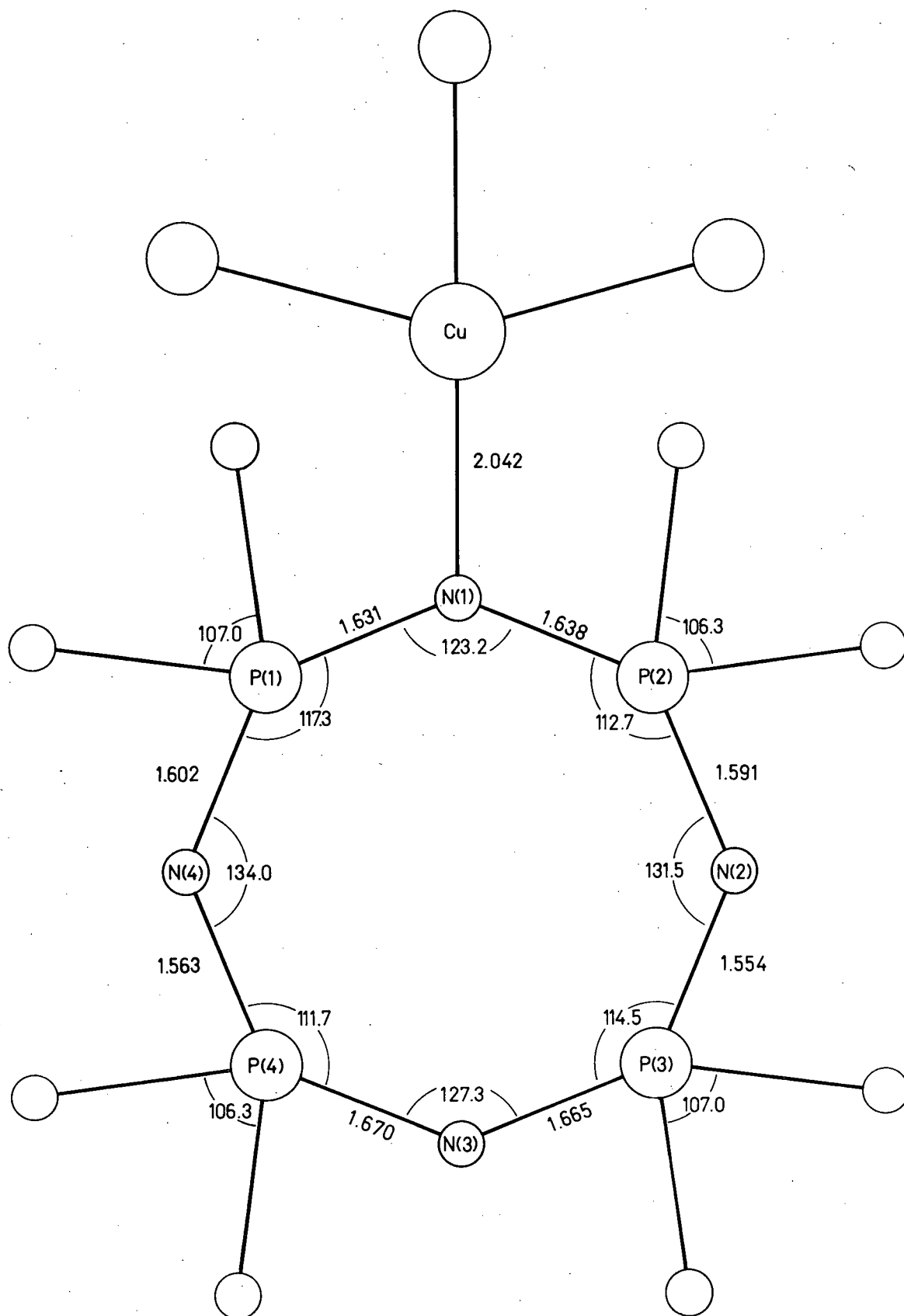


Figure 4. Bond lengths and angles within the phosphonitrilic ring.

Table VI. Bond distances (\AA) and valency angles (degrees).

P(1)-N(1)	1.631	P(1)-N(1)-P(2)	123.2
P(1)-N(4)	1.602	P(2)-N(2)-P(3)	131.5
P(2)-N(1)	1.638	P(3)-N(3)-P(4)	127.3
P(2)-N(2)	1.591	P(4)-N(4)-P(1)	134.0
P(3)-N(2)	1.554	Mean P-N-P	129.0
P(3)-N(3)	1.665	N(4)-P(1)-N(1)	117.3
P(4)-N(3)	1.670	N(1)-P(2)-N(2)	112.7
P(4)-N(4)	1.563	N(2)-P(3)-N(3)	114.5
P(1)-C(1)	1.768	N(3)-P(4)-N(4)	111.7
P(1)-C(2)	1.804	Mean N-P-N	114.0
P(2)-C(3)	1.775	C(1)-P(1)-C(2)	107.0
P(2)-C(4)	1.774	C(3)-P(2)-C(4)	106.3
P(3)-C(5)	1.781	C(5)-P(3)-C(6)	107.0
P(3)-C(6)	1.772	C(7)-P(4)-C(8)	106.3
P(4)-C(7)	1.758	Mean C-P-C	106.6
P(4)-C(8)	1.826		
Mean P-C	1.782		
Cu-Cl(1)	2.218	Cl(1)-Cu-Cl(2)	143.2
Cu-Cl(2)	2.217	Cl(1)-Cu-Cl(3)	97.6
Cu-Cl(3)	2.262	Cl(1)-Cu-N(1)	96.7
Cu-N(1)	2.042	Cl(2)-Cu-Cl(3)	97.7
Mean Cu-Cl	2.232	Cl(2)-Cu-N(1)	96.4
		Cl(3)-Cu-N(1)	133.9
$\sigma(\text{P-N})$	= 0.02 \AA	$\sigma(\text{P-N-P})$	= 1.4 $^\circ$
$\sigma(\text{P-C})$	= 0.04	$\sigma(\text{N-P-N})$	= 1.2
$\sigma(\text{Cu-Cl})$	= 0.01	$\sigma(\text{C-P-C})$	= 1.5
$\sigma(\text{Cu-N})$	= 0.02	$\sigma(\text{Cl-Cu-Cl})$	= 0.5
		$\sigma(\text{Cl-Cu-N})$	= 0.7

would seem to occur, however, with overlap from a phosphorus d_{xz} or d_{yz} orbital into a singly occupied p_z orbital on the nitrogen for the bond length is less than the value of 1.77 Å for a single P-N bond distance.^{45,46} The length is very similar to the P-N bond lengths in the metaphosphimate structures $\text{Na}_3(\text{NHPO}_2)_3 \cdot 4\text{H}_2\text{O}$ ⁴⁷ (1.68 Å), and $(\text{NH})_4\text{P}_4\text{O}_8\text{H}_4 \cdot 2\text{H}_2\text{O}$ ⁴⁸ (1.66 Å) where only a single system of π -bonds can exist. Adjacent to this long P-N bond is the shortest bond distance in the ring, 1.56 Å. The shortness can be accounted for in the following way. The absence of electron drift from the N(3) lone pair electrons to the $d_{\pi s}$ orbitals of phosphorus (3) and (4), and the formal positive charge on N(3) would combine to make these phosphorus atoms more receptive to $d_{\pi}-p_{\pi}$ bonding via acceptance of the lone pair electrons from nitrogen (2) and nitrogen (4) respectively. The next bonds, 1.60 Å between N(4)-P(1) and N(2)-P(2) are more like normal phosphonitrilic ring bonds. The effect of the anomalous N(3) is no longer felt and the normal overlaps can occur once more. At N(1), the lone pair is again required for bonding an exocyclic atom. Hybridization at nitrogen into sp^2 orbitals again is likely both from the P(1)-N(1)-P(2) angle of 123° and from the fact that the nitrogen is only 0.1 Å off the P(1)P(2)Cu plane. The P-N bond distances show an increase to 1.63 Å as the double bond character (especially the π_s -component) is once more decreased. It would seem that the copper is not as strong an acceptor as is the proton, however, for here the effect on the bond length is less severe.

The interbond angles in $[\text{NPMe}_2]_4\text{H.CuCl}_3$ also tend to support this bonding scheme, the angles at nitrogen being the most indicative. At N(1) and N(3) where the lone pair electrons are required for bonding, the angles are 123° and 127° respectively. These approach the equilibrium angles expected for three co-planar bonds and suggest that the postulated sp^2 hybridization is not unreasonable. The angles are similar to the P-N-P angles in tri- and tetrametaphosphimates (123° and 126°) where the nitrogen atom is also protonated. The angles at N(2) and N(4) (131.5° and 134°) which are bonded only to phosphorus atoms, are similar to values observed in other tetrameric phosphonitriles. The larger angle is consistent with some donation of electron density from these nitrogen atoms into the π_s -system. These angles are greater than at N(1) and N(3) because of the increased electronic repulsions between the bonds. The angles at phosphorus are considerably different from those of the parent compound $[\text{NPMe}_2]_4$. The average N-P-N angle here is 114° compared to 119.8° ; the exocyclic angle is larger, 106.6° compared to 104° . In no unperturbed phosphonitrilic structure has the endocyclic angle deviated far from 120° , nor the exocyclic angle exceeded 104° . The ring angles, on the other hand, are larger than those of the metaphosphimates (104.5° and 107°) where the secondary π_s -system is not possible. The angles at phosphorus in $[\text{NPMe}_2]_4\text{H.CuCl}_3$ are thus about midway between these two cases. The effect this decreased angle will have on the phosphonitrilic bonding system is difficult to assess, but it is probable that the overlap of bonding orbitals would not be as great here as it is in the case of normal phosphonitrilic rings.

Considerable attention has been given to the shape of tetrameric phosphonitrilic rings with the purpose of distinguishing the relative importance of the π_a and π_s -bonding systems. Paddock¹⁷ has demonstrated that the "tub" configuration permits strong π -interactions between adjacent atoms displaced on the same side of the molecular plane. The organic analogue of this, cyclo-octatetraene⁴⁹ illustrates the limiting case where double bonds between two such atoms alternate with single bonds. While this treatment has been useful with unperturbed phosphonitriles it is not as fruitful in the present case. As can be seen in Figure 4, equivalent bond lengths occur on either side of the molecule. This cannot therefore be used to support stronger bond formation between adjacent phosphorus and nitrogen atoms displaced in the same direction. It would seem that the "tub" conformation is adopted (at least in the present case) mainly for steric reasons. This shape, although somewhat constraining the CuCl_3 group, permits the methyl groups on adjacent phosphorus atoms to be approximately staggered.

The arrangement about the copper atom is a distorted one. The deviation from a tetrahedral environment is considerably greater in this case than in the tetrahedrally co-ordinated Cs_2CuCl_4 .^{50,51} There the angles around the central copper atom are 124.9° , 123.3° , 102.5° and 102.9° , but in the present compound the corresponding angles are 143° , 134° , 98° and 96° indicating that the tetrahedron here is much more flattened. The distortion is much greater than that expected from the Jahn Teller effect.⁵² Theoretical calculations based on

changing the screening constant of Cu(II) and varying the polarizability of the ligands in Cs_2CuCl_4 have indicated that 122.4° and 103.4° are the angles expected in the distorted tetrahedron.⁵³ It seems more appropriate to consider the arrangement as a deviation from square planar co-ordination, which although less common than an octahedral environment in Cu(II) complexes is found in the complex $\text{Cu}(\text{pyO})_4(\text{ClO}_4)_2$ ⁵⁴ and in $(\text{NH}_4)_2\text{CuCl}_4$ ⁵⁵ where the Cl-Cu-Cl angle is required by symmetry to be 90° . (There are no atoms about the copper in the present structure which could complete the four short and two long bonds of a distorted octahedron.) To investigate the steric interactions that would arise in a square planar arrangement, positions for atoms Cl(2) and Cl(3) were calculated on the Cl(1)CuN(1) plane using the observed bond distances from the copper. This plane seemed a likely one from a model and was almost perpendicular to the ring. Several unacceptably close contacts occur. The distance from Cl(2) to C(3) of the same molecule is about 2.7 \AA and C(6) of the molecule at $1/2 - x, y - 1/2, z$ there is a contact of 2.9 \AA . Between Cl(3) and C(5) of the molecule at $x - 1/2, 1/2 - y, -z$ there is a distance of 2.8 \AA . These distances can be compared with the sum of the van der Waals radii of 3.8 \AA . The distortion of Cl(2) and Cl(3) away from the plane increases all these non-bonded contacts and presumably leads to a more stable configuration.

There are, however, several intermolecular distances remaining which are somewhat less than the sums of the van der Waals radii. The shortest of these, a Cl(3)...N(3) distance of 3.20 \AA (van der Waals

sum = 3.3 Å), and a Cl(1)...C(3) distance of 3.57 Å occur between the standard molecule and the one at $x - 1/2, 1/2 - y, -z$. The first of these, the Cl(3)...N(3) distance very likely involves a hydrogen bond. The P(3)N(3)...Cl(3) angle is 126°, and the P(4)N(3)...Cl(3) angle is 104° so the molecular arrangement is suitable for such a bond.

Although the hydrogen atom could not be located on the difference map the observed N(3)...Cl(3) distance is the expected value for a N-H...Cl hydrogen bond.⁵⁶ As well as these, there are several methyl...methyl interactions less than the sum of the van der Waals radii (4.0 Å). Those less than 3.8 Å are 3.69 Å from C(1) to C(3) at $x, 1/2 - y, 1/2 + z$, and 3.75 Å from C(2) to the corresponding C(2) in the molecule at $-x, 1 - y, -z$. These are not to be considered unduly compressed, however, since C...C contacts of less than 4.0 Å are not uncommon. Recently Hanson has reported contacts between methyl groups of adjacent molecules to be as small as 3.13 Å.⁵⁷ With non-rotating methyl groups these need not involve unreasonably small H...H distances.

C. THE STRUCTURE OF BIS-(OCTAMETHYLCYCLOTETRAPHOSPHONITRILIUM)
TETRACHLOROCOBALTATE(II)

Experimental

$[(\text{NPMe}_2)_4\text{H}^+]_2\text{CoCl}_4^{2-}$ crystallizes as pale blue platelets from methyl ethyl ketone. The platelets are elongated along c with the (010) face developed. Space group and unit cell information were obtained in the usual manner from oscillation and Weissenberg photographs. Some thirty diffractometer-measured 2θ values were used in a least squares technique to refine the cell parameters.

Crystal Data (λ , Mo- \underline{K}_α = 0.7107 Å)

$[(\text{NPMe}_2)_4\text{H}^+]_2\text{CoCl}_4^{2-}$, \underline{M} = 803.17.

Monoclinic, \underline{a} = 10.43₅ ± 0.01 Å, \underline{b} = 32.83₇ ± 0.02 Å, \underline{c} = 11.17₄ ± 0.01 Å, β = 102.29 ± 0.1°. (Here ± refers to σ).

\underline{U} = 3740.7 Å³, \underline{D}_m = 1.45 g.cm.⁻³ (flotation), \underline{Z} = 4, \underline{D}_c = 1.43 g.cm.⁻³.

$\underline{F}(000)$ = 1668.

Absorption coefficient, $\mu(\text{Mo-}\underline{K}_\alpha)$ = 11.6 cm⁻¹.

Absent reflexions : $h0\ell$ when $h + \ell = 2n + 1$, and $0k0$ when $k = 2n + 1$.

Space group $P2_1/n$.

Considerable difficulty was encountered during the data collection because of the small crystalline size of the sample and the long b -axis of the unit cell. Numerous attempts to prepare larger crystals by varying solvents and crystallizing conditions were unsuccessful. After a systematic examination of the entire sample, the crystal having

the greatest thickness was selected for the intensity measurements. This crystal, however, was still very small and measured 0.2 mm. in length, 0.1 mm. in breadth, but only 0.02 mm. in thickness. The small size of the crystal resulted, unfortunately, in a large number of weak and barely detectable intensities. Also the long b -axis caused certain types of reflexions to fall close together in reciprocal space. Reflexions of the class $0k\ell$, in particular, overlapped badly when measured on the diffractometer with $0k + 1, \ell$ reflexions since their 2θ values were close together and the differences in χ were not great enough to properly separate the intensities.

The seriousness of these problems was not fully appreciated until midway through the analysis. The intensities were recorded initially on a card-automated General Electric XRD-6 Spectrogoniometer equipped with a scintillation counter and a pulse height analyser. Zirconium-filtered Mo-K_{α} radiation was used with a θ - 2θ scan. The measurements were corrected for background, Lorentz and polarization factors were applied, and the three-dimensional Patterson function was summed.

As will be explained in the Structure Analysis section, the reliability of these intensity measurements later became questionable. Consequently it became necessary to recollect large portions, if not all of the data, in a different manner. A consideration of the choices of X-ray radiation available indicated that Mo-K_{α} was probably still preferable. The linear absorption coefficient for Mo-K_{α} ($\mu = 11.6 \text{ cm.}^{-1}$) is much smaller than for other radiations : for Cu-K_{α} , $\mu = 95.8 \text{ cm.}^{-1}$,

for Fe- K_{α} , $\mu = 127.6 \text{ cm.}^{-1}$, and for Cr- K_{α} radiation, $\mu = 204.7 \text{ cm.}^{-1}$. Copper radiation was especially unsuitable since the compound contained cobalt atoms which would probably fluoresce. Since iron radiation might have proved useful, a study was made of the characteristics of this radiation diffracted by the crystal. Although the reflected radiation was more intense than with molybdenum, and there was far less overlap of reflexions, the absorption was much more serious. At $\chi = 90^{\circ}$, a reflexion of the type $00L$ was found to vary in intensity by a factor of ten as the crystal was rotated about the ϕ dial. With filtered molybdenum radiation, by comparison, there was little detectable variation.

For recollecting the intensity measurements manual operation of the diffractometer seemed desirable. This would permit operator intervention where necessary to reduce overlapping of reflexions. The 2θ scan increment was reduced to 1° and the entire set of intensity data was recollected on a manual General Electric diffractometer. In an effort to compensate for the weak reflexions the scanning speed was reduced to 2° a minute from the usual 4° per minute. This, however, was not as beneficial as had been hoped for the general background from the molybdenum radiation was often comparable to the peak height. Once again this resulted in a large number of weak and unreliable intensities. As will be explained later, many of these were included in the analysis only as "unobserveds". These were assigned a value of $F_0 = 0.6 F(\text{threshold})$, and because of the relatively large scaling factor (about 20) required to place the observed structure factors on the same

scale as the calculated ones, have fairly large magnitudes in the final structure factor table. Of the 3483 reflexions measured with $2\theta \leq 40^\circ$, only 1324 (38%) had total counts greater than 1.5 times the minimum background count.

Structure Analysis

The incorrect starting formula made the three-dimensional Patterson function more difficult to interpret than had been anticipated. The measured density of 1.45 g.cm.^{-3} implied that there were probably eight molecules of the postulated $[\text{NPMe}_2]_4\text{CoCl}_2$ in the unit cell. (The calculated density for this assumption is 1.53 g.cm.^{-3} .) With two molecules per asymmetric unit a strong Co-Co vector should occur between non-equivalent cobalt atoms in the Patterson map. This was not apparent. In addition, neither the Harker line at $1/2, 2y, 1/2$ nor the Harker section at $y = 1/2$ contained well resolved unambiguous peaks. However, the orientation of a set of two chlorines about a cobalt atom could be determined from the near-origin region and when this same orientation was found about the Harker positions, the co-ordinates of one cobalt (and then two chlorine atoms) were tentatively determined. A structure factor calculation based on this possibility using the appropriate scattering factors from the International Tables and assuming isotropic temperature parameters of 4.0 \AA^2 , gave an encouraging residual of $R = 0.63$. A three-dimensional Fourier summation based on these positions indicated that the postulated formula was incorrect: there appeared to be two eight-membered phosphonitrilic rings but only

one cobalt atom in the asymmetric unit. Positions for the eight phosphorus atoms were obtained and a second Fourier was summed although the residual factor was still 0.59. From this the co-ordinates of the nitrogen atoms in the phosphonitrilic rings could be located. In addition, it became clear that two other chlorine atoms completed a tetrahedral arrangement about the cobalt. The presence of these atoms discredited the initial assignment of two molecules per asymmetric unit: instead of two molecules each containing one phosphonitrilic ring and a CoCl_2 group, the actual unit consists of two rings and a CoCl_4^{2-} ion. Each formula has approximately the same chemical composition and without a chemical analysis for the percentage of cobalt in the sample, it is difficult to distinguish between the two. The partial chemical analysis together with the chemical composition of the postulated and actual structures are compared in Table VII.

Table VII. Comparison of the postulated and actual composition of the compound with the chemical analysis.

Element	Analysis*(%)	Theoretical Composition (%)	
		Postulated $[\text{N}(\text{PMe}_2)_4\text{CoCl}_2]$	Actual $[(\text{N}(\text{PMe}_2)_4\text{H}^+)]_2\text{CoCl}_4^{2-}$
P	29.03	28.81	30.85
N	13.56	13.03	13.95
C	23.29	22.34	23.93
H	6.03	5.63	6.27
Cl	17.07	16.49	17.66

* J. Dyson. Ph.D. Thesis, Victoria University of Manchester, 1964.

One final Fourier summation was required to locate the methyl carbons. This was based on the positions of one cobalt, four chlorine, eight phosphorus and eight nitrogen atoms, the residual being 0.44. The sixteen methyl carbons were readily located and least squares refinement was commenced with $R = 0.28$. Refinement of the positional and isotropic thermal parameters began normally, but converged quickly. In successive cycles the residual decreased from 0.28 to 0.24, to 0.23 and to 0.225. The relatively poor agreement between the observed and calculated structure factors was surprising since all non-hydrogen atoms had been located on the electron density map. Also the structure was chemically feasible and the density calculated from it was in good accord with the measured density. Furthermore a Difference Fourier summed at this stage showed general fluctuations of up to $2 \text{ e.}\text{\AA}^{-3}$ but no regions having large excesses of electron density.

At this time an examination of the worst discrepancies between the measured and calculated structure factors indicated that sections of the observed data were unreliable. Some serious differences between the amplitudes measured on the automated-diffractometer and the corresponding spot intensities on the photographs were noticed. In some cases, also, backgrounds measured on the counter were unreasonably large. The crystal was remounted on the diffractometer and a more thorough study of intensity profiles indicated some serious overlapping of reflexions. For example, within the 2θ scan of 1° either side of the weak 061 reflexion ($2\theta = 8.33^\circ$), significant contributions

from the 051 ($2\theta = 7.24$) and the 071 ($2\theta = 9.45$) reflexions were included even though the χ values differed by a minimum of 2.4° . This problem was worsened by the white radiation streaks accompanying the molybdenum radiation. In addition, the presence of intensities only slightly above the background - some of which were apparent on the Weissenberg photographs - prompted remeasurement of the entire data. As described earlier this was undertaken, and the intensity estimates then appeared to be more reasonable. The remainder of the analysis was carried out using these new manually-collected measurements. At a later stage, a number of reflexions for which the observed intensities disagreed radically with the calculated structure factors were remeasured. In most cases a missetting of the angles on the manual diffractometer was responsible, since the remeasured values were more realistic. For some reflexions an anomalously high background or the residual of an extraneous peak were detected and the count was adjusted accordingly. For one reflexion, 032 ($2\theta = 8.34$) an accurate intensity could not be assigned because the streaking from the strong 022 reflexion ($2\theta = 7.87$) almost completely masked it even though the difference in χ was 8.1° . A value for this reflexion was estimated by visual comparison with neighbouring spots on the second level Weissenberg film.

The overall agreement of this second set of data appeared substantially better than the first. The initial R using the previously determined coordinates was 0.20 and decreased to 0.16 in a few least squares cycles. At this stage the treatment of weak reflexions was

reconsidered. Until this point a somewhat arbitrary figure of 3 counts had been taken as the minimum observable count. In view of the high random background present this seemed unreasonably low. The standard deviation of a peak count given by counting statistics⁵⁸ takes into account the magnitude of the background as well as the scan count

$$\sigma = \sqrt{B_1 + \text{scan} + B_2}$$

where the backgrounds B_1 and B_2 are counts for half the scan time. On the basis of a minimum background of 120 counts (measured as 12), intensities were classified as "unobserveds" if they were less than three times their standard deviation. This is approximately equivalent to eliminating reflexions having net intensities below a threshold value of 6 measured counts. Unfortunately, this procedure resulted in a greatly depleted number of observed intensities. The least squares refinement was continued, however, for even in the final stages of refinement when a total of sixteen atoms were refined anisotropically there were still more than five observed reflexions per parameter.

The weighting scheme used in the least squares refinement was varied slightly during the course of the refinement. This was chiefly to adjust the weights applied to the unobserved reflexions. These were given weights varying from 0.0 to 0.5 and finally set at 0.2 which made their $w\Delta^2$ comparable to the first range of observed reflexions. In keeping $w\Delta^2$ approximately constant for ranges of F_0 the weights applied to the observed reflexions were of the form $\sqrt{w} = |F_0|/F^*$ for $|F_0| < F^*$ and $\sqrt{w} = F^*/|F_0|$ when $|F_0| \geq F^*$ with F^* finally set at 80.

After reclassification of the unobserved reflexions, and with very little change in the parameters the residual became 0.11. Three cycles of refinement of the anisotropic thermal parameters of the cobalt, chlorine, phosphorus and nitrogen atoms reduced R to 0.089. At this stage a three-dimensional difference map indicated the positions of most of the methyl hydrogens which had peaks of 0.3 to 0.5 e.Å⁻³. Forty-four of the forty-eight possible methyl hydrogen atoms were located having C-H bond lengths between 0.8 Å and 1.2 Å, but the hydrogen atoms on each of the phosphonitrilic rings were not apparent. Inclusion of the forty-four hydrogen atoms in a structure factor calculation further reduced the residual to 0.082 indicating that the assigned positions were probably valid. No least squares refinement of the hydrogen atom positions was attempted. Refinement of the heavier atoms was essentially complete after one further cycle at which time the indicated shifts were all less than the standard deviations. The final residual was 0.077 for the observed reflexions. A list of observed and calculated structure factors is given in Table VIII, and the final atomic co-ordinates and thermal parameters are listed in Table IX, the hydrogen atom positions being in Table X. In Figure 5 sections of the final electron-density distribution are shown and in Figure 6 there is a drawing of the structure viewed along the c*-axis.

Table VIII (continued)

2	8	2	87.4	-85.6	3	16	2	-22.8	-5.3	4	26	2	-29.0	-22.8	6	6	3	-25.2	32.4	7	14	3	56.0	-62.7	C	25	3	-26.6	24.7
-2	8	2	-16.9	-6.7	3	16	2	-16.9	55.9	-4	26	2	48.8	36.0	-6	6	3	-23.3	22.5	-7	14	3	-23.3	22.5	1	25	3	-70.4	55.4
3	8	2	100.4	101.1	4	16	2	-24.7	-16.1	-5	26	2	-24.9	37.9	7	6	3	-27.1	-31.1	-8	14	3	-28.8	-17.9	-1	25	3	-26.0	-1.1
-3	8	2	-40.4	-45.5	4	16	2	-40.4	45.5	5	26	2	-27.2	22.8	-7	6	3	-29.0	-38.1	1	15	3	-28.4	63.3	2	25	3	-27.1	2.6
4	8	2	178.1	-174.2	5	16	2	-27.5	-58.1	1	27	2	-27.2	22.8	8	6	3	-29.0	-38.1	1	15	3	-28.4	63.3	-2	25	3	-26.5	-45.1
-4	8	2	-19.4	0.1	-5	16	2	-24.6	75.7	-1	27	2	-26.7	-13.1	-8	6	3	-26.7	-5.2	2	15	3	44.2	-39.3	3	25	3	-23.0	4.7
5	8	2	91.1	-74.3	6	16	2	-26.7	9.8	2	27	2	-27.6	-29.2	-9	6	3	-27.2	-60.8	-2	15	3	53.2	42.3	-4	25	3	-25.2	-65.9
-5	8	2	-26.3	114.8	-6	16	2	-26.0	16.0	-2	27	2	-27.6	39.1	0	7	3	-28.9	-74.5	2	15	3	-21.5	-41.2	5	25	3	-25.7	-20.1
6	8	2	-25.1	-26.3	7	16	2	-28.1	-27.8	3	27	2	-28.6	-17.4	1	7	3	-17.4	18.3	3	15	3	73.4	77.6	-6	25	3	-26.3	-13.1
-6	8	2	-23.4	13.2	-7	16	2	-27.1	-69.1	-3	27	2	-28.4	-52.6	-1	7	3	137.3	159.0	-3	15	3	-122.7	-8.3	-5	25	3	-29.2	-4.4
7	8	2	45.2	-43.3	8	16	2	-29.5	31.9	4	27	2	-29.5	21.2	2	7	3	32.3	-21.4	4	15	3	-24.3	12.9	8	26	3	-27.2	-12.7
-7	8	2	-65.3	61.3	0	17	2	-25.7	-73.3	-4	27	2	-29.5	43.4	-2	7	3	-29.5	43.4	-4	15	3	-29.9	73.8	1	26	3	-27.1	168.8
8	8	2	-28.4	11.2	1	17	2	-29.3	21.4	-5	27	2	-30.0	-38.3	3	7	3	161.4	161.1	5	15	3	-25.6	45.9	-1	26	3	-26.6	-26.2
-8	8	2	-27.2	18.0	-1	17	2	128.6	138.9	0	28	2	-27.9	3.6	-3	7	3	78.6	82.2	-5	15	3	54.9	61.1	2	26	3	-27.6	18.3
9	8	2	-28.8	-18.5	2	17	2	-22.2	18.8	1	28	2	-25.8	-34.3	4	7	3	39.8	-42.9	6	15	3	-27.1	29.6	-7	26	3	-27.1	17.1
0	9	2	90.3	-90.7	-2	17	2	-22.0	4.4	-2	28	2	-27.1	29.4	-4	7	3	-20.2	-1.7	-6	15	3	-26.1	37.2	3	26	3	-28.6	21.1
1	9	2	112.9	119.1	3	17	2	-21.1	28.0	2	28	2	-28.2	-35.2	5	7	3	65.7	81.4	7	15	3	-28.5	5.4	-3	26	3	60.4	-25.6
-1	9	2	-16.5	-1.8	-3	17	2	50.8	60.1	-2	28	2	80.4	-79.4	-5	7	3	44.5	-44.7	-7	15	3	-27.7	-37.0	4	26	3	-24.6	-4.4
2	9	2	58.6	54.9	4	17	2	53.8	50.0	3	28	2	-29.2	-147.4	6	7	3	60.6	5.1	-8	15	3	-26.1	67.5	5	26	3	-26.3	-51.3
-2	9	2	-17.5	23.6	-4	17	2	72.9	72.8	-3	28	2	-28.3	-7.3	-6	7	3	-23.5	12.2	0	16	3	84.2	-87.0	-5	26	3	-27.7	-45.1
3	9	2	127.1	126.0	5	17	2	-22.6	22.0	-4	28	2	-30.1	71.3	7	7	3	-27.2	49.3	1	16	3	36.9	-37.6	0	27	3	-27.8	13.2
-3	9	2	-108.7	-110.5	-6	17	2	-25.1	-27.9	5	28	2	-28.5	-46.4	-7	7	3	-25.3	-25.0	-1	16	3	-21.9	-73.6	1	27	3	64.5	-56.6
4	9	2	-20.9	11.4	6	17	2	-24.8	56.3	1	29	2	48.1	-43.8	8	7	3	29.1	23.7	3	16	3	61.0	-28.6	-1	27	3	-27.1	-17.6
-4	9	2	-20.3	11.4	-6	17	2	48.3	56.3	-1	29	2	-27.0	-5.1	-8	7	3	-26.9	11.8	-2	16	3	-22.0	9.0	2	27	3	51.4	-51.6
5	9	2	146.1	143.5	7	17	2	48.5	47.8	2	29	2	-28.9	-29.4	-9	7	3	-28.7	-30.5	3	16	3	64.9	54.2	-2	27	3	-27.7	64.2
-5	9	2	-33.2	45.2	-7	17	2	-21.5	-28.7	-2	29	2	49.8	51.0	-9	7	3	-28.7	-30.5	3	16	3	64.9	54.2	-2	27	3	-27.7	64.2
6	9	2	43.2	-45.2	-8	17	2	48.4	17.5	3	29	2	76.9	-80.1	-1	8	3	54.9	-57.3	4	16	3	65.7	-69.5	-3	27	3	-28.8	-13.7
-6	9	2	-23.7	21.9	0	18	2	48.8	59.1	-3	29	2	-24.6	29.5	-2	8	3	109.2	-105.5	-4	16	3	-24.0	6.4	4	27	3	-29.4	2.5
7	9	2	-23.1	-4.4	1	18	2	86.4	-94.1	1	30	2	-29.1	9.8	-1	8	3	95.0	-90.8	-1	16	3	-26.6	8.0	5	27	3	-28.4	52.5
-7	9	2	-28.5	48.8	2	18	2	45.5	48.8	2	30	2	-29.9	-79.9	0	9	3	136.1	-131.2	-2	16	3	-26.1	78.7	6	27	3	-27.8	-11.1
8	9	2	-29.0	-1.7	2	18	2	-22.9	9.9	-1	30	2	-28.5	1.7	3	8	3	39.2	-31.4	4	16	3	-27.5	25.0	-1	27	3	-27.1	11.1
-8	9	2	-27.4	32.6	-2	18	2	41.2	-48.0	-2	30	2	-29.3	-5.3	-3	8	3	50.6	-54.9	-5	16	3	56.3	67.4	2	28	3	61.5	66.0
9	9	2	-28.3	18.1	3	18	2	-21.1	-21.1	0	29	2	-28.5	-46.4	4	8	3	-28.5	-46.4	-7	16	3	-21.9	-73.6	1	27	3	64.5	-56.6
0	10	2	44.0	49.5	-3	18	2	-23.6	-30.6	0	31	2	-29.7	-11.5	-4	8	3	37.6	-42.9	-7	16	3	47.9	51.1	1	28	3	-29.6	-16.4
-0	10	2	-161.8	-144.6	4	18	2	-25.6	-42.1	1	0	3	94.8	-81.2	5	8	3	88.5	85.1	-8	16	3	-29.6	10.9	-3	28	3	-29.7	9.6
1	10	2	17.1	12.1	-4	18	2	113.1	-123.7	-1	0	3	-15.0	-13.8	-5	8	3	-22.1	-27.8	0	17	3	-22.0	-10.9	-4	28	3	-30.4	-11.1
-1	10	2	-13.0	12.1	5	18	2	-21.9	-21.9	-2	0	3	117.6	-102.2	-6	8	3	-29.2	15.5	-7	16	3	-21.2	-65.6	-5	27	3	-28.7	-25.4
2	10	2	47.0	-42.0	-5	18	2	43.6	71.6	-3	0	3	48.6	-57.3	-6	8	3	61.3	55.1	-1	17	3	-21.5	7.1	1	29	3	-28.7	19.6
-2	10	2	-64.1	60.7	6	18	2	-27.4	-18.3	5	0	3	125.3	134.7	-7	8	3	-27.8	-17.8	2	17	3	66.5	74.1	-1	29	3	-28.1	-29.7
3	10	2	176.9	-175.1	-6	18	2	-22.8	19.4	-5	0	3	117.6	-102.2	-8	8	3	-25.5	40.1	-2	17	3	133.7	147.2	-2	29	3	-29.3	-27.2
-3	10	2	-17.0	12.5	-7	18	2	-26.0	50.6	7	0	3	-27.0	51.4	-8	8	3	-29.2	15.5	-3	17	3	-21.2	-65.6	-2	29	3	-29.3	-27.2
4	10	2	-20.7	12.5	-8	18	2	-28.4	-12.9	-7	0	3	84.1	-83.8	-9	8	3	-27.3	-31.1	-3	17	3	59.1	-60.4	-3	29	3	-29.9	3.1
-4	10	2	-23.0	10.5	-8	18	2	-30.0	48.2	-9	0	3	-28.5	17.0	-9	8	3	-28.9	-47.4	4	17	3	-26.0	-2.4	0	30	3	-29.6	18.5
5	10	2	42.2	-45.7	-9	18	2	-27.6	-21.2	-2	1	3	39.9	-37.7	-9	9	3	35.7	85.9	-1	17	3	-27.7	65.9	-2	30	3	-29.7	18.5
-5	10	2	-54.5	58.3	1	19	2	44.1	98.4	1	1	3	42.4	-32.4	1	9	3	42.4	-32.4	5	17	3	-27.0	10.7	-2	10	3	-24.4	-14.5
6	10	2	-24.0	26.6	-1	19	2	42.5	35.7	-1	1	3	184.4	-185.7	-1	9	3	34.4	33.6	-5	17	3	-25.4	6.7	0	0	69.0	67.5	
-6	10	2	-27.4	26.6	2	19	2	-23.1	-2.6	2	1	3	214.3	-209.3	2	9	3	44.5	-43.5	6	17	3	-27.8	-7.5	2	0	4	-18.6	13.0
7	10	2	44.6	-48.8	3	19	2	43.9	48.6	-2	1	3	70.1	-70.5	3	9	3	48.7	51.9	-7	17	3	-27.8	-7.5	2	0	4	-18.6	13.0
-7	10	2	-29.2	-17.4	3	19	2	42.9	56.0	3	1	3	70.1	-70.5	3	9	3	110.4	-109.4	7	17	3	53.3	59.2	4	0	4	-22.8	14.3
8	10	2	-27.6	21.5	-3	19	2	-23.8	-3.2	-3	1	3	171.9	5.0	-3	9	3	-19.4	21.3	-7	17	3	-28.4	-10.0	4	0	4	-26.2	-20.2
-8	10	2	-28.3	18.1	-4	19	2	-21.1	-29.9	-4	1	3	70.1	-70.5	-3	9	3	70.1	-70.5	-7	17	3	-28.4	-10.0	4	0	4	-26.2	-20.2
9	10	2	-17.4	20.1	-4	19	2	-25.1	29.9	-4	1	3	171.9	5.0	-4	9	3	104.7	101.5	0	18	3	41.2	44.1	-6	0	4	67.2	72.5
-9	10	2	-17.8	-1.3	5	19	2	-27.4	14.7	-5	1	3	-22.9	9.1	5	9	3	70.1	69.6	1	18	3	63.8	-59.0	8	0	4	67.1	75.2
0	11	2	29.6	-17.6	-5	19	2	-28.3	-5.5	-5	1	3	78.7	82.5	-5	9	3	-22.5	53.1	-1	18	3	77.9	-83.8	8	0	4	-27.5	-28.8
-0	11	2	-28.5	30.7	6	19	2	43.9	48.6	-6	1	3	-24.6	-6.1	-6	9	3												

Table VIII (continued)

-3	11	6	67.7	-67.4	-1	23	6	-29.4	-15.5	-3	9	7	-25.9	22.4	0	23	7	-29.5	19.5	-7	11	8	-31.2	22.9	0	7	6	-26.8	-20.8
4	11	6	-29.6	-20.4	-2	23	6	-29.1	-18.0	-4	9	4	-26.7	-13.8	-1	23	7	-30.6	-17.7	0	12	8	-28.6	0.9	1	7	7	-28.6	6.2
-4	11	6	-27.5	31.4	-2	23	6	-26.8	14.9	-4	9	7	-26.4	33.6	-2	23	7	-31.0	-6.0	1	12	8	-31.7	59.4	-1	7	7	-28.6	-11.6
5	11	6	-27.8	10.5	-3	23	6	-29.9	-18.5	-5	9	7	-31.3	12.4	-3	23	7	-31.1	-44.7	-1	12	8	-28.1	16.8	2	7	7	-29.4	-16.2
-5	11	6	-26.5	-28.2	-4	23	6	-30.7	-31.9	-5	9	7	-46.6	51.4	0	0	8	-25.8	-20.7	2	12	8	-28.0	-24.3	-2	7	7	-28.5	-2.6
6	11	6	-27.1	-2.6	-5	23	6	-31.4	10.7	-6	9	7	-28.1	37.6	2	2	8	-29.1	3.4	-2	12	8	-28.1	37.6	-2	7	7	-28.5	35.4
-6	11	6	-27.7	-44.2	0	24	6	-28.0	20.0	-7	9	7	-28.9	-18.4	-2	0	8	-29.3	-71.2	3	12	8	-29.8	-4.4	-3	7	7	-28.8	33.4
7	11	6	-29.0	24.7	-1	24	6	-26.6	74.1	-8	9	7	-30.3	-4.7	4	0	8	-29.3	44.1	-3	12	8	-28.1	5.7	-4	7	7	-29.2	10.1
-8	11	6	-29.8	-12.5	-1	24	6	-31.1	52.2	0	10	7	-24.4	-18.0	-2	0	8	-29.7	29.7	4	12	8	-29.3	44.1	-5	7	7	-29.2	35.0
0	12	6	-23.4	-13.4	2	24	6	-30.3	-13.9	-1	10	7	-25.2	20.0	-8	0	8	-29.8	-45.2	-5	12	9	-29.5	-6.7	-6	7	7	-30.0	10.0
1	12	6	-24.1	-45.1	-7	24	6	-30.3	-14.4	-1	10	7	-25.6	29.0	-8	0	8	-29.6	-109.8	-6	12	9	-29.4	-3.2	0	8	7	-27.4	24.2
-1	12	6	-24.7	-36.1	-3	24	6	-30.4	10.0	2	10	7	-26.7	-18.7	0	1	8	-24.5	5.5	0	13	8	-26.9	4.6	1	8	7	-28.1	-14.4
2	12	6	-25.0	38.2	-4	24	6	-31.7	18.0	-2	10	7	-26.4	59.0	1	1	8	-26.0	12.8	1	13	8	-27.1	-24.4	-1	7	7	-28.6	14.1
-2	12	6	-24.8	40.6	0	25	6	-29.7	-5.1	3	10	7	-27.4	-24.6	-1	1	8	-29.5	-94.1	-1	13	8	-28.4	-14.5	2	8	7	-28.8	3.6
3	12	6	-26.6	28.5	1	25	6	-29.3	7.4	-3	10	7	-25.9	40.4	2	1	8	-26.8	-8.9	2	13	8	-28.4	-24.3	-2	8	7	-28.7	-39.5
-3	12	6	-25.1	-45.2	-1	25	6	-30.5	9.2	4	10	7	-27.9	14.4	-2	1	8	-25.4	54.6	-2	13	8	-28.1	90.4	-3	8	7	-29.1	17.6
4	12	6	-26.5	11.7	-2	25	6	-30.4	-19.4	-4	10	7	-26.8	3.5	3	1	8	-27.8	-29.5	3	13	8	-28.1	90.4	-4	9	7	-29.6	15.4
-4	12	6	-26.0	-36.1	-1	25	6	-31.3	-26.2	5	10	7	-31.5	47.5	-3	1	8	-26.4	16.6	-3	13	8	-28.6	-8.3	-5	8	7	-30.2	-26.2
5	12	6	-28.0	-29.3	-1	26	6	-31.0	-29.4	-5	10	7	-27.5	24.6	4	1	8	-26.4	-83.6	-4	13	8	-28.3	-9.7	-6	8	7	-30.2	74.3
-5	12	6	-29.8	11.7	-2	26	6	-31.4	5.2	-6	10	7	-28.6	23.4	-4	1	8	-26.4	16.6	-4	13	8	-28.3	-9.7	-7	9	7	-29.6	-17.3
6	12	6	-32.0	24.3	1	0	7	-27.4	42.7	-7	10	7	-29.1	-26.8	-5	1	8	-27.7	25.4	-6	13	8	-29.6	18.7	1	9	7	-29.4	16.4
-6	12	6	-34.2	-37.6	-1	0	7	-28.3	-103.3	-8	10	7	-25.3	-73.8	-6	1	8	-27.2	-26.5	0	14	8	-27.2	2.0	-1	9	7	-29.4	-2.1
7	12	6	-35.6	-61.7	3	0	7	-27.9	-126.1	0	11	7	-24.6	4.4	-7	1	8	-24.6	40.4	1	14	8	-27.6	14.8	2	9	7	-27.4	-31.5
-8	12	6	-30.3	-43.7	0	0	7	-29.2	-95.2	-1	11	7	-26.0	-18.1	-6	1	8	-26.8	12.2	-4	14	8	-28.0	14.8	-3	9	7	-29.1	-25.4
0	13	6	82.4	-85.0	-5	0	7	-32.2	-143.0	-1	11	7	-26.0	26.4	0	2	8	-24.5	-26.8	2	14	8	-27.6	-25.8	-1	0	7	-29.3	-14.5
1	13	6	64.2	61.9	-7	0	7	-30.2	-54.2	2	11	7	-25.8	47.1	1	2	8	-27.7	45.7	-2	14	8	-26.5	-10.0	-4	9	7	-29.5	74.1
-1	13	6	-25.1	-2.6	0	1	7	-22.7	10.7	-2	11	7	-26.1	-21.5	-1	2	8	-26.2	11.3	1	14	8	-30.4	-29.0	-5	9	7	-29.2	71.4
2	13	6	-31.4	-31.6	-1	1	7	-27.8	3.1	-3	11	7	-27.7	-29.8	-1	2	8	-26.5	-49.1	-2	14	8	-29.4	-49.1	-6	0	7	-29.6	-21.7
-2	13	6	-25.0	-35.4	-1	1	7	-23.7	-8.1	-3	11	7	-28.1	71.0	-2	2	8	-26.4	-57.0	-4	14	8	-28.6	70.7	0	10	7	-27.3	22.5
3	13	6	55.0	64.4	2	1	7	-25.0	-23.2	4	11	7	-28.1	-7.7	3	2	8	-26.7	83.7	-5	14	8	-30.1	3.6	1	10	7	-26.7	17.8
-3	13	6	-28.1	-103.9	-2	1	7	-26.4	100.1	-4	11	7	-27.1	-23.8	-3	2	8	-26.5	-89.9	-6	15	8	-30.9	30.6	-1	10	7	-29.4	-27.7
4	13	6	-27.8	-10.1	3	1	7	-26.0	17.1	-5	11	7	-27.8	-19.4	-4	2	8	-26.5	-89.9	-6	15	8	-30.9	32.4	7	10	7	-30.2	21.6
-4	13	6	-26.1	44.3	-3	1	7	-27.4	69.4	-5	11	7	-27.8	4.4	-4	2	8	-26.1	-44.4	1	15	8	-27.4	-2.4	-2	10	7	-29.3	1.8
5	13	6	48.6	-56.7	1	1	7	-27.2	-38.3	-6	11	7	-27.1	66.9	-5	2	8	-27.8	-39.4	-1	15	8	-29.1	-2.0	-1	10	7	-29.4	18.5
-5	13	6	-29.5	18.2	-4	1	7	-28.4	15.2	-7	11	7	-26.8	13.5	-6	2	8	-29.8	15.1	-2	15	8	-29.8	45.4	-5	10	7	-30.7	-7.4
6	13	6	-28.3	2.1	5	1	7	-29.6	-16.0	-8	11	7	-30.7	19.8	-7	2	8	-29.4	-39.1	-2	15	8	-30.7	45.4	-5	10	7	-30.7	-7.4
-6	13	6	-28.3	2.1	5	1	7	-29.6	-16.0	-8	11	7	-30.7	19.8	-7	2	8	-29.4	-39.1	-2	15	8	-30.7	45.4	-5	10	7	-30.7	-7.4
7	13	6	78.8	83.3	-5	1	7	-26.2	4.3	0	12	7	-24.9	-42.3	-8	2	8	-31.3	12.1	3	15	8	-30.7	-33.5	-6	10	7	-31.1	-29.9
-7	13	6	-31.0	5.2	6	1	7	-30.5	-9.0	1	12	7	-25.7	30.5	0	3	8	-24.6	-15.8	-3	15	8	-28.6	81.7	0	10	7	-28.0	8.4
8	13	6	-29.1	38.5	-2	1	7	-30.1	12.2	2	12	7	-25.7	30.5	0	3	8	-24.6	-15.8	-3	15	8	-28.6	81.7	0	10	7	-28.0	8.4
-8	13	6	-24.5	13.2	-7	1	7	-28.4	31.8	2	12	7	-26.5	30.9	-1	3	8	-26.4	-1.8	-5	15	8	-30.5	3.4	-1	11	7	-29.6	14.8
1	14	6	-25.5	2.3	-8	1	7	-29.8	-73.5	-2	12	7	-26.4	5.2	2	3	8	-25.7	-56.1	-6	15	8	-31.3	-23.3	2	11	7	-29.6	14.8
-1	14	6	-22.2	103.5	-7	1	7	-29.2	-7.7	-3	12	7	-27.1	63.0	-1	3	8	-25.7	26.1	-1	15	8	-27.8	26.5	-2	12	7	-29.6	14.8
2	14	6	103.8	-100.9	-1	2	7	-29.7	-40.3	-3	12	7	-26.5	24.0	3	3	8	-27.9	9.3	1	16	8	-28.2	-1.2	-3	11	7	-29.5	14.4
-2	14	6	55.7	59.6	-1	2	7	-24.3	-18.0	4	12	7	-28.4	-1.4	-3	3	8	-24.3	-40.9	-1	16	8	-29.4	2.2	-4	11	7	-29.2	-49.4
3	14	6	-26.0	5.5	2	2	7	-28.4	48.3	-4	12	7	-27.4	-21.7	4	3	8	-29.0	6.4	2	16	8	-29.1	-34.1	-1	11	7	-29.6	-58.1
-3	14	6	-26.0	5.5	2	2	7	-28.4	48.3	-4	12	7	-27.4	-21.7	4	3	8	-29.0	6.4	2	16	8	-29.1	-34.1	-1	11	7	-29.6	-58.1
4	14	6	-26.5	-41.3	3	2	7	-28.2	-68.7	-5	12	7	-28.1	12.6	-5	3	8	-27.8	-33.6	-3	16	8	-29.7	19.0	0	12	7	-29.1	-1.0
-4	14	6	-28.7	13.2	-3	2	7	-24.7	-9.3	-6	12	7	-29.1	5.8	-6	3	8	-28.8	-9.2	-4	16	8	-29.6	-66.4	-1	12	7	-29.8	-54.5
5	14	6	-28.1	12.1	-4	2	7	-28.1	12.6	-7	12	7	-29.1	5.8	-6	3	8	-28.8	-9.2	-4	16	8	-29.6	-66.4	-1	12	7	-29.8	-54.5
-5	14	6	-28.6	-10.4	-4	2	7	-24.1	-49.4	0	13	7	-25.1	-28.1	-1	3	8	-31.1	18.6	0	17	8	-28.2	-24.4	-2	12	7	-29.8	-42.5
6	14	6	-29.9	-19.2	-5	2	7	-22.3	-44.9	1	13	7	-25.7	-0.5	0	4	8	-24.7	11.3	1	17	8	-28.5	-2.2	-3	12	7	-29.8	-47.3
-6	14	6	-31.3	-10.4	-5	2	7	-26.1	-50.4	-1	13	7	-23.2	76.7	1	4	8	-26.7	32.4	-1	17	8	-29.8	8.0	-4	12	7	-30.4	-7.8
7	14	6	-29.1	19.2	-6	2	7	-26.3	-34.6	-2	13	7	-26.8	61.3	-1	4	8	-26.7	32.4	-1	17	8	-29.8	8.0	-4	12	7	-30.4	-7.8
-7	14	6	-24.9	40.1	-6	2	7	-27.4	-49.7	-2	13	7	-26.0	25.2	2	4	8	-26.4	-9.5	-2	17	8	-29.6	-2.2	0	13			

Table IX. Final fractional positional and thermal parameters.

	x	y	z	mean σ	$B(\text{\AA}^2)$	$\sigma(B)$
Co	0.4613	0.1178	0.2881	0.0054		
C1(1)	0.3034	0.1298	0.1126	0.0101		
C1(2)	0.5639	0.1762	0.3666	0.0111		
C1(3)	0.6009	0.0733	0.2321	0.0117		
C1(4)	0.3590	0.0927	0.4368	0.0108		
P(1)	0.0780	0.3327	0.3794	0.0098		
P(2)	0.2942	0.2883	0.5231	0.0097		
P(3)	0.1348	0.2186	0.4595	0.0099		
P(4)	-0.0907	0.2677	0.4571	0.0099		
P(5)	0.2628	-0.0149	0.2350	0.0096		
P(6)	0.1131	-0.0823	0.3057	0.0102		
P(7)	-0.1147	-0.0318	0.2865	0.0097		
P(8)	0.0201	0.0379	0.2146	0.0096		
N(1)	-0.0329	0.3157	0.4597	0.027		
N(2)	0.2110	0.3126	0.4032	0.028		
N(3)	0.2327	0.2462	0.5494	0.028		
N(4)	-0.0020	0.2384	0.3992	0.028		
N(5)	0.1807	0.0247	0.2748	0.025		
N(6)	0.1903	-0.0552	0.2209	0.026		
N(7)	0.0007	-0.0618	0.3572	0.025		
N(8)	-0.0764	0.0010	0.1942	0.025		
C(1)	-0.0002	0.3268	0.2173	0.044	5.25	1.06
C(2)	0.0857	0.3842	0.4144	0.042	4.52	0.96
C(3)	0.3138	0.3213	0.6606	0.049	4.03	0.90
C(4)	0.4552	0.2813	0.4930	0.042	4.58	1.01
C(5)	0.2016	0.2036	0.3291	0.042	4.66	1.03
C(6)	0.1191	0.1718	0.5369	0.044	5.16	1.04
C(7)	-0.1005	0.2582	0.6085	0.038	3.60	0.89
C(8)	-0.2482	0.2703	0.3654	0.040	4.43	0.94
C(9)	0.3150	-0.0032	0.0955	0.038	3.69	0.88
C(10)	0.4135	-0.0143	0.3524	0.042	4.70	0.97
C(11)	0.2275	-0.1031	0.4407	0.035	3.04	0.81
C(12)	0.0526	-0.1248	0.2112	0.044	5.01	1.03
C(13)	-0.2479	-0.0606	0.1966	0.048	3.76	0.88
C(14)	-0.1847	-0.0092	0.4051	0.051	2.89	0.79
C(15)	-0.0041	0.0759	0.3215	0.036	2.98	0.82
C(16)	0.0051	0.0615	0.0686	0.039	3.89	0.93

..../continued

Table IX (continued). Anisotropic thermal parameters (\underline{U}_{ij} in $\text{\AA}^2 \times 10^2$).

	\underline{U}_{11}	\underline{U}_{12}	\underline{U}_{13}	\underline{U}_{22}	\underline{U}_{23}	\underline{U}_{33}	mean $\sigma(\underline{U})$
Co	3.69	-0.39	1.24	3.06	0.44	5.11	0.28
C1(1)	3.68	-0.14	0.81	4.53	0.10	5.04	0.57
C1(2)	5.13	-0.54	1.35	4.04	1.00	7.83	0.61
C1(3)	6.17	3.15	1.84	5.52	0.65	8.21	0.68
C1(4)	5.83	-0.94	1.69	4.37	0.53	5.49	0.60
P(1)	1.87	0.17	1.49	3.17	0.72	5.12	0.54
P(2)	2.56	-0.01	1.16	3.17	0.90	4.00	0.52
P(3)	2.99	0.14	1.52	2.46	0.74	4.55	0.53
P(4)	2.91	-1.06	1.56	3.77	-1.37	3.44	0.54
P(5)	2.46	0.00	0.45	3.61	0.19	2.44	0.52
P(6)	3.76	-0.19	1.84	2.79	0.12	3.85	0.54
P(7)	3.63	-0.86	0.68	3.28	0.33	2.05	0.52
P(8)	2.45	0.21	0.83	3.00	0.30	3.05	0.51
N(1)	2.78	-1.69	1.25	1.09	1.70	6.01	1.61
N(2)	4.29	0.91	1.00	2.84	-0.03	3.21	1.63
N(3)	2.99	-1.61	-0.38	3.06	1.35	3.87	1.65
N(4)	3.28	0.06	1.43	1.91	-0.95	5.31	1.62
N(5)	1.63	1.70	1.73	1.86	0.94	4.03	1.40
N(6)	2.96	0.47	0.68	3.11	-0.41	1.32	1.48
N(7)	0.99	0.68	-0.49	1.04	-0.24	2.84	1.40
N(8)	3.31	0.54	0.93	2.79	0.91	1.23	1.45

Table X. Hydrogen atom positions located on difference map.

	x	y	z	$B(\text{Å}^2)$
H(1-1)	-0.061	0.317	0.167	4.0
H(1-2)	0.086	0.302	0.217	
H(1-3)	0.000	0.353	0.200	
H(2-1)	0.086	0.384	0.483	
H(2-2)	0.000	0.399	0.400	
H(2-3)	0.077	0.384	0.317	
H(3-1)	0.374	0.308	0.733	
H(3-2)	0.335	0.298	0.617	
H(3-3)	not located			
H(4-1)	0.431	0.253	0.450	
H(4-2)	0.374	0.298	0.500	
H(4-3)	0.489	0.268	0.583	
H(5-1)	0.134	0.183	0.283	
H(5-2)	0.172	0.201	0.400	
H(5-3)	0.297	0.207	0.333	
H(6-1)	0.182	0.149	0.550	
H(6-2)	0.201	0.198	0.550	
H(6-3)	0.058	0.164	0.604	
H(7-1)	-0.134	0.225	0.600	
H(7-2)	-0.201	0.274	0.600	
H(7-3)	-0.067	0.250	0.700	
H(8-1)	-0.262	0.247	0.392	
H(8-2)	-0.214	0.283	0.292	
H(8-3)	-0.339	0.295	0.367	
H(9-1)	0.364	0.030	0.100	
H(9-2)	0.240	0.000	0.050	
H(9-3)	0.402	-0.015	0.075	
H(10-1)	0.402	-0.030	0.417	
H(10-2)	0.460	0.015	0.350	
H(10-3)	0.364	0.015	0.383	
H(11-1)	0.230	-0.131	0.375	
H(11-2)	0.192	-0.116	0.500	
H(11-3)	not located			
H(12-1)	0.000	-0.116	0.142	
H(12-2)	0.125	-0.134	0.233	
H(12-3)	0.019	-0.146	0.283	
H(13-1)	-0.192	-0.070	0.150	
H(13-2)	-0.316	-0.040	0.183	
H(13-3)	not located			
H(14-1)	-0.240	-0.030	0.383	
H(14-2)	-0.125	0.003	0.450	
H(14-3)	-0.240	0.009	0.350	
H(15-1)	-0.096	0.082	0.333	
H(15-2)	0.096	0.085	0.325	
H(15-3)	0.038	0.046	0.317	
H(16-1)	0.067	0.082	0.092	
H(16-2)	-0.058	0.067	0.133	
H(16-3)	not located			

Discussion

The structure of $[\text{NPMe}_2]_4\text{H}\cdot\text{CuCl}_3$ showed that a phosphonitrilic ring could be associated with a transition metal atom by means of a covalent bond between the metal and a nitrogen atom of the ring. In $[(\text{NPMe}_2)_4\text{H}^+]_2\text{CoCl}_4^{2-}$ by contrast, the association is an ionic one with the CoCl_4^{2-} ion hydrogen-bonded to two protonated phosphonitrilic rings. In both compounds the addition of a proton to a ring nitrogen atom destroys the equality of the P-N bond lengths and causes them to deviate from the ideal values found in the symmetric parent compound, $[\text{NPMe}_2]_4$.⁴⁰

The phosphonitrilic rings in $[\text{NPMe}_2]_4$ and $[\text{NPMe}_2]_4\text{H}\cdot\text{CuCl}_3$ approximate the "tub" conformation. It is interesting, therefore, to note that in $[(\text{NPMe}_2)_4\text{H}^+]_2\text{CoCl}_4^{2-}$ one of the rings approaches the "saddle" shape. The two conformations can be distinguished on the basis of the deviation of the phosphorus and nitrogen atoms from the best plane through the ring atoms as well as from the dihedral angles between successive NPN/PNP planes. In the "tub" form, as has been noted previously, the ring atoms occur in pairs alternately above and below the ring. The dihedral angles in this conformation would then vary around the ring as the atoms alternatively have their z-axes approximately aligned (when the atoms are on the same level) or mismatched (when they are not). In the idealized "saddle" conformation on the other hand, the phosphorus atoms are planar with successive nitrogen atoms deviating in opposite directions from the plane. This

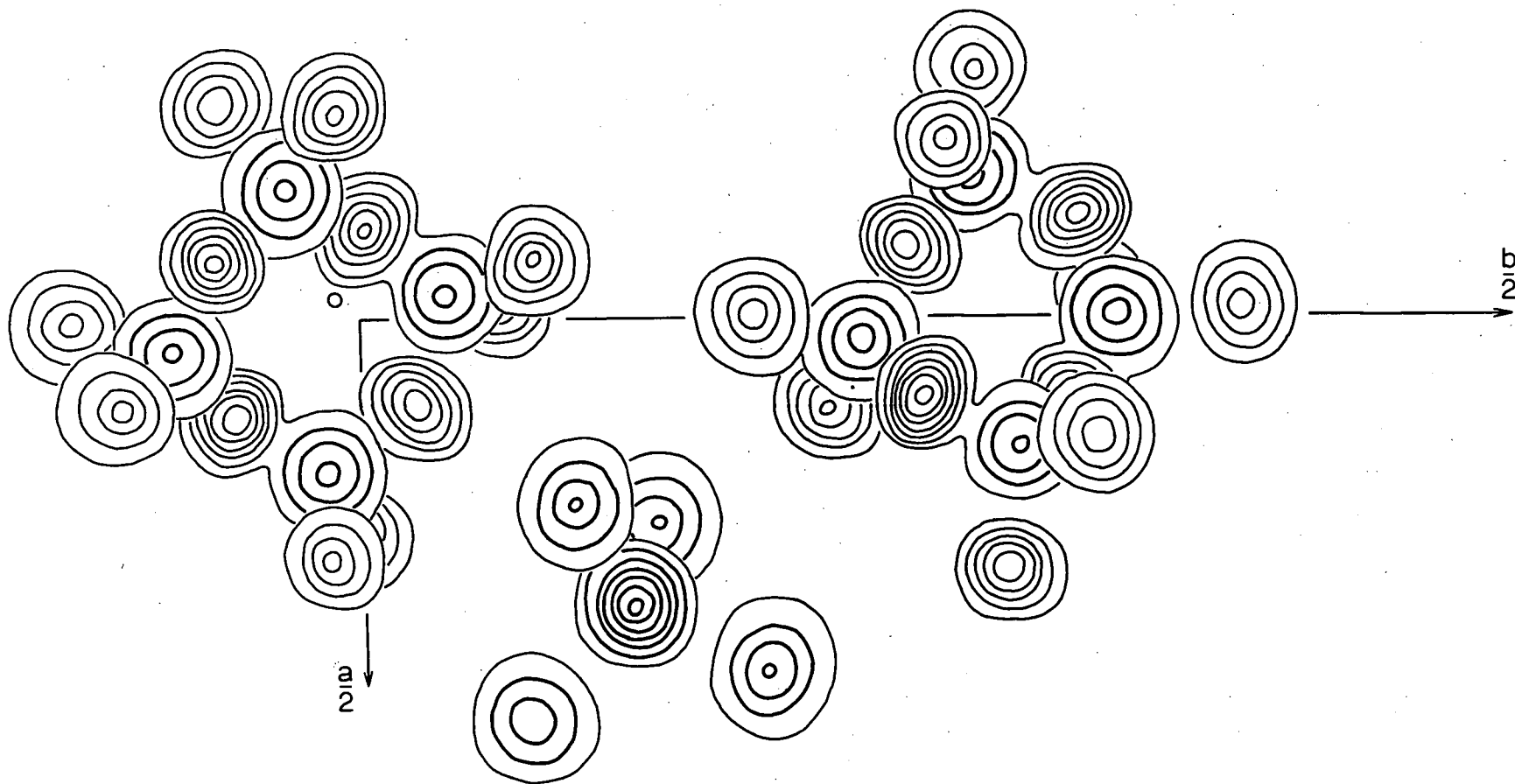


Figure 5. Superimposed sections of the final three-dimensional electron density distribution. Contours are drawn at 1,2,3 ... e.Å⁻³ for the nitrogen and carbon atoms, and at 1,5,10 ... e.Å⁻³ for the copper, chlorine and phosphorus atoms.

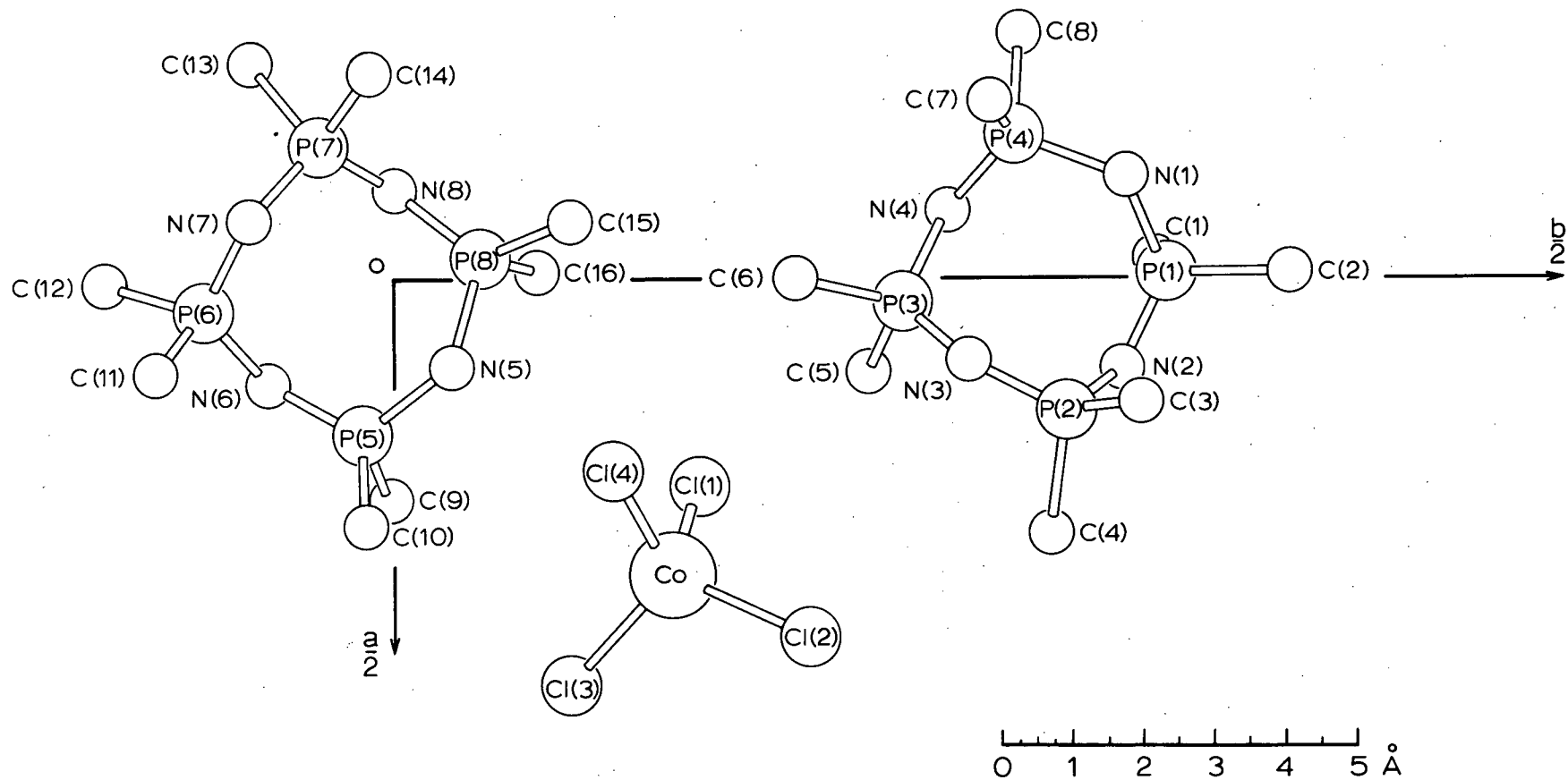


Figure 6. A drawing of the molecule viewed along the c^* -axis.

arrangement requires the dihedral angles to be approximately equal around the ring. Ring I (P(1)-P(4)) is similar to the unperturbed parent compound and has adjacent P-N segments alternately up and down. In common with most phosphonitrilic structures (a recent exception being $[\text{NP}(\text{NMe})_2]_6$ ⁵⁹) the nitrogen atoms are displaced more from the ring plane (0.59 Å) than are the phosphorus atoms (0.40 Å). The dihedral angles between successive PNP/NPN planes are 59.7°, 25.0°, 68.1°, 21.5°, 60.0°, 38.9°, 80.1° and 15.0° beginning from the protonated nitrogen atom and progressing clockwise around the ring. In ring II (P(5)-P(8)), however, the phosphorus atoms are very nearly planar with the mean deviation from the plane being only 0.02 Å. The nitrogen atoms are displaced alternately above and below the plane an average distance of 0.61 Å. In this ring the dihedral angles are more regular. Around the ring they are 39.0°, 63.1°, 60.2°, 42.6°, 45.1°, 52.5°, 54.2° and 43.1°. On the basis of the atomic displacements and the trends in the dihedral angles, ring II tends more toward the "saddle" shape although it lacks the symmetry required to equalize the π -interactions. It would seem from this analysis that the distinction between the two conformations can not be very great, for there is no indication of an overall preference towards a shape which favours predominantly π_a or π_s -bonding within the compound.

In the crystal structures of $\text{N}_3\text{P}_3\text{Cl}_2(\text{NHPr}^i)_4$, HCl^{35} and $[\text{NPMe}_2]_4\text{H}\cdot\text{CuCl}_3$ the protonation of the phosphonitrilic ring was shown to have a marked effect on the ring bond lengths and angles. The phosphonitrilic rings in both these compounds had other perturbing

features: in the first, the ring bond lengths were probably influenced by the different substituents on the ring, and in second, the bond to copper would disrupt the π -electron system. $[(\text{NPMe}_2)_4\text{H}^+]_2\text{CoCl}_4^{2-}$ would appear to be a good structure in which to see the effect of disturbing the ring bonding systems only by the addition of a single proton.

Although the present analysis is not as accurate as the other two, (the standard deviation of the P-N bonds being about 0.03 Å) some conclusions can be based upon the intramolecular bond lengths and angles listed in Table XI.

The phosphorus-nitrogen bond lengths vary considerably within the rings and it is surprising that corresponding bonds having the same relationship to the protonated nitrogen are not more nearly equal. Rather than considering individual bond lengths in detail, it would seem more appropriate to examine averaged values for these are more regular in the two phosphonitrilic rings. In each ring the pattern is the same: moving from the protonated nitrogen, the longest P-N bond is followed by the shortest, then a longer one is followed by a shorter. The mean values averaged over four chemically equivalent bonds are 1.695 Å, 1.538 Å, 1.614 Å, and 1.582 Å, ($\sigma = 0.02$ Å). This is the same sort of order found in $[\text{NPMe}_2]_4\text{H}\cdot\text{CuCl}_3$ except that there the final pair of bond lengths is longer because of the attached copper atom. A pattern of this nature cannot arise from inductive effects, and would appear instead to be a phenomenon associated with the interactions of the π -electron system.⁶⁰

Table XI. Bond lengths (\AA) and valency angles ($^\circ$).P-N bond lengths ($\sigma = 0.03 \text{ \AA}$)

Ring I				Average		
N(1)-P(1)	=	1.702	N(1)-P(4)	=	1.686	1.694
P(1)-N(2)	=	1.509	P(4)-N(4)	=	1.565	1.537
N(2)-P(2)	=	1.641	N(4)-P(3)	=	1.583	1.612
P(2)-N(3)	=	1.576	P(3)-N(3)	=	1.561	1.568

Ring II

N(5)-P(5)	=	1.668	N(5)-P(8)	=	1.723	1.696
P(5)-N(6)	=	1.516	P(8)-N(8)	=	1.559	1.538
N(6)-P(6)	=	1.632	N(8)-P(7)	=	1.600	1.616
P(6)-N(7)	=	1.565	P(7)-N(7)	=	1.624	1.594

P-C bond lengths ($\sigma = 0.04 \text{ \AA}$)

P(1)-C(1)	=	1.831	P(1)-C(2)	=	1.733
P(2)-C(3)	=	1.855	P(2)-C(4)	=	1.797
P(3)-C(5)	=	1.813	P(3)-C(6)	=	1.789
P(4)-C(7)	=	1.745	P(4)-C(8)	=	1.745
P(5)-C(9)	=	1.799	P(5)-C(10)	=	1.820
P(6)-C(11)	=	1.845	P(6)-C(12)	=	1.782
P(7)-C(13)	=	1.801	P(7)-C(14)	=	1.804
P(8)-C(15)	=	1.782	P(8)-C(16)	=	1.783
mean P-C	=	1.795			

Co-Cl bond lengths ($\sigma = 0.02 \text{ \AA}$)

Co-Cl(1)	=	2.311
Co-Cl(2)	=	2.280
Co-Cl(3)	=	2.246
Co-Cl(4)	=	2.308
mean Co-Cl	=	2.286

..../continued

Table XI (continued)

Angles at nitrogen ($\sigma = 1.8^\circ$)

	P-N-P		P-N-P	Average
N(1)	125.3	N(5)	127.1	126.2
N(2)	131.6	N(6)	135.5)	132.2
N(4)	129.4	N(8)	132.1)	128.5
N(3)	128.7	N(7)	128.2	

Angles at phosphorus

	N-P-N ($\sigma = 1.5^\circ$)	C-P-C ($\sigma = 2.0^\circ$)
P(1)	117.8	108.4
P(2)	114.4	106.7
P(3)	116.3	104.2
P(4)	109.9	109.6
P(5)	115.8	104.3
P(6)	118.7	106.3
P(7)	117.4	104.0
P(8)	114.0	108.1
mean	115.5	106.4

Angles at cobalt ($\sigma = 0.5^\circ$)

C1(1)-Co-C1(2)	=	112.0	C1(2)-Co-C1(3)	=	112.1
C1(1)-Co-C1(3)	=	105.2	C1(2)-Co-C1(4)	=	105.9
C1(1)-Co-C1(4)	=	108.4	C1(3)-Co-C1(4)	=	113.3

As was the case in $[\text{NPMe}_2]_4\text{H.CuCl}_3$, the longest P-N bonds are those involving the protonated nitrogen atoms. The mean value of 1.695 Å again suggests only weak π -overlap. With the nitrogen lone pair electrons required for bonding the hydrogen atom, only the π_a -system can be operative. The bond length is again similar to those found in the metaphosphimate compounds^{47,48} where the bonding system is analogous. It is significant also that the smallest P-N-P angle in each ring occurs at the protonated site suggesting weaker inter-bond repulsions and hence less electron density in these links than in any of the other P-N bonds.

The parameters which are unaffected by the perturbation are very similar to those in $[\text{NPMe}_2]_4\text{H.CuCl}_3$ when averaged values are considered. The angles at phosphorus, N-P-N = 115.5° and C-P-C = 106.4° are close to the values of 114.0 and 106.6° found in the copper compound. Also, although the phosphorus-carbon bond lengths vary somewhat, the mean value 1.795 Å is in good accord with the 1.782 Å in $[\text{NPMe}_2]_4\text{H.CuCl}_3$ and the 1.805 Å value for the P-C bond length in $[\text{NPMe}_2]_4$.⁴⁰

The phosphonitrilic rings are linked by hydrogen bonding to the tetrahedral CoCl_4^{2-} ion in much the same way as different molecules of $[\text{NPMe}_2]_4\text{H.CuCl}_3$ were connected. The distance between Cl(1) of the standard unit and the protonated N(1) atom of ring I at position $x + 1/2, 1/2 - y, z - 1/2$ is 3.21 Å; similarly, the separation between Cl(4) and N(5) of ring II is also 3.21 Å. These distances correspond

to the average $\text{N}^+-\text{H}\dots\text{Cl}^-$ separation usually reported.⁶¹ The distance can be compared with the sum of the van der Waals radii for nitrogen and chlorine of 3.3 Å. The angles around these nitrogen atoms also support the hydrogen bond assignment. In the first instance the P(1)N(1)...Cl(1) angle is 126.6° and the P(4)N(1)...Cl(1) angle is 107.6°. In the second case the P(5)N(5)...Cl(4) angle is 115.1°, the P(8)N(5)...Cl(4) angle, 116.4°. The hydrogen bonding is shown in Figure 7 where the packing in the unit cell is drawn viewed down the c-axis.

Apart from these hydrogen-bonded distances the shortest intermolecular contacts occur between the nitrogen and carbon atoms. The shortest of these is a distance of 3.44 Å between N(6) and C(16) at $-x, -y, -z$. There are two other contacts less than 3.6 Å: that between N(4) and C(3) at $x - 1/2, 1/2 - y, z - 1/2$ of 3.53 Å; and that between N(3) and C(8) at $x + 1/2, 1/2 - y, z + 1/2$ of 3.54 Å. In addition there is an approach of 3.53 Å between C(10) and the centrosymmetrically related atom translated a unit cell in the x and z directions. As was mentioned in the discussion of $[\text{NPMe}_2]_4\text{H.CuCl}_3$, none of these distances are unreasonably small.

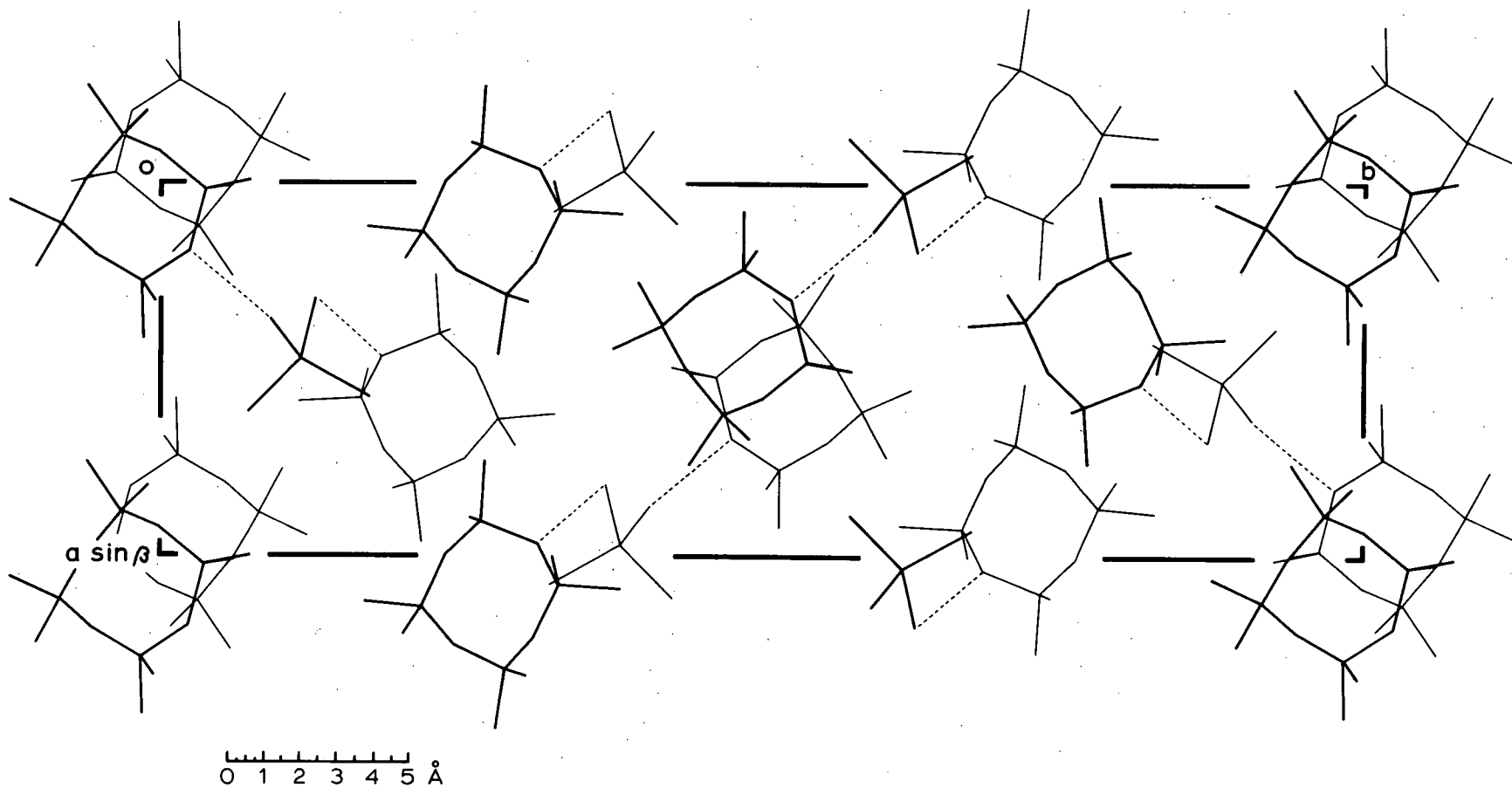


Figure 7. Packing of the unit cell viewed along the c -axis showing hydrogen-bonding.

PART II

THE STRUCTURE DETERMINATION OF

HEXADECAMETHOXYCYCLO-OCTAPHOSPHONITRILE

A. INTRODUCTION

In the Introduction to Part I, the crystal structure determinations of six- and eight-member phosphonitriles were reviewed. The major structural features were mentioned, and in some cases explanations for these were attempted in terms of the bonding theory described. While many of the same principles hold for larger rings, there are also differences which should be examined. Before discussing the present analysis of a sixteen-member ring it would be wise to complete the survey of structural information available for the phosphonitriles by reviewing the X-ray work which has been published on compounds greater than the tetramer in size. In this way, features which are peculiar to the larger rings may be anticipated and looked for in the structure of $[\text{NP}(\text{OMe})_2]_8$.

Very few X-ray studies have been carried out on the larger phosphonitriles, the conformations of the trimers and tetramers having received the most attention. The two structures which have been reported are summarized in Table XII. With the larger rings, planar

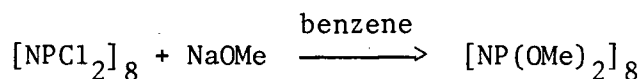
Table XII. X-ray structure determinations of the larger phosphonitriles.

Compound	P-N(\AA)	Angle PNP($^\circ$)	Angle NPN($^\circ$)	Ring Shape	Reference
$[\text{NPCl}_2]_5$	1.49 to 1.55(.015)	148.6	118.4	nearly planar, re-entrant nitrogen atoms	62
$[\text{NP}(\text{NMe}_2)_2]_6$	1.56(.01) 1.67(exo.)	147.5	120.0	puckered, 3, (tub)	59

shapes with equal angles are not readily attainable because the angles at phosphorus and nitrogen would have to become unreasonably large. This obstacle is overcome in the pentameric chloride by means of re-entrant nitrogen atoms and the molecule is able to remain nearly planar. As a consequence of this, the average angle at nitrogen (148°) is rather large. Although the range in individual bond lengths is considerable, the average P-N bond length (1.52 \AA) is shorter than in the corresponding trimeric and tetrameric chlorides suggesting that a planar shape and large P-N-P angles permit maximum π -interactions. In addition, Molecular Orbital theory predicts that π -electron energies per electron increase slightly with increasing ring size.²¹ Thus if the ligands on phosphorus are the same, larger rings are likely to be more strongly bound. This tendency is also found to a smaller extent in the hexameric dimethylamide. The twelve-member ring has a puckered conformation with pairs of adjacent phosphorus and nitrogen atoms alternately up and down. This is reminiscent of the "tub" conformation found in the tetrameric series and it would seem that in this case also the steric requirements of the exocyclic groups are the major factor in determining the shape. In common with its tetrameric analogue, some secondary bonding occurs between the ring and the exocyclic nitrogen atoms.

The structure of $[\text{NP}(\text{OMe})_2]_8$ was undertaken to extend the information available about cyclic phosphonitriles to larger rings. The sixteen-member ring is the largest phosphonitrile to have been analyzed by X-ray diffraction to the present time. The octameric

methoxy compound is prepared by replacement of the chlorine atoms on the corresponding chloride.⁶³



The geometrical shapes which a phosphonitric ring might assume increase rapidly with increasing ring size. In the present octameric compound the steric interactions of exocyclic groups might well have less influence upon the resulting conformation than in the smaller rings since the diameter of the ring will probably be large. The actual shape which is found may be determined primarily by π -bonding preferences and thus the structural principles observed in the tetramers might apply again. Also, the geometric freedom of the large ring may permit regions of local planarity which would aid π -overlap. It might be hoped that accurate structural information for larger rings will permit the bonding theory for phosphonitriles to be developed still further.

B. THE STRUCTURE OF HEXADECAMETHOXYCYCLO-OCTAPHOSPHONITRILE

Experimental

Crystals of $[\text{NP}(\text{OMe})_2]_8$ from carbon tetrachloride are colourless needles elongated along \underline{a} . Crystallographic data were obtained from various rotation, Weissenberg and precession photographs. The data refer to the primitive reduced cell.⁶⁴

Crystal Data (λ , Cu- \underline{K}_α = 1.5418 Å; λ , Mo- \underline{K}_α = 0.7107 Å) $[\text{NP}(\text{OCH}_3)_2]_8$,
 $\underline{M} = 856.4$

Triclinic, $\underline{a} = 8.40$, $\underline{b} = 11.07$, $\underline{c} = 11.67$ Å (all ± 0.01 Å), $\alpha = 62^\circ 7'$,
 $\beta = 84^\circ 18'$, $\gamma = 76^\circ 14'$ (all $\pm 5'$)

$\underline{U} = 931.6$ Å³, $\underline{D}_m = 1.52$, $\underline{Z} = 1$, $\underline{D}_c = 1.53$ g.cm.⁻³, $\underline{F}(000) = 448$.

Absorption coefficients, $\mu(\text{Cu-}\underline{K}_\alpha) = 41$ cm.⁻¹, $\mu(\text{Mo-}\underline{K}_\alpha) = 4.5$ cm.⁻¹

No systematically absent reflexions. Space group $P1$ or $P\bar{1}$. $P\bar{1}$ from $N(Z)$ plot and structure analysis.

Three-dimensional data were collected on a General Electric XRD-5 Spectrogoniometer with a scintillation counter, Mo- \underline{K}_α radiation (zirconium filter and pulse height analyser), and a θ - 2θ scan. Of the 2368 reflexions with $2\theta \leq 45^\circ$ (corresponding to a minimum interplanar spacing $\underline{d} = 0.92$ Å), 1786 (75%) were observed. After correcting for background, Lorentz and polarization factors were applied, and the structure amplitudes were derived. Reflexions with intensity less than 1.5 times background were classified as unobserved and given $|F_o| = \sqrt{0.4} F(\text{threshold})$. The crystal used for recording the intensities was

mounted with a^* parallel to the ϕ axis of the goniostat and was approximately cylindrical with length 0.60 mm. and diameter 0.20 mm. No absorption corrections were applied.

Structure Analysis

A statistical $N(Z)$ plot suggested that the intensities approximated a centric distribution, and with one molecule per unit cell this implied that the molecule possesses a centre of symmetry. Full details and a listing of the Fortran program written for the $N(Z)$ test are given in the Appendix. The results of the $N(Z)$ test and the Wilson Ratio test are tabulated in Table XIII together with the theoretical values. The actual $N(Z)$ plot is shown in Figure 8. The centric distribution was confirmed by the appearance of the three-dimensional Patterson function which contained a number of strong peaks consistent with a centrosymmetric structure. The positions of the phosphorus atoms were determined from the P-P vectors in the Patterson function. Structure factors were calculated based on these phosphorus positions and the initial R was 0.46. The nitrogen, oxygen and carbon atoms were located from a three-dimensional Fourier synthesis. Structure factors were calculated for all the reflexions with the usual scattering factors, with $B = 4.0 \text{ \AA}^2$, and R was 0.26.

Refinement of the positional and thermal parameters proceeded by block-diagonal least-squares with minimization of $\sum w(F_o - F_c)^2$ with $\sqrt{w} = |F_o|/12$ when $|F_o| < 12$ and $\sqrt{w} = 12/|F_o|$ when $|F_o| \geq 12$. Unobserved reflexions were given $\sqrt{w} = 0.50$. Analysis of the values of $w(F_o - F_c)^2$ at

Table XIII. Results of statistical tests to distinguish between centric and acentric distributions of intensities.

N(Z) Test			
Fraction of local average (Z)	Experimental N(Z)	Theoretical N(Z)	
		centric	acentric
0.1	.2240	.2481	.0952
0.2	.2954	.3453	.1813
0.3	.4002	.4187	.2592
0.4	.4612	.4738	.3297
0.5	.5129	.5205	.3935
0.6	.5519	.5614	.4512
0.7	.5834	.5972	.5034
0.8	.6158	.6289	.5507
0.9	.6426	.6572	.5934
1.0	.6642	.6833	.6321

Ratio Test		
Experimental Ratio	Theoretical Ratio	
	centric	acentric
0.682	0.637	0.785

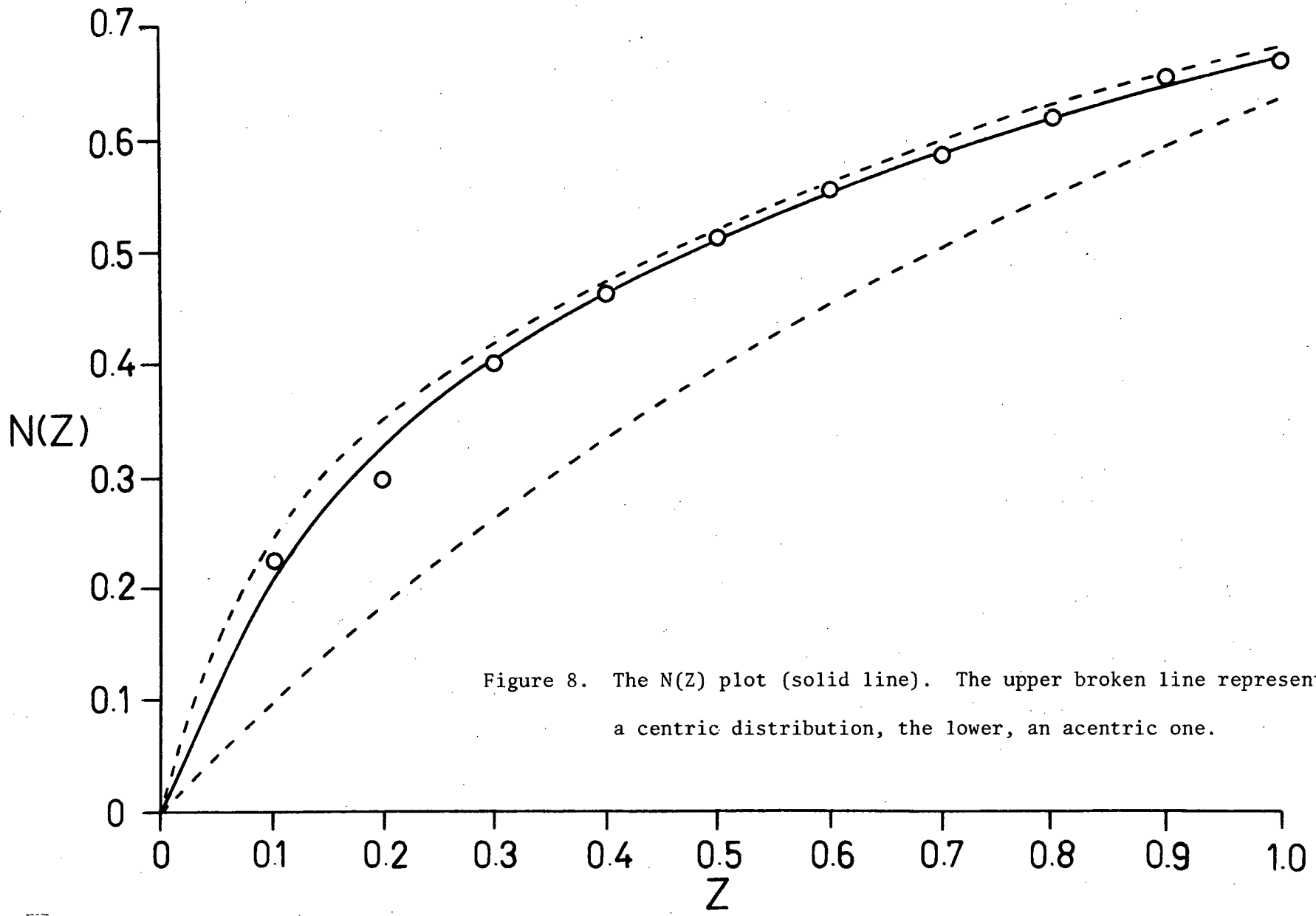


Figure 8. The $N(Z)$ plot (solid line). The upper broken line represents a centric distribution, the lower, an acentric one.

each stage of refinement indicated that this weighting scheme was appropriate. Six least-squares cycles with isotropic thermal parameters reduced R to 0.089. At this stage an $(F_o - F_c)$ synthesis was computed and nineteen of the twenty-four independent hydrogen atoms were located, with peak heights 0.6 - 0.8 $e \cdot \text{\AA}^{-3}$ and C-H bond distances 0.7 - 1.3 \AA . These were included in the structure factor calculations, but the hydrogen positions were not refined. Two further least-squares cycles with anisotropic temperature factors for the ring atoms N and P, and isotropic temperature factors for the O, C and H atoms gave a final R of 0.079. Measured and calculated structure factors are compared in Table XIV. Sections of the final three-dimensional electron-density distribution are shown in Figure 9, and in Figure 10 there is a drawing of the molecule, giving the atom numbering. A final difference synthesis had maximum fluctuations of $\pm 0.5 e \cdot \text{\AA}^{-3}$.

The final positional and thermal parameters and their standard deviations are listed in Table XV. The hydrogen atoms are numbered according to the carbon atoms to which they are bonded; the hydrogen positions are not to be considered accurate. The bond distances and angles are given in Table XVI. Figure 11 shows the molecular packing arrangement viewed along the c -axis. All the shorter intermolecular distances involve contacts between the methoxy groups, which cover the outside of the molecule, and all the separations correspond to van der Waals interactions. The shortest distance is an O...C contact of 3.20 \AA , between O(1) of the standard molecule and C(8) of the molecule at $(x, 1 + y, z)$. The shortest O...O and C...C contacts are 3.70 \AA and 3.67 \AA respectively.

Table XIV. Measured and calculated structure factors. Unobserved

reflexions have $|F_0| = 0.6 F(\text{threshold})$ and are indicated by a negative sign.

h	k	l	F _o	F _c	0 6 9	10 9	-11.2	1 1	-1 10	27.7	-29.4	1	-5	1	4.7	3.0	-1	8	10	5.7	-6.7	-2	1	10	-2.1	-3.7	
0 0 0	1	65.4	55.0	0 6 10	12.7	-14.4	-1	1	10	12.4	-14.4	-1	1	1	22.8	-18.5	-1	8	11	14.1	-11.3	-2	2	0	-1.7	1.6	
0 0 0	2	101.1	-97.3	0 6 11	5.7	3.3	-1	1	11	12.9	10.2	-1	5	2	52.6	48.4	1	9	0	8.8	-3.7	2	2	1	26.1	22.5	
0 0 0	3	85.7	-63.0	0 7 0	12.4	-11.4	-1	1	2	0	-63.4	-1	-5	2	-2.4	-1.9	1	-9	0	11.2	9.7	-2	-2	1	31.3	-32.4	
0 0 0	4	13.4	-23.2	0 7 1	14.8	-15.5	-1	-2	0	21.9	-17.3	1	5	-2	36.0	-34.8	1	9	1	17.1	-16.7	2	2	4	51.1	47.8	
0 0 0	5	8.0	15.7	0 7 2	-4.1	4.2	1	2	1	70.8	-58.5	-1	5	2	32.8	-31.8	1	-9	1	-3.2	-3.9	-2	-2	1	20.1	19.0	
0 0 0	6	36.2	38.7	0 7 3	13.9	13.6	-1	-2	1	7.6	-10.2	-1	5	3	37.4	-34.0	1	-9	1	-3.1	-1.2	2	2	2	23.6	22.9	
0 0 0	7	12.7	12.2	0 7 4	47.7	54.4	-1	-2	1	47.7	48.7	-1	-5	3	23.1	22.1	-1	9	1	32.2	31.9	-2	-2	2	21.5	21.3	
0 0 0	8	44.3	-64.4	0 7 5	10.6	-11.2	-1	-2	1	11.3	-10.0	-1	5	-2	20.2	-20.3	1	-9	1	-4.7	-11.6	2	-2	2	52.3	-51.3	
0 0 0	9	28.0	29.0	0 7 6	4.8	48.6	1	2	2	80.6	-74.3	-1	5	3	5.7	3.4	1	-9	2	-3.3	-5.3	-2	-2	2	-1.8	2.4	
0 0 0	10	-5.0	8.6	0 7 7	10.4	-10.6	-1	-2	2	32.4	-29.6	-1	5	4	16.1	16.9	1	-9	2	-3.2	-0.2	2	2	3	9.3	-8.8	
0 0 0	11	9.7	-9.9	0 7 8	4.1	3.4	1	2	-2	51.8	59.6	-1	-5	4	5.0	5.7	1	9	2	20.0	19.2	-2	-2	3	41.0	40.4	
0 0 0	12	96.0	37.0	0 7 9	-5.9	7.1	-1	-2	2	35.4	34.0	-1	5	-4	16.9	15.5	1	9	3	11.3	-33.0	-2	-2	3	17.8	-21.7	
0 0 0	13	42.2	36.9	0 7 10	40.2	-42.0	-1	2	3	-1.6	1.4	-1	-5	4	-2.2	-0.9	-1	9	3	33.5	-32.3	-2	-2	3	-1.8	-5.4	
0 0 0	14	80.1	-71.2	0 7 11	35.7	-36.6	-1	-2	3	44.5	43.7	-1	5	5	12.5	14.4	1	9	4	-4.6	-3.2	2	2	4	47.6	-47.2	
0 0 0	15	14.4	16.4	0 7 12	12.6	-13.6	-1	-2	3	21.5	-18.7	-1	5	6	6.8	6.8	1	9	4	-4.7	-2.6	2	-2	4	16.2	16.1	
0 0 0	16	-35.1	30.4	0 7 13	26.2	25.7	-1	-2	3	39.7	33.1	-1	5	-5	24.1	23.8	1	9	5	8.5	-9.2	2	-2	4	24.3	25.3	
0 0 0	17	39.4	38.3	0 7 14	13.0	13.0	1	2	4	58.3	56.1	-1	-5	5	29.7	28.3	-1	9	5	5.9	6.7	-2	-2	4	22.2	-24.1	
0 0 0	18	9.7	-9.9	0 7 15	10.9	10.7	-1	-2	4	36.4	37.9	-1	5	6	36.0	-38.0	-1	9	6	-4.9	0.8	2	-2	5	41.0	40.4	
0 0 0	19	4.5	7.5	0 7 16	14.9	-16.8	1	2	4	8.4	-7.6	-1	-5	6	6.8	-6.7	-1	9	6	17.3	16.2	-2	-2	5	14.4	16.0	
0 0 0	20	30.9	-33.3	0 8 0	11.0	-10.0	-1	-2	4	18.5	15.1	-1	5	-6	-3.0	1.8	1	9	7	15.0	13.4	-2	-2	5	4.3	5.6	
0 0 0	21	15.9	-15.1	0 8 1	-12.6	-12.9	1	2	5	35.8	29.2	-1	-5	6	32.4	29.3	-1	9	7	14.6	13.4	-2	-2	5	1.9	3.8	
0 0 0	22	14.8	-17.3	0 8 2	13.5	15.1	-1	-2	5	19.7	-18.9	-1	5	7	38.4	-38.1	-1	9	8	-4.9	0.8	2	-2	6	16.3	15.8	
0 0 0	23	12.9	-12.0	0 8 3	8.6	-8.8	-1	2	-5	14.1	14.7	-1	-5	7	8.3	-7.2	-1	9	8	14.1	12.7	-2	-2	6	9.3	-8.9	
0 0 0	24	42.7	43.4	0 8 4	3.4	-4.4	-1	2	2	13.0	-9.6	-1	-5	7	7.1	7.2	-1	9	9	-5.0	4.8	-2	-2	6	20.5	22.1	
0 0 0	25	11.2	12.2	0 8 5	7.5	-8.4	-1	2	2	3.9	-3.5	-1	-5	7	6.4	6.3	-1	9	10	5.9	-12.2	-2	-2	6	21.3	-21.7	
0 0 0	26	13.8	12.4	0 8 6	4.4	-4.4	-1	-2	6	24.9	-24.1	-1	5	8	11.0	11.0	-1	9	10	5.9	-0.6	-2	-2	7	-2.8	-2.4	
0 0 0	27	8.7	-6.9	0 8 7	9.0	7.2	-1	-2	6	10.2	7.4	-1	5	9	5.0	-5.0	-1	9	11	12.5	-14.6	-2	-2	7	6.6	7.1	
0 0 0	28	42.8	-42.8	0 8 8	28.3	-29.4	-1	-2	7	2.8	0.5	-1	5	10	5.3	-5.1	1	10	0	17.8	18.0	-2	-2	8	10.1	10.2	
0 0 0	29	13.5	14.5	0 8 9	4.7	-1.3	1	2	7	-2.7	-17.1	-1	-5	10	10.7	10.8	-1	10	0	6.7	-8.9	-2	-2	8	-3.0	-1.1	
0 0 0	30	18.0	19.1	0 8 10	-10.5	-7.1	-1	2	7	1.7	-11.1	-1	-5	11	10.0	8.6	-1	10	0	3.5	4.6	-2	-2	8	11.4	11.4	
0 0 0	31	-10.5	-7.1	0 8 11	12.1	-12.7	1	2	8	13.0	14.4	-1	-5	11	3.1	-1.5	1	10	1	12.0	-0.0	-2	-2	8	6.8	5.9	
0 0 0	32	76.8	-74.7	0 8 12	11.1	10.4	-1	-2	8	-2.9	-1.1	-1	6	0	9.1	-8.1	-1	10	1	6.0	3.1	-2	-2	9	-4.5	2.3	
0 0 0	33	92.8	-85.6	0 9 0	-3.1	-0.7	1	-2	9	-2.9	-0.6	-1	-6	0	6.3	1.4	-1	10	2	-5.1	-1.8	-2	-2	9	-3.2	-2.2	
0 0 0	34	37.9	-38.2	0 9 1	7.4	-7.4	-1	-2	9	5.8	-5.8	-1	-6	1	15.8	-17.5	-1	10	3	-5.0	0.1	-2	-2	9	17.7	-17.3	
0 0 0	35	36.7	-33.5	0 9 2	-3.1	-5.1	1	-2	9	33.6	-32.8	-1	-6	1	15.8	-17.5	-1	10	3	-5.0	0.1	-2	-2	9	17.7	-17.3	
0 0 0	36	44.8	42.2	0 9 3	20.6	23.0	-1	-2	9	9.9	8.9	-1	-6	1	47.4	46.4	-1	10	3	-3.1	-1.1	-2	-2	10	-4.8	-9.3	
0 0 0	37	138.3	134.1	0 9 4	-3.2	-4.3	1	-2	9	13.8	-15.1	-1	-6	1	14.4	15.2	-1	10	3	17.5	-17.2	-2	-2	10	11.2	-11.6	
0 0 0	38	49.4	46.4	0 9 5	2.9	-0.9	-1	-2	9	21.7	21.2	-1	-6	1	14.4	15.2	-1	10	4	-4	-4	-2	-2	10	11.2	-11.6	
0 0 0	39	-1.8	6.3	0 9 6	38.3	-40.1	1	2	10	20.4	-20.2	-1	-6	2	15.0	15.2	-1	10	5	9.0	-9.7	-2	-2	10	-1.9	-3.1	
0 0 0	40	4.3	-3.1	0 9 7	12.1	-6.5	-1	2	10	-3.2	-1.4	-1	-6	2	6.2	7.7	-1	10	5	-3.1	0.4	-2	-2	10	12.7	-11.9	
0 0 0	41	15.6	-17.5	0 9 8	4.9	0.1	1	2	11	7.1	-8.5	-1	-6	3	41.4	-40.0	-1	10	6	7.5	-8.6	-2	-2	10	3.5	3.9	
0 0 0	42	25.7	-28.3	0 9 9	25.3	24.3	1	2	11	-5.1	5.5	-1	-6	3	14.8	-9.2	-1	10	6	8.4	-7.3	-2	-2	10	25.3	25.5	
0 0 0	43	30.0	-29.6	0 9 10	4.9	0.1	1	2	11	7.1	-8.5	-1	-6	3	24.5	25.3	-1	10	7	10.3	9.5	-2	-2	10	1.5	1.9	
0 0 0	44	-6.5	-1.2	0 9 11	30.2	-32.0	-1	-2	11	7.7	-11.3	-1	-6	3	29.5	-31.0	-1	10	7	9.5	-8.6	-2	-2	10	3.5	3.9	
0 0 0	45	23.9	-24.0	0 9 12	3.3	-2.2	1	2	11	3.6	2.9	-1	-6	4	-3.7	-4.0	-1	10	8	12.3	-10.1	-2	-2	10	3.5	3.9	
0 0 0	46	17.1	-18.1	0 10 0	-5.3	4.5	-1	-3	1	21.0	21.3	-1	-6	4	-2.9	1.3	-1	10	9	17.2	15.9	-2	-2	10	2.8	3.1	
0 0 0	47	2.2	-2.2	0 10 1	6.1	-3.3	-1	-3	1	6.1	-3.3	-1	-6	4	12.9	-13.2	-1	10	9	12.9	-13.2	-2	-2	10	2.8	3.1	
0 0 0	48	22.1	-20.7	0 10 2	-5.2	6.4	-1	-3	1	3.1	-6.7	-1	-6	4	28.2	28.1	-1	10	10	-6.4	0.7	-2	-2	10	9.5	-9.2	
0 0 0	49	7.4	7.1	0 10 3	-5.1	5.8	1	3	2	6.2	8.6	-1	-6	5	14.2	15.2	-1	10	10	6.9	-4.2	-2	-2	10	13.7	11.0	
0 0 0	50	-4.7	-5.4	0 10 4	-5.0	-7.8	-1	-3	2	12.5	-15.1	-1	-6	5	11.2	-13.4	-1	10	11	-5.4	-16.0	-2	-2	10	5.8	-5.4	
0 0 0	51	6.7	-9.0	0 10 5	4.4	-4.4	-1	-3	2	10.6	-10.6	-1	-6	5	5.5	6.2	-1	10	11	5.5	-6.7	-2	-2	10	11.4	8.5	
0 0 0	52	11.1	1.9	0 10 6	-5.0	0.2	-1	-3	2	5.4	51.7	-1	-6	5	-2.4	-1.7	-1	10	11	2	-5.0	-6.7	-2	-2	10	11.4	8.5
0 0 0	53	18.4	-16.9	0 10 7	10.4	10.1	-1	-3	3	69.2	-70.3	-1	-6	6	11.9	10.9	-1	10	11	3	-5.4	-1.9	-2	-2	10	9.4	-9.8
0 0 0	54	15.4	15.5	0 10 8	14.5	15.3	-1	-3	3	8.1	-5.3	-1	-6	6	9.2	-9.2	-1	10	11	3	-5.4	-1.9	-2	-2	10	9.4	-9.8
0 0 0	55	-4.5	-7.8	0 10 9	10.9	10.1	1	3	3	8.7	10.5	-1	-6	6	8.2	-11.4	-1	10	11	4	-5.3	1.4	-2	-2	10	9.4	-9.8
0 0 0	56	30.7	-61.6	0 10 10	14.1	-17.2	-1	-3	3	54.6	50.0	-1	-6	6	8.2	-7.6	-1	10	11	4	15.7	14.1	-2	-2	10	-2.6	0.8
0 0 0	57	71.1	27.3	0 11 2	-5.5	-10.1	-1	-3	4	28.9	-22.4	-1	-6	7	8.6	-9.2	-1	10	11	5	-5.3	-1.4	-2	-2	10	-2.6	0.8
0 0 0	58	3.3	3.2	0 11 3</																							

Table XV. Final positional parameters (fractional) with mean standard deviations (\AA), and thermal parameters and standard deviations (B in \AA^2 , U_{ij} in $\text{\AA}^2 \times 10^2$).

Atom	\underline{x}	\underline{y}	\underline{z}	mean σ	\underline{B}	$\sigma(\underline{B})$
P(1)	-0.1315	0.3154	-0.1258	0.0041	-	-
P(2)	0.2114	0.2593	-0.2020	0.0044	-	-
P(3)	0.2511	0.0714	-0.3144	0.0044	-	-
P(4)	0.1884	-0.2048	-0.1498	0.0041	-	-
N(1)	0.0585	0.2572	-0.1156	0.014	-	-
N(2)	0.2183	0.2157	-0.3118	0.013	-	-
N(3)	0.2040	-0.0523	-0.1894	0.013	-	-
N(4)	0.2161	-0.3074	-0.0017	0.013	-	-
O(1)	-0.1860	0.4732	-0.2273	0.011	3.14	0.21
O(2)	-0.2189	0.2477	-0.1878	0.012	3.83	0.24
O(3)	0.3670	0.1664	-0.1129	0.011	3.22	0.21
O(4)	0.2364	0.4147	-0.2665	0.012	3.49	0.22
O(5)	0.4363	0.0214	-0.3402	0.013	3.96	0.24
O(6)	0.1702	0.0975	-0.4420	0.013	4.02	0.25
O(7)	0.3069	-0.2742	-0.2266	0.012	3.45	0.22
O(8)	0.0164	-0.1914	-0.2048	0.012	3.35	0.22
C(1)	-0.1626	0.5203	-0.3645	0.022	4.91	0.42
C(2)	-0.1994	0.1009	-0.1312	0.019	3.95	0.36
C(3)	0.3969	0.1866	-0.0025	0.021	4.52	0.41
C(4)	0.3740	0.4539	-0.3464	0.022	5.09	0.44
C(5)	0.5288	0.1174	-0.4376	0.023	5.89	0.50
C(6)	-0.0114	0.1440	-0.4568	0.024	5.31	0.48
C(7)	0.4732	-0.3371	-0.1892	0.024	5.43	0.48
C(8)	-0.0403	-0.3140	-0.1767	0.022	4.99	0.44

Atom	\underline{U}_{11}	\underline{U}_{12}	\underline{U}_{13}	\underline{U}_{22}	\underline{U}_{23}	\underline{U}_{33}	mean $\sigma(\underline{U})$
P(1)	3.02	-0.50	0.37	3.17	-1.16	3.18	0.15
P(2)	2.92	-0.50	0.12	3.01	-1.50	3.53	0.15
P(3)	3.59	-0.99	0.40	3.32	-1.89	2.68	0.16
P(4)	3.48	-0.47	0.58	3.40	-1.41	3.15	0.16
N(1)	3.74	-0.53	-0.73	4.68	-1.73	3.52	0.55
N(2)	4.58	-0.89	0.52	3.04	-1.45	3.71	0.55
N(3)	4.40	-0.19	0.46	3.86	-2.09	3.86	0.53
N(4)	3.67	-0.27	0.31	4.17	-1.45	4.68	0.50

Table XV (continued)

Atom	<u>x</u>	<u>y</u>	<u>z</u>	<u>B</u>
H(1)	-0.067	0.542	-0.383	5.0
H(1)	-0.083	0.508	-0.342	
H(1)	not located			
H(2)	-0.217	0.058	-0.042	
H(2)	-0.100	0.050	-0.133	
H(2)	-0.275	0.083	-0.108	
H(3)	0.367	0.125	-0.058	
H(3)	0.500	0.217	-0.042	
H(3)	0.408	0.283	-0.033	
H(4)	0.450	0.400	-0.300	
H(4)	0.400	0.433	-0.275	
H(4)	0.433	0.408	-0.400	
H(5)	0.575	0.083	-0.383	
H(5)	0.475	0.167	-0.483	
H(5)	not located			
H(6)	0.100	0.142	-0.467	
H(6)	-0.033	0.233	-0.433	
H(6)	not located			
H(7)	0.542	-0.333	-0.158	
H(7)	0.350	-0.233	-0.242	
H(7)	not located			
H(8)	-0.033	-0.373	-0.108	
H(8)	0.042	-0.375	-0.192	
H(8)	not located			

Discussion

The $[\text{PN}(\text{OMe}_2)]_8$ molecule is centrosymmetrical, and has the general shape shown in Figure 10. The sixteen-membered phosphonitric ring consists of two approximately planar and parallel segments, P(2), N(2), P(3), N(3), P(4), N(4) and the centrosymmetrically related set of atoms, joined by a step at P(1), N(1) and P(1'), N(1'). The methoxy groups cover the outside of the ring very evenly, and the whole molecule is quite compact.

The P-N bond distances are in the range 1.550 - 1.569 Å. The least-squares standard deviations of the individual lengths are 0.014 Å, and the standard deviations calculated from the internal consistency, if all the distances are equal, are only 0.005 Å, so that the least-squares estimates of the accuracy appear to be on the pessimistic side. The same conclusion is suggested from a study of variations in measured values of the other bonds and the angles in the molecule. It seems appropriate to use the less-optimistic least-squares standard deviations in the remainder of the discussion. The P-N bond lengths are all equal within experimental error, the mean value being 1.561 Å ($\sigma = 0.005$ Å). The P-O and O-C distances also show no significant differences among the individual values, the mean lengths being P-O = 1.576 Å ($\sigma = 0.005$ Å), and O-C = 1.440 Å ($\sigma = 0.009$ Å).

The mean N-P-N angle is 116.7°, but three of the angles are 114.2, 115.6, and 115.8°, mean value 115.2° ($\sigma = 0.4^\circ$), while the N(1)-P(2)-N(2) angle is significantly (7.5σ) larger at 121.2° ($\sigma = 0.7^\circ$).

Table XVI. Bond lengths (\AA) and angles (degrees).

P(1)-N(1)	1.566	N(4')-P(1)-N(1)	115.6
P(2)-N(1)	1.550	N(1)-P(2)-N(2)	121.2
P(2)-N(2)	1.558	N(2)-P(3)-N(3)	115.8
P(3)-N(2)	1.569	N(3)-P(4)-N(4)	114.2
P(3)-N(3)	1.559		
P(4)-N(3)	1.564	O(1)-P(1)-O(2)	99.2
P(4)-N(4)	1.565	O(3)-P(2)-O(4)	105.6
P(1')-N(4)	1.556	O(5)-P(3)-O(6)	100.2
		O(7)-P(4)-O(8)	100.3
P(1)-O(1)	1.567		
P(1)-O(2)	1.580	P(1)-O(1)-C(1)	122.0
P(2)-O(3)	1.574	P(1)-O(2)-C(2)	120.5
P(2)-O(4)	1.580	P(2)-O(3)-C(3)	119.4
P(3)-O(5)	1.572	P(2)-O(4)-C(4)	121.5
P(3)-O(6)	1.570	P(3)-O(5)-C(5)	121.7
P(4)-O(7)	1.576	P(3)-O(6)-C(6)	118.3
P(4)-O(8)	1.586	P(4)-O(7)-C(7)	121.6
		P(4)-O(8)-C(8)	120.2
O(1)-C(1)	1.441		
O(2)-C(2)	1.413	N(4')-P(1)-O(1)	104.2
O(3)-C(3)	1.460	N(4')-P(1)-O(2)	111.3
O(4)-C(4)	1.428	N(1)-P(1)-O(1)	114.1
O(5)-C(5)	1.453	N(1)-P(1)-O(2)	111.1
O(6)-C(6)	1.488	N(1)-P(2)-O(3)	109.1
O(7)-C(7)	1.414	N(1)-P(2)-O(4)	105.6
O(8)-C(8)	1.427	N(2)-P(2)-O(3)	106.6
		N(2)-P(2)-O(4)	107.6
P(1)-N(1)-P(2)	141.0	N(2)-P(3)-O(5)	111.8
P(2)-N(2)-P(3)	134.1	N(2)-P(3)-O(6)	107.5
P(3)-N(3)-P(4)	136.0	N(3)-P(3)-O(5)	106.6
P(4)-N(4)-P(1')	135.7	N(3)-P(3)-O(6)	113.9
		N(3)-P(4)-O(7)	113.3
		N(3)-P(4)-O(8)	106.4
		N(4)-P(4)-O(7)	107.7
		N(4)-P(4)-O(8)	114.2

Standard deviations

$$\begin{aligned}\sigma(\text{P-N}) &= 0.014 \text{ \AA} \\ \sigma(\text{P-O}) &= 0.013 \\ \sigma(\text{O-C}) &= 0.025\end{aligned}$$

$$\begin{aligned}\sigma(\text{P-N-P}) &= 1.0^\circ \\ \sigma(\text{N-P-N}) &= 0.7 \\ \sigma(\text{O-P-O}) &= 0.7\end{aligned}$$

$$\begin{aligned}\sigma(\text{P-O-C}) &= 1.2 \\ \sigma(\text{N-P-O}) &= 0.7\end{aligned}$$

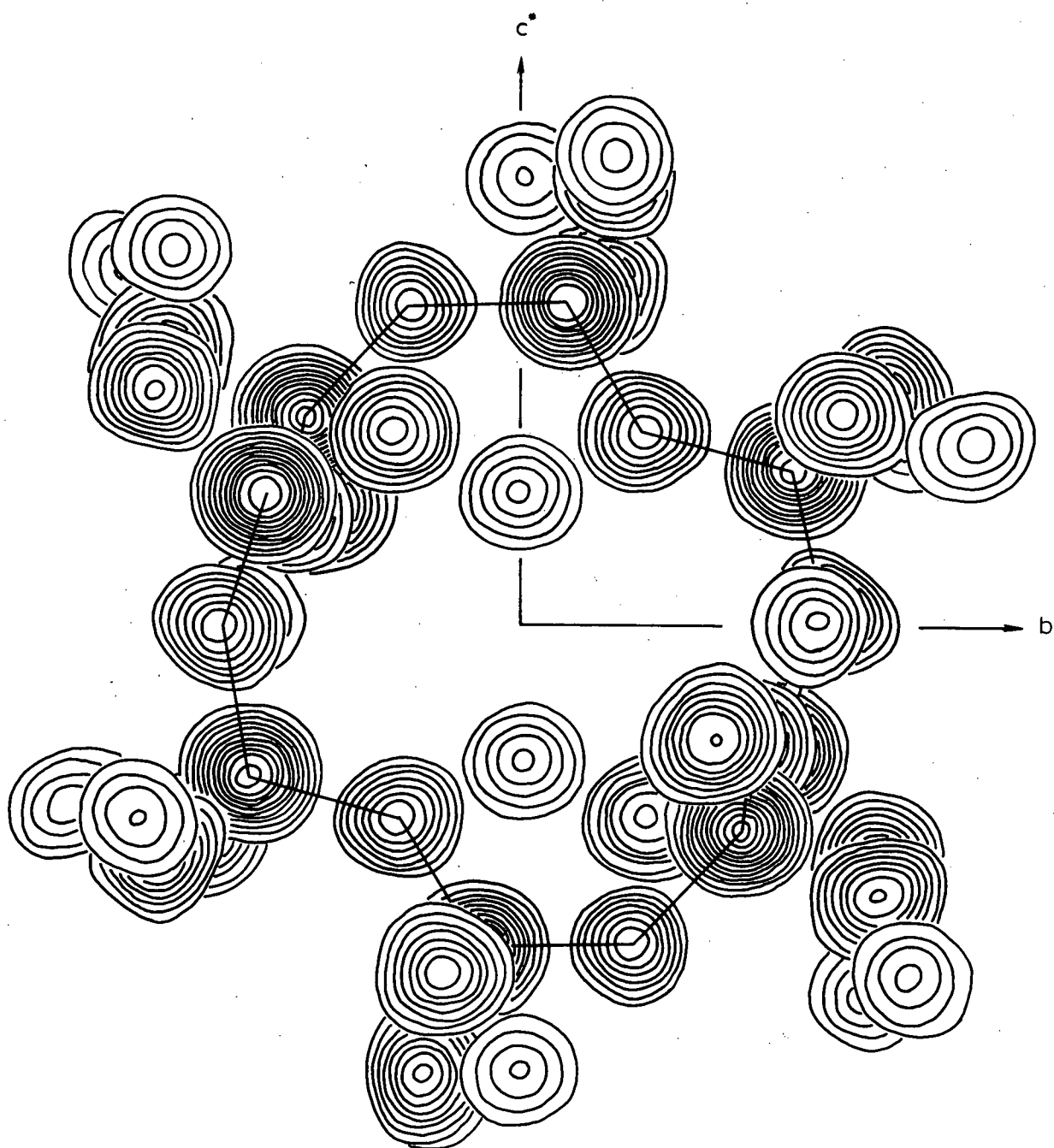


Figure 9. Sections of the three-dimensional electron-density distribution. Contours are at $2 \text{ e.}\text{\AA}^{-3}$ at phosphorus, and $1 \text{ e.}\text{\AA}^{-3}$ at nitrogen, oxygen, and carbon with the lowest contour at $2 \text{ e.}\text{\AA}^{-3}$.

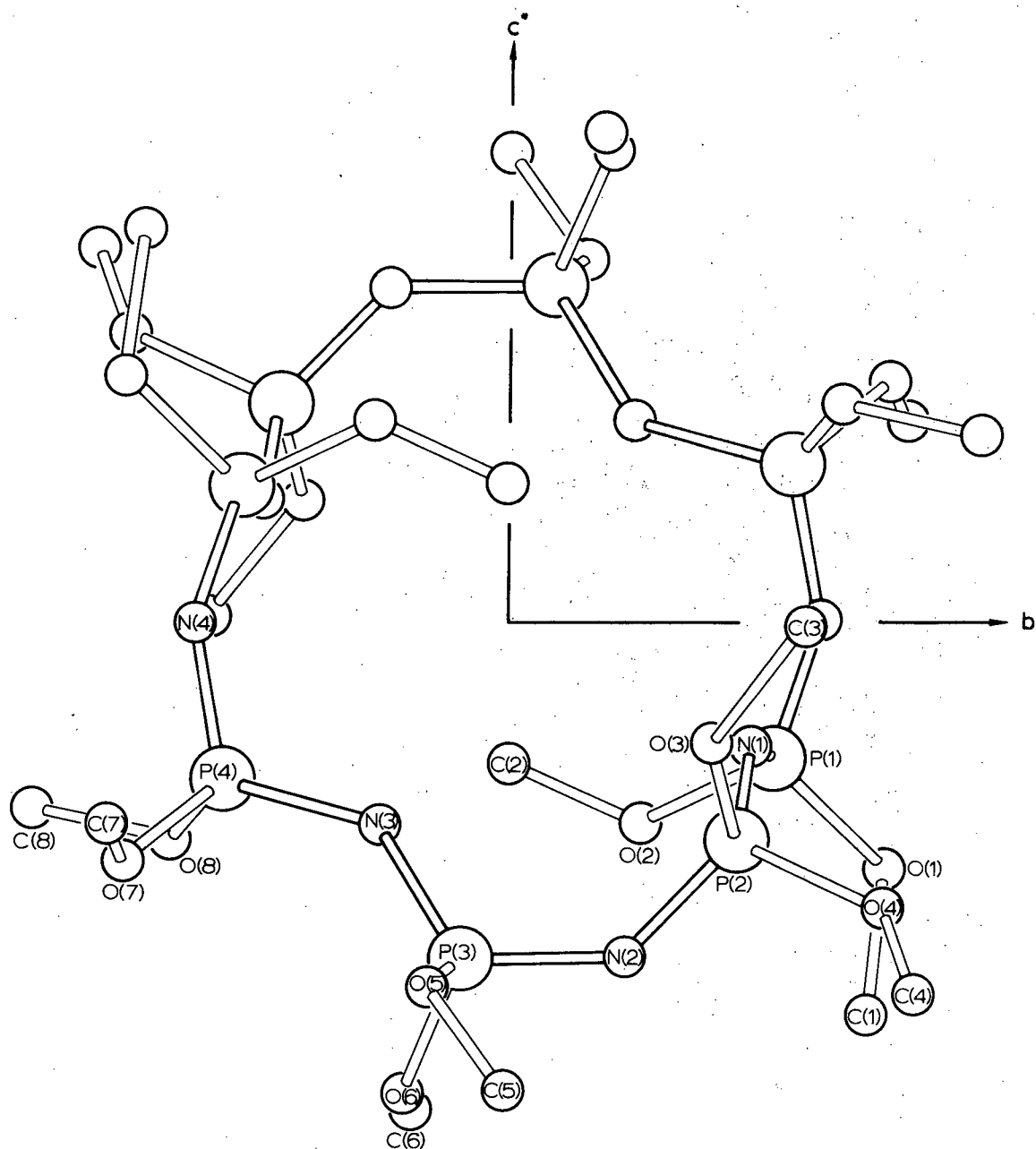


Figure 10. A diagram of the structure viewed along the a' -axis of the orthogonal set a' , b , c^* .

Similarly the mean P-N-P angle is 136.7° , but the angle at N(1), 141.0° ($\sigma = 1.0^\circ$), is significantly (5σ) larger than the other three, 134.1 , 135.7 , and 136.0° , mean 135.3° ($\sigma = 0.6^\circ$). The O-P-O angles show a similar effect, that at P(2), 105.6° ($\sigma = 0.7^\circ$), being 7σ larger than the other three, 99.2 , 100.2 , and 100.3° , mean 99.9° ($\sigma = 0.4^\circ$). The P-O-C angles are in the range $118.3 - 122.0^\circ$, with no significant variations from the mean value of 120.6 ($\sigma = 0.4^\circ$).

Averaged molecular parameters of the molecules $[\text{NP}(\text{OMe})_2]_8$ and $[\text{NP}(\text{OMe})_2]_4^{40}$ are compared in Table XVII. It would appear from the

Table XVII. Comparison of molecular parameters of $[\text{NP}(\text{OMe})_2]_4$ and $[\text{NP}(\text{OMe})_2]_8$.

	$[\text{NP}(\text{OMe})_2]_4$	$[\text{NP}(\text{OMe})_2]_8$
P-N(Å)	1.58	1.561
P-O	1.60	1.576
O-C	1.47	1.440
Angle P-N-P($^\circ$)	132	136.7
Angle N-P-N	122	116.7
Angle O-P-O	105	101.3
Angle P-O-C	120.4	120.6

bond lengths that the larger molecule is more strongly bound, but the differences are small and may well be within experimental error. The effect, however, is in the direction predicted by a Molecular Orbital treatment²¹ and has previously been observed in $[\text{NPCl}_2]_5^{62}$ where the average P-N bond is shorter than in the corresponding smaller rings. In any case, the P-N bond distance in $[\text{NP}(\text{OMe})_2]_8$ of 1.56 \AA is 0.21 \AA

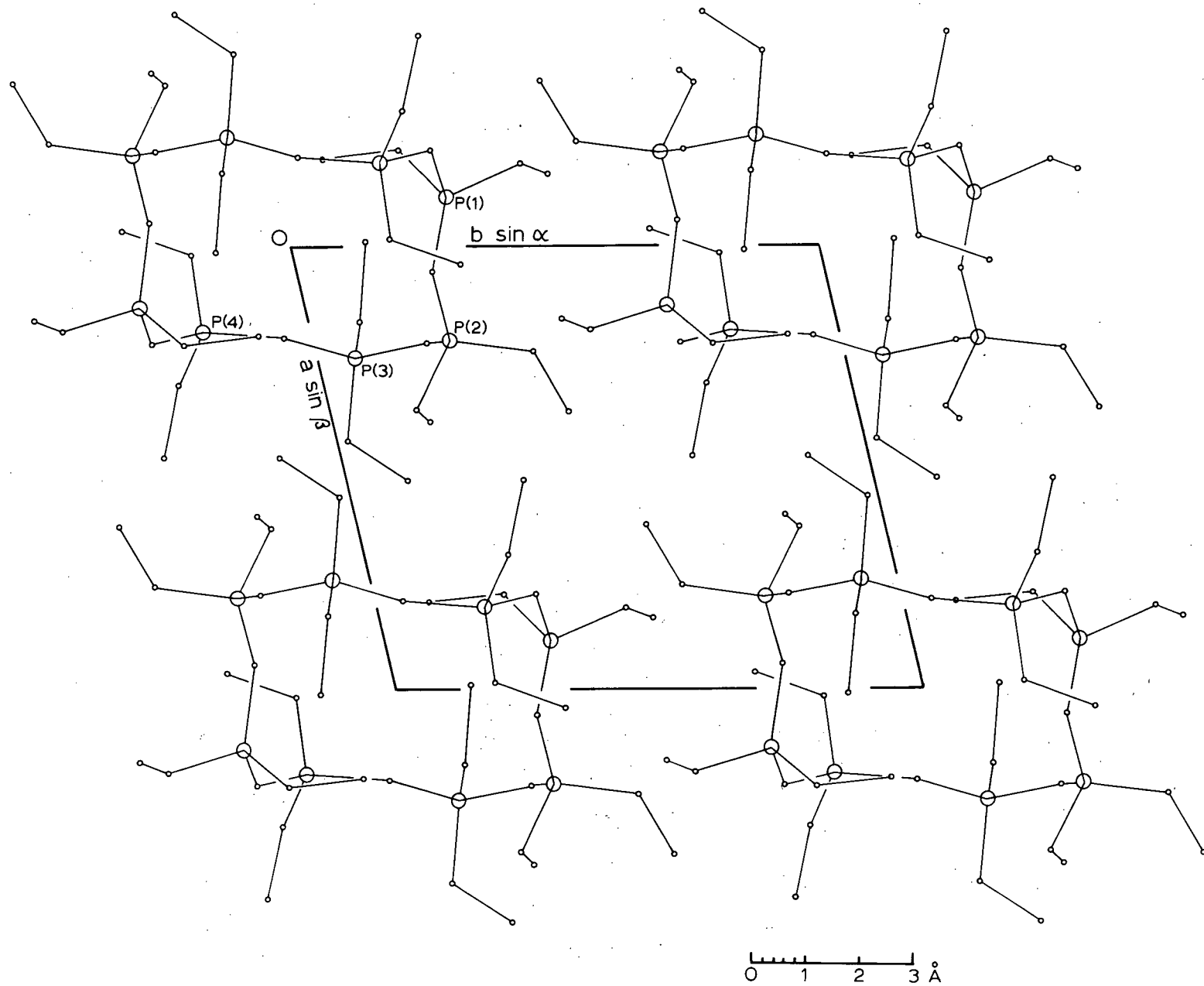


Figure 11. The molecular packing viewed along the c -axis.

shorter than the single-bond length of 1.77 Å found in sodium phosphoramidate.^{45,46} This bond distance and the equality of bonds around the ring are both consistent with findings in other phosphonitrilic structures. The average ring angle at nitrogen in $[\text{NP}(\text{OMe})_2]_8$ is greater than in the tetramer suggesting an increased participation of the nitrogen lone pair electrons in π -bonding within the larger ring. It is surprising, however, that this angle is not larger than in $[\text{NP}(\text{NMe}_2)_2]_6$ where it is 147° for the methoxy groups on phosphorus would be expected to enhance the electron delocalization from nitrogen more than the dimethylamido substituents. The N-P-N angle is also smaller than the 120° usually found in phosphonitriles. In the present case it is more comparable with the O=P-O angle of 117.2° in dibenzylphosphoric acid.⁶⁵

The phosphonitrilic skeleton in $[\text{NP}(\text{OMe})_2]_8$ has a definite tendency towards planarity. In common with $[\text{NPCl}_2]_5$ this is partially attained through re-entrant angles at N(1), N(1'), N(3) and N(3'). A convenient way of describing the shape is to consider the ring as being derived from the idealized planar configuration illustrated in Figure 12(a). This structure would be strained at the nitrogen atoms N(1) and N(1') where the angles would be about 60° if normal values were assigned to the other angles. The strain at these atoms can be relieved by displacing one half of the molecule relative to the other as shown in Figure 12(b). This would permit the angles at N(1) and N(1') to increase while allowing large portions of the ring to remain approximately planar. This does appear to be an acceptable picture

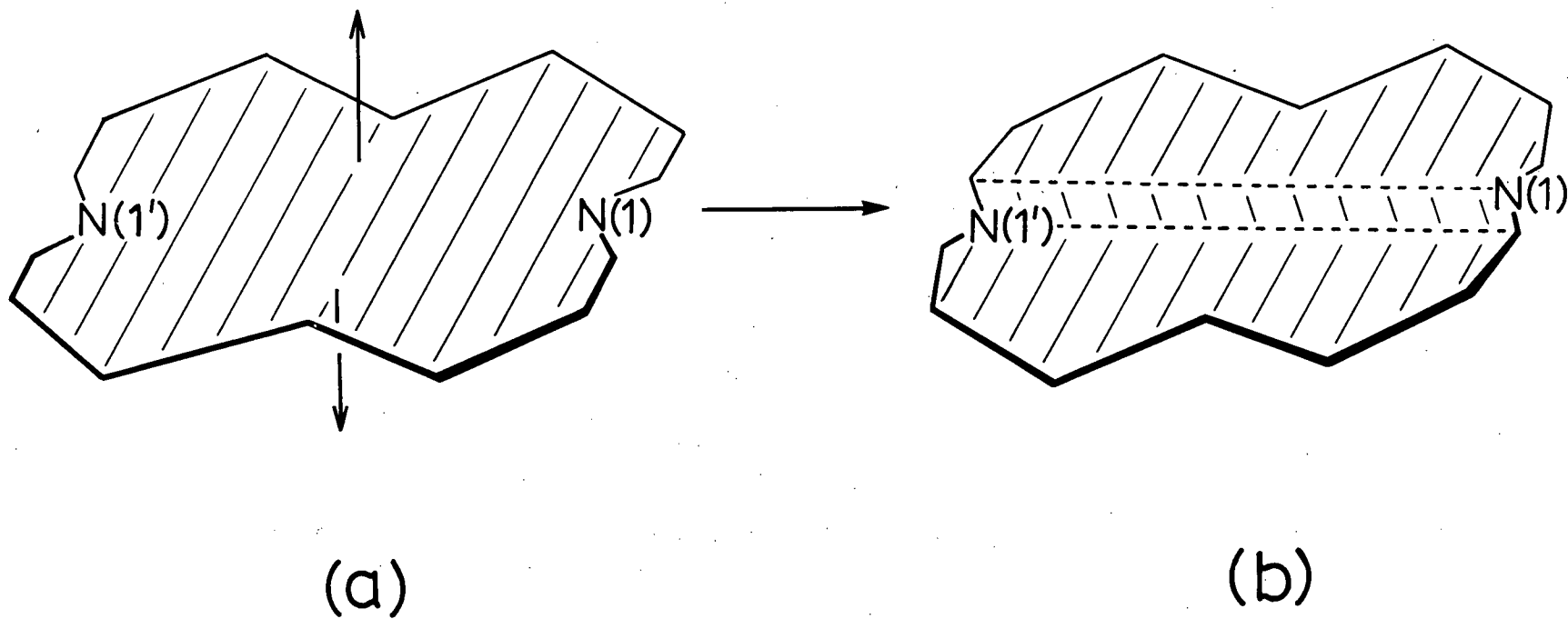


Figure 12. Idealized structures indicating the distortion of the phosphonitrilic ring from planarity.

for the angle at these nitrogen atoms is significantly larger than the others, and the mean deviation of the atom sequence P(2)N(2)P(3)-N(3)P(4)N(4) is only 0.12 Å from the mean plane. In addition, the six-atom sequence P(4')N(4')P(1) N(1)P(2)N(2) is also nearly planar, the mean deviation being 0.26 Å. These planar segments would tend to make possible both π_a and π_s bonding within the ring.

The configuration about the individual phosphorus atoms can be seen in Figure 13 where the atom positions are plotted with respect to a particular three-atom plane. The centre diagram represents an idealized configuration which allows the exterior atoms to be arranged about the central atom with a minimum of steric interference. This is the arrangement found in pentaerythritol tetranitrate⁶⁶ where the absence of π -bonding probably assures that the shape is determined by the steric repulsions of the outermost atoms. In this configuration, the exterior atoms can be considered related by a four-fold inversion axis (A,B) or by a two-fold axis (A,C). It is convenient to discuss the configuration about the phosphorus atoms in relation to this model. All the phosphorus environments show some similarity to the idealized arrangement in that the terminal bonds are all displaced in opposite directions from the three-atom planes. Furthermore, the positions of the outermost atoms about P(2), P(3), and P(4) are all analogous to the model which would tend to reduce steric interactions. The configuration at P(1) is slightly different. It is situated at the junction between major planar sections of the ring and the steric interactions about it are not the same as for the other phosphorus atoms. In particular, the

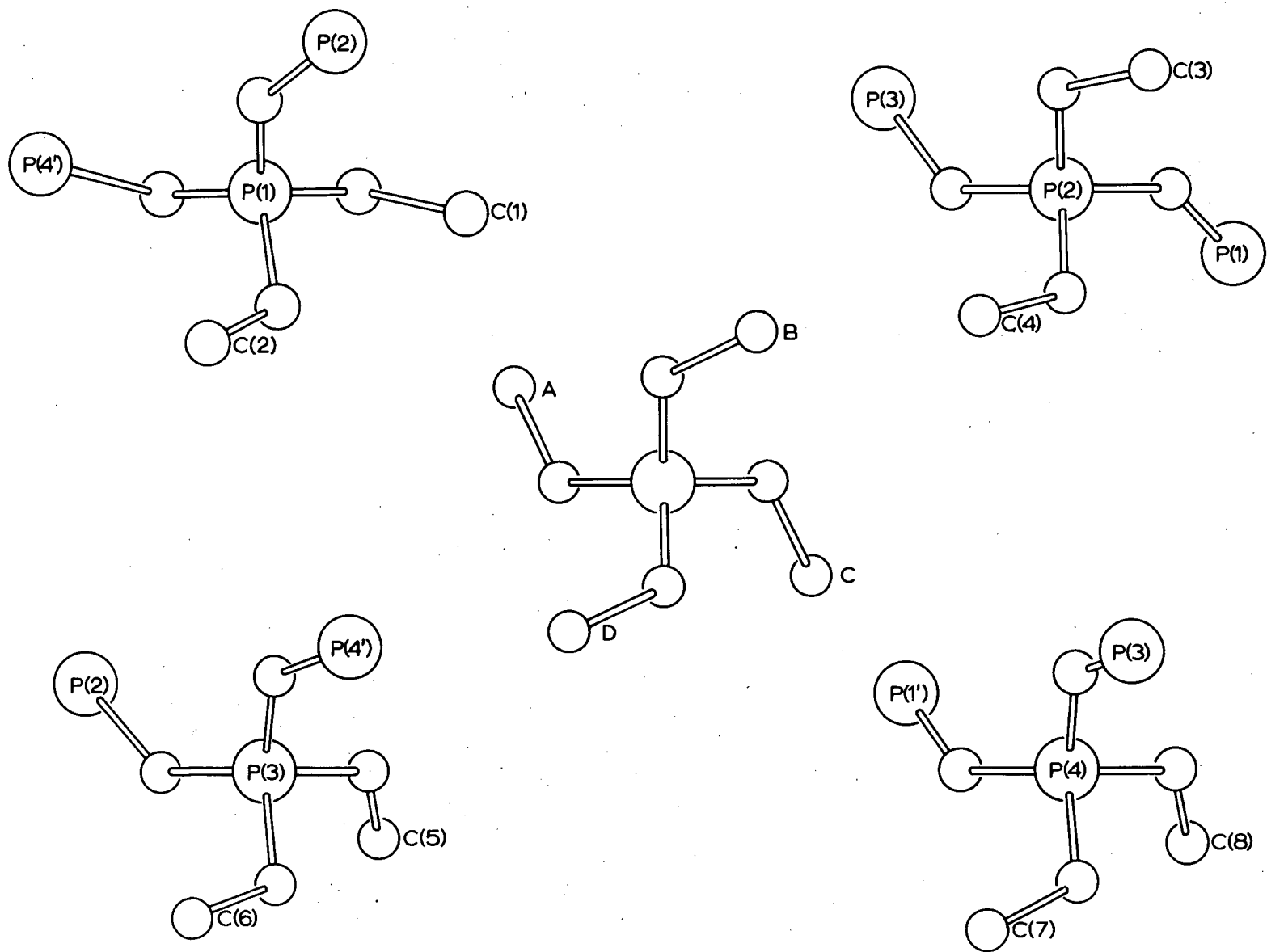


Figure 13. Configurations about phosphorus. The centre diagram shows an idealized $\text{P}(\text{OC})_4$ group, the others indicate the atomic arrangements about the phosphorus atoms in $[\text{NP}(\text{OMe})_2]_8$.

re-entrant angle at N(1) causes a close approach (3.48 Å) between the O(1) and O(4) oxygen atoms. Although a reorientation of the methoxy groups on P(1) towards the pentaerythritol configuration could increase the separation, this could only occur at the expense of leaving the centre of the ring open.

The relationship of one POC group to the other at a particular phosphorus atom is also interesting because of the possibility of exocyclic π -bonding. Two different types of arrangements are generally found in the esters of phosphoric acid. At P(1), P(3), and P(4) the methoxy groups are related approximately by a $\bar{4}$ axis (see Figure 13). This is the configuration found in dibenzyl phosphoric acid⁶⁵ and in vitamin B₁₂.⁶⁷ At P(2), by contrast, the methoxy groups are related by an approximate two-fold axis as is found in di-p-chlorophenyl phosphoric acid,⁶⁸ for example. These two different orientations make possible different π -overlaps between the phosphorus atom and its exocyclic groups. In both situations there is a tendency towards a preferred alignment of the POC planes with the π -orbitals on phosphorus. Accurate alignment of one dimethylamido group for maximum overlap with one set of $d_{-\pi}$ orbitals and partial overlap for the other were found in the case of $[\text{NP}(\text{NMe}_2)_2]_4$. The situation at P(1), P(3), and P(4) for the present molecule is rather similar to the case of dibenzyl phosphoric acid. In this compound, $p_{-\pi}$ orbitals at two different oxygens can each overlap with a different π -orbital at phosphorus because of the large dihedral angle of 88.6° between the POC planes. Although in $[\text{NP}(\text{OMe})_2]_8$ the average dihedral angle is reduced to 70°

for steric reasons, this still permits at least partial overlap at these phosphorus atoms with the separate π_a and π_s -orbital systems. At P(2), however, the situation is different. As before, the normal to the POC plane can be taken to indicate the lone pair electrons in the oxygen p orbital capable of π -bonding. Unlike the other cases, at P(2) the normals to both POC planes tend to align with the YZ plane. This would suggest involvement between the lone pairs on both oxygen atoms with the same π_s -system on phosphorus. The overlap between the exocyclic groups at P(2) is thus distinct from the π -bonding possibilities at the other phosphorus atoms. This difference, and the fact that P(2) is near the end of a long planar section may help to explain the large angles at this atom. There are no variations in the P-O bond lengths which can be attributed to π -bonding involving a particular π -system. Since the π_a and π_s -orbitals are primarily involved in the ring bonds it is likely that a balance of orbital participation with the exocyclic atoms is maintained. Also, the effective π -bonding to the methoxy groups will be weaker here than in $[\text{NP}(\text{NMe}_2)_2]_4$ because it involves delocalization of the lone pairs from the more electronegative oxygen atoms. In spite of this some exocyclic π -bonding must occur for the average P-O bond length of 1.58 Å is 0.13 Å less than the expected value of 1.71 Å for a true single bond.

PART III

THE STRUCTURE DETERMINATION OF

CAESIUM DIFLUOROPHOSPHATE

A. INTRODUCTION

In the thesis until now the bonding and structural features of phosphonitrilic compounds have been described. In this section the structure of CsPO_2F_2 will be discussed and the bonding from phosphorus to oxygen and fluorine will be considered in a slightly different manner from the phosphorus-nitrogen bonding of the phosphonitriles.

The difluorophosphate anion, like the phosphonitriles, contains bonds between tetrahedrally co-ordinated phosphorus and first-row elements. Such bonds are often considerably shorter than the expected single bond distances. Some common values for the P-O and P-F bonds in isolated tetrahedra are given in Table XVIII together with the distance predicted from the Schomaker-Stevenson equation.⁶⁹ The usual form of this semi-empirical equation

$$r_{AB} = r_A + r_B - 0.09 (x_A - x_B)$$

modifies the atomic radii, r_A and r_B , by a correction depending upon the difference in their electronegativities, x_A and x_B , but makes no allowance for π -bonding.

Table XVIII. Bond lengths (\AA) between tetrahedrally co-ordinated phosphorus and the first-row elements oxygen and fluorine.

Bond	Calculated bond length	Observed	Reference
P-O	1.71	1.54	LiMnPO_4 (70)
P-F	1.65	1.53	POF_3 , PSF_3 (71,72)

The contraction of the observed bond lengths from the calculated values indicates that the bond order in each instance must be greater than one. Ionic resonance structures suggest a way of accounting for the bond shortening. Another explanation can be given in terms of \underline{d}_{π} - \underline{p}_{π} overlap, and this will be described briefly here because of the analogy with phosphonitrilic bonding. The theory is mainly due to Cruickshank who has considered the possibilities for multiple bonding between first row elements and tetrahedrally coordinated second row elements.⁷³ In this treatment the orientation of the \underline{d} orbitals at phosphorus is chosen differently from the cases previously discussed. To preserve the tetrahedral symmetry at phosphorus, the axes are chosen to be coincident with the $\bar{4}$ axes of the tetrahedron. Cruickshank shows that although the $3p$ orbitals of phosphorus are required for σ -bonding some π -bonding is feasible with the phosphorus \underline{d} orbitals, especially the \underline{d}_{z^2} and $\underline{d}_{x^2-y^2}$. The \underline{d}_{xz} , \underline{d}_{yz} , and \underline{d}_{xy} , although also potentially π -bonding orbitals, combine much less strongly with the appropriate ligand orbitals. Complete tetrahedral symmetry about phosphorus would allow the $\underline{d}_{x^2-y^2}$ and \underline{d}_{z^2} orbitals to interact equally with the four ligands. Simultaneous involvement at the ligands with each of these \underline{d} orbitals is possible because there are two orthogonal p -type orbitals available having the proper symmetry. A diagram of the orbitals involved and the geometrical proximities for overlap in the two systems are illustrated in Figure 14.

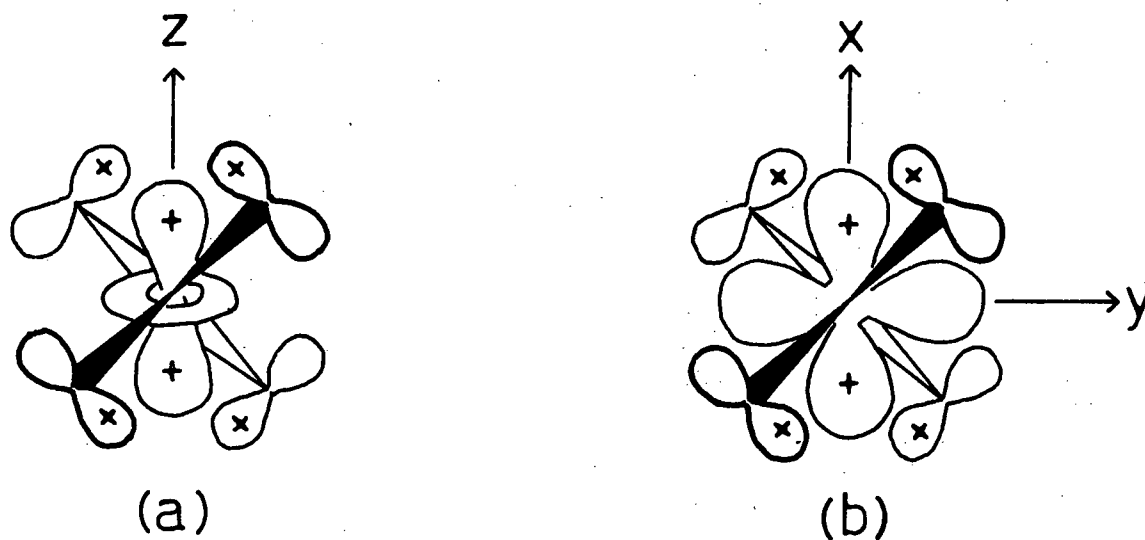


Figure 14. π -overlap between phosphorus d orbitals and ligands. (a) overlap of d_{z^2} with ligand p_{π} orbitals, (b) overlap of $d_{x^2-y^2}$ with ligand p_{π} orbitals.

It should be noted at this point that a plausible explanation of phosphonitrilic bonding can also be formulated using this axial system and the d_{z^2} and $d_{x^2-y^2}$ orbitals.⁷³ In this approach the ring is considered as built up tetrahedra linked together. This bonding scheme is not as satisfactory, however, for the phosphonitriles as it is for isolated tetrahedral configurations. In the case of the phosphonitriles the symmetry at phosphorus is always less than tetrahedral

because of the ring formation and the different electronegativities of the nitrogen and exocyclic atoms. The equality of the participation by these two orbitals is therefore removed. In the phosphonitriles there were advantages to selecting the orbital directions relative to the ring in order to stress the symmetric and antisymmetric aspects of overlap; in isolated tetrahedra the axial directions are chosen along the symmetry axes and this distinction is no longer necessary.

The alkali-metal difluorophosphates are prepared by the reaction of the metal chlorides with difluorophosphoric acid.⁷⁴ For the caesium salt the equation is



The difluorophosphate anion can be considered in terms of the bonding theory described. A shortening of the P-O and P-F bond lengths to values less than the accepted single bond distances should be expected on the basis of this theory, but the relative amount of double bond character in each type of bond is not easy to predict. As will be shown the geometry of the anion in CsPO_2F_2 is very similar to the parameters determined in the isomorphous KPO_2F_2 . The structure of the potassium salt was begun at the same time as the caesium compound but completed sooner by a colleague, R. Harrison.⁷⁵ The X-ray analysis of CsPO_2F_2 was continued, nevertheless, in order to detect any differences which might arise from the larger size of the Cs^+ cation. The singly charged caesium atom with a radius of 1.69 Å is the largest stable monatomic cation. Replacement of a cation by a similar but larger one

often results in an isomorphous structure having increased interionic distances and correspondingly larger cell dimensions. This effect is observed for the cations of potassium, rubidium, and caesium in the perchlorates and fluoroborates which have the barium sulfate structure.⁷⁶

To provide comparable crystallographic data for the difluorophosphate series which has the same basic structure, the cell dimensions of

RbPO_2F_2 were also measured.

B. THE STRUCTURE OF CAESIUM DIFLUOROPHOSPHATE

Experimental

Crystals of CsPO_2F_2 from methanol are colourless needles elongated along \underline{c} . The unit cell dimensions were measured from a \underline{c} -axis rotation photograph, and by the extrapolation method of Farquhar and Lipson⁷⁷ from high-angle reflexions on $hk0$ Weissenberg photographs. The space group was determined from various Weissenberg and precession films, and the density was measured by flotation in a mixture of diiodomethane and iodoform.

Crystal data for the potassium, rubidium, and caesium salts are summarized in Table XIX (λ , $\text{Cu-K}_{\alpha 1} = 1.54051 \text{ \AA}$; λ , $\text{Cu-K}_{\alpha 2} = 1.54433 \text{ \AA}$; λ , $\text{Cu-K}_{\alpha} = 1.5418 \text{ \AA}$).

The intensities for all reflexions with $2\theta(\text{Mo-K}_{\alpha}) \leq 54^\circ$ were measured on a General Electric XRD-5 Spectrogoniometer with a scintillation counter, approximately monochromatic Mo-K_{α} radiation (zirconium filter and pulse-height analyser), and a θ - 2θ scan. Of the 563 reflexions measured, 506 (90%) were observed. The observed intensities were corrected for background, Lorentz and polarization factors were applied, and the structure amplitudes were derived. The crystal used for recording the intensities was mounted with \underline{c} parallel to the ϕ axis of the goniostat and had dimensions $0.25 \times 0.25 \times 0.60$ mm. parallel to \underline{a} , \underline{b} , and \underline{c} respectively. No absorption corrections were applied.

Table XIX

Crystal data for $\underline{M}PO_2F_2$.

<u>M</u>	K	Rb	Cs
Formula	KPO_2F_2	$RbPO_2F_2$	$CsPO_2F_2$
Mol. wt.	140.07	186.44	233.87
Radius of \underline{M}^+ (Å)	1.33	1.48	1.69
Crystal system		Orthorhombic	
<u>a</u> (Å)	8.03 ₉	8.15	8.43 ₇
<u>b</u> (Å)	6.20 ₅	6.45	6.79 ₆
<u>c</u> (Å)	7.63 ₅	7.79	8.06
<u>U</u> (Å ³)	380.9	409.5	462.1
<u>D_m</u> (g.cm. ⁻³)	-	-	3.3
<u>Z</u>	4	4	4
<u>D_c</u> (g.cm. ⁻³)	2.44	3.02	3.36
<u>F</u> (000)	272	344	416
μ (Cu-K α) (cm ⁻¹)	155	215	654
μ (Mo-K α) (cm ⁻¹)	17	130	84
Space group		Pnma (D _{2h} ¹⁶)	

Structure Analysis

Since it was likely that caesium difluorophosphate would be isomorphous with the potassium salt,⁷⁵ structure factors were calculated directly, using the final atomic coordinates of potassium difluorophosphate with isotropic temperature factors. The initial R factor was 0.28. Refinement of the positional and thermal parameters proceeded by block-diagonal least-squares methods, the function minimized being $\sum w(F_o - F_c)^2$ with $\sqrt{w} = |F_o|/15$ when $|F_o| < 15$, and $\sqrt{w} = 15/|F_o|$ when $|F_o| \geq 15$. Unobserved reflexions were given zero weight. Three strong reflexions (102, 210, 400), for which the observed structure factors appeared to be too low, were corrected for secondary extinction by the procedure of Pinnock, Taylor, and Lipson.⁷⁸ Four cycles of refinement with isotropic thermal parameters, and six further cycles with anisotropic thermal parameters reduced R to 0.070 for the 506 observed reflexions. The measured structure factors together with the final calculated values are listed in Table XX.

The final positional and anisotropic thermal parameters are given in Table XXI, together with their standard deviations calculated from the least squares residuals. The significant interatomic distances and angles are compared with those of KPO_2F_2 in Table XXII, and the distances involving the Cs^+ ion are also shown in views of the structure in Figures 15 and 16.

Table XX. Measured and calculated structure factors.

h	k	l	F _o	F _c	h	k	l	F _o	F _c	h	k	l	F _o	F _c	h	k	l	F _o	F _c	h	k	l	F _o	F _c	
0	0	2	76.9	-75.0	1	7	1	22.0	23.4	3	2	9	7.5	-6.5	5	0	5	29.7	15.4	7	0	5	47.8	-10.2	
0	0	4	89.3	-95.8	1	7	2	45.9	46.6	3	2	9	1	43.5	46.9	5	0	6	43.4	-45.8	7	0	7	32.7	30.5
0	0	6	51.5	57.8	1	7	3	29.9	-30.3	3	3	2	97.7	-102.4	5	0	7	18.3	-18.4	7	1	0	0.0	-3.1	
0	0	8	14.4	20.7	1	7	4	21.6	-21.2	3	3	3	21.8	-18.9	5	0	8	28.7	28.4	7	1	1	0.0	-3.1	
0	0	10	28.0	-31.4	1	7	5	13.6	-13.4	3	3	4	55.0	55.3	5	0	9	0.0	-5.9	7	1	2	60.0	-63.0	
0	1	1	73.4	-83.7	1	7	6	14.5	-14.9	3	3	5	33.2	-32.1	5	1	1	53.5	62.2	7	1	3	0.0	-4.3	
0	1	3	87.5	-95.5	1	7	8	13.8	14.8	3	3	6	40.3	39.8	5	1	2	47.8	56.2	7	1	4	22.2	21.6	
0	1	5	147.9	123.5	1	7	10	23.8	-39.7	3	3	7	31.4	29.1	5	1	3	60.1	-66.7	7	1	5	0.0	-4.3	
0	1	7	28.9	26.5	1	7	12	16.1	-16.6	3	3	8	29.0	-27.2	5	1	4	30.9	-33.0	7	1	6	28.8	28.1	
0	1	9	59.2	-49.9	1	7	14	18.0	18.3	3	3	9	0.0	-0.0	5	1	5	14.7	-13.7	7	1	7	11.0	12.2	
0	2	0	238.8	-242.1	2	0	0	10.2	-11.8	3	4	1	59.9	56.0	5	1	6	41.2	44.1	7	2	0	0.0	-3.1	
0	2	2	15.0	-3.9	2	0	2	14.7	-7.8	3	4	2	56.7	55.7	5	1	7	11.9	12.1	7	2	1	47.9	47.5	
0	2	4	144.3	128.3	2	0	4	103.6	-114.1	3	4	3	43.1	41.9	5	1	8	0.0	-3.1	7	2	2	10.4	12.4	
0	2	6	86.1	-72.3	2	0	6	18.4	17.6	3	4	4	21.7	20.6	5	2	1	20.5	21.5	7	2	3	0.0	-0.3	
0	2	8	16.9	-12.4	2	0	8	5.9	9.0	3	4	5	22.4	22.7	5	2	2	85.1	-97.7	7	2	4	36.5	-30.8	
0	2	10	25.4	26.6	2	0	10	6.5	-9.0	3	4	6	42.0	-38.3	5	2	3	5.5	-4.8	7	2	5	0.0	0.0	
0	3	1	104.2	106.9	2	0	12	12.7	14.1	3	4	7	46.4	-44.8	5	2	4	38.5	39.1	7	3	0	57.1	-55.3	
0	3	3	15.9	18.8	2	0	14	2.5	4.5	3	4	8	18.8	-17.1	5	2	5	19.4	-20.7	7	3	1	0.0	0.0	
0	3	5	89.3	-81.0	2	1	0	238.1	-231.2	3	5	1	25.9	30.0	5	2	6	36.7	37.4	7	3	2	22.0	21.4	
0	3	7	29.6	-28.0	2	1	1	24.7	10.1	3	5	2	67.6	65.5	5	2	7	21.7	21.8	7	3	3	13.4	13.9	
0	3	9	46.0	45.8	2	1	2	70.7	77.6	3	5	3	20.8	20.8	5	2	8	25.0	-23.7	7	3	4	6.9	-6.9	
0	3	11	171.9	180.5	2	1	3	3.4	4.2	3	5	4	34.7	-32.0	5	3	1	46.9	-49.6	7	3	5	25.4	-22.9	
0	3	13	27.6	-27.6	2	1	4	93.4	104.7	3	5	5	15.7	16.8	5	3	2	48.9	-50.6	7	3	6	12.8	-12.8	
0	3	15	89.8	-84.8	2	1	5	17.3	-18.8	3	5	6	33.3	-33.5	5	3	3	46.9	-50.6	7	3	7	0.0	0.0	
0	3	17	16.9	51.3	2	1	6	66.2	-70.0	3	5	7	20.1	-18.3	5	3	4	31.2	31.7	7	4	0	28.4	25.4	
0	3	19	16.4	16.7	2	1	7	6.7	3.0	3	5	8	26.0	24.1	5	3	5	15.7	18.2	7	4	1	10.7	11.8	
0	3	21	34.5	-36.2	2	1	8	21.8	-24.5	3	5	9	35.6	35.6	5	3	6	10.7	10.7	7	4	2	9.2	-10.1	
0	3	23	46.3	-48.9	2	1	9	5.9	3.7	3	5	10	39.3	40.7	5	3	7	40.4	-40.7	7	4	3	0.0	-1.8	
0	3	25	12.4	11.5	2	1	10	25.0	24.5	3	5	11	16.8	-17.2	5	3	8	8.2	-8.1	7	4	4	41.8	-41.8	
0	3	27	120.6	-116.7	2	2	0	22.4	23.0	3	6	1	23.9	-23.7	5	3	9	18.7	-18.7	7	4	5	28.0	28.0	
0	3	29	29.3	30.1	2	2	1	115.6	120.7	3	6	2	15.7	16.1	5	3	10	14.7	-14.6	7	4	6	0.0	-1.8	
0	3	31	52.7	53.6	2	2	2	4.5	-3.2	3	6	3	29.6	26.1	5	3	11	13.9	15.6	7	4	7	0.0	-1.8	
0	3	33	33.4	-34.2	2	2	3	44.5	53.1	3	6	4	11.4	-9.3	5	3	12	31.1	-31.4	7	4	8	21.0	-21.0	
0	3	35	10.9	10.9	2	2	4	11.4	9.3	3	6	5	17.3	-17.3	5	3	13	17.7	-16.3	7	4	9	39.3	-38.9	
0	3	37	10.9	10.9	2	2	5	74.3	-66.7	3	6	6	7.4	7.3	5	3	14	34.9	36.0	7	4	10	64.0	65.1	
0	3	39	83.4	-84.8	2	2	6	0.0	4.2	3	6	7	24.1	-23.1	5	3	15	32.0	34.1	7	4	11	42.2	-43.1	
0	3	41	62.3	64.0	2	2	7	24.1	-23.1	3	6	8	27.1	-26.9	5	3	16	17.2	-18.1	7	4	12	0.0	0.0	
0	3	43	10.9	10.9	2	2	8	50.2	45.5	3	6	9	7.4	7.3	5	3	17	17.2	-18.1	7	4	13	7.6	-6.8	
0	3	45	10.9	10.9	2	2	9	133.7	136.4	3	6	10	193.7	196.4	5	3	18	10.2	-12.1	7	4	14	19.7	19.2	
0	3	47	39.9	42.0	2	2	10	11.8	-11.8	3	6	11	11.8	8.3	5	3	19	28.8	27.5	7	4	15	16.4	20.7	
0	3	49	62.3	64.0	2	2	11	11.8	-11.8	3	6	12	7.3	-4.0	5	3	20	6.0	10.4	7	4	16	0.0	0.0	
0	3	51	10.9	10.9	2	2	12	6.7	-7.9	3	6	13	77.0	83.8	5	3	21	46.0	-46.6	7	4	17	16.0	-16.1	
0	3	53	10.9	10.9	2	2	13	41.3	-39.2	3	6	14	25.2	-23.6	5	3	22	8.3	-8.3	7	4	18	37.5	-36.5	
0	3	55	32.7	32.4	2	2	14	19.4	17.6	3	6	15	6.4	5.0	5	3	23	19.0	19.0	7	4	19	0.0	0.0	
0	3	57	37.6	33.8	2	2	15	74.1	68.2	3	6	16	74.1	68.2	5	3	24	8.3	-8.4	7	4	20	19.5	-19.6	
0	3	59	62.3	64.0	2	2	16	11.8	-11.8	3	6	17	8.2	-8.3	5	3	25	21.7	-22.9	7	4	21	21.3	20.7	
0	3	61	10.9	10.9	2	2	17	17.3	-17.3	3	6	18	8.2	-8.3	5	3	26	14.0	12.8	7	4	22	0.0	-0.1	
0	3	63	10.9	10.9	2	2	18	8.2	-8.3	3	6	19	8.2	-8.3	5	3	27	21.7	-22.9	7	4	23	0.0	0.0	
0	3	65	10.9	10.9	2	2	19	8.2	-8.3	3	6	20	30.4	32.8	5	3	28	14.0	12.8	7	4	24	0.0	0.0	
0	3	67	10.9	10.9	2	2	20	17.3	-17.3	3	6	21	61.3	70.2	5	3	29	15.0	-15.0	7	4	25	0.0	0.0	
0	3	69	10.9	10.9	2	2	21	8.2	-8.3	3	6	22	5.9	6.7	5	3	30	27.1	-27.1	7	4	26	0.0	0.0	
0	3	71	10.9	10.9	2	2	22	4.2	-4.2	3	6	23	67.6	76.8	5	3	31	15.4	15.4	7	4	27	28.6	27.5	
0	3	73	10.9	10.9	2	2	23	62.3	61.3	3	6	24	6.0	6.8	5	3	32	12.1	-12.1	7	4	28	0.0	0.0	
0	3	75	10.9	10.9	2	2	24	92.4	93.2	3	6	25	6.0	6.8	5	3	33	12.1	-12.1	7	4	29	0.0	0.0	
0	3	77	10.9	10.9	2	2	25	184.1	139.9	3	6	26	6.0	6.8	5	3	34	12.1	-12.1	7	4	30	0.0	0.0	
0	3	79	10.9	10.9	2	2	26	0.0	-4.9	3	6	27	6.0	6.8	5	3	35	12.1	-12.1	7	4	31	0.0	0.0	
0	3	81	10.9	10.9	2	2	27	40.4	39.3	3	6	28	6.0	6.8	5	3	36	12.1	-12.1	7	4	32	0.0	0.0	
0	3	83	10.9	10.9	2	2	28	111.1	119.7	3	6	29	6.0	6.8	5	3	37	12.1	-12.1	7	4	33	0.0	0.0	
0	3	85	10.9	10.9	2	2	29	16.3	16.4	3	6	30	6.0	6.8	5	3	38	12.1	-12.1	7	4	34	0.0	0.0	
0	3	87	10.9	10.9	2	2	30	47.8	46.5	3	6	31	6.0	6.8	5	3	39	12.1	-12.1	7	4	35	0.0	0.0	
0	3	89	10.9	10.9	2	2	31	0.0	0.8	3	6	32	6.0	6.8	5	3	40	12.1	-12.1	7	4	36	0.0	0.0	
0	3	91	10.9	10.9	2	2	32	5.0	5.0	3	6	33	6.0	6.8	5	3	41	12.1	-12.1	7	4	37	0.0	0.0	
0	3	93	10.9	10.9	2	2	33	16.3	16.4	3	6														

Table XXI. Final positional parameters (fractional) with standard deviations (\AA), and anisotropic thermal parameters ($\text{\AA}^2 \times 10^2$).

Atom	\underline{x}	\underline{y}	\underline{z}	$\sigma(x)$	$\sigma(y)$	$\sigma(z)$
Cs ⁺ (1)	0.1365	0.2500	0.1423	0.0020	0	0.0022
P (2)	0.1099	0.2500	-0.3198	0.0089	0	0.0097
F (3)	0.2510	0.2500	-0.4511	0.029	0	0.027
F (4)	-0.0273	0.2500	-0.4433	0.030	0	0.026
O (5)	0.1125	0.0606	-0.2325	0.016	0.022	0.022

Atom	\underline{U}_{11}	\underline{U}_{12}	\underline{U}_{13}	\underline{U}_{22}	\underline{U}_{23}	\underline{U}_{33}	mean $\sigma(\underline{U})$
Cs ⁺ (1)	4.46	0	0.24	2.82	0	3.62	0.10
P (2)	3.96	0	-0.12	3.06	0	2.87	0.36
F (3)	7.17	0	2.35	7.24	0	5.40	1.44
F (4)	8.05	0	-4.61	9.15	0	5.42	1.42
O (5)	6.40	0.04	1.52	2.87	0.62	5.24	0.90

Discussion

Comparison of the anisotropic thermal parameters of the atoms in caesium difluorophosphate (Table XXI) with the corresponding values in the potassium salt,⁷⁵ indicates that the translational motion of the difluorophosphate ion as a whole is slightly greater in the caesium compound, the root mean square amplitudes of vibration of the phosphorus atom being 0.20, 0.18, 0.17 Å in the a, b, and c directions respectively, as against 0.16, 0.14, 0.16 Å in the potassium compound. The rotational oscillational motions of the PO_2F_2^- ions are very similar in both compounds, and the corrections to the P-O (+ 0.01 Å) and P-F (+ 0.02 Å) bond distances in CsPO_2F_2 are not significantly different from the corrections in the potassium salt. The corrected distances are included in Table XXII.

An analysis of the π -bonding in the difluorophosphate ion has been given for KPO_2F_2 .⁷⁵ The arguments apply equally to the anion in the present compound in view of the similar dimensions obtained. Essentially the X-ray results are in excellent accord with parameters derived from infrared stretching frequencies and indicate a bond order of 1.83 for the P-O bonds with the P-F bonds containing a smaller amount of π -bond character. This π -bonding would presumably occur through overlap between the p orbitals on the ligands and the $\underline{d}_{x^2-y^2}$ and \underline{d}_{z^2} orbitals of phosphorus. Utilizing both d orbitals a total π -bond order of 2 should be attainable in the ion. Fluorine is more reluctant than oxygen to enter into a π -bonding system but the shortened bond does indicate some participation and an assumption of 17% double bond character is not unreasonable.⁷⁵ The greater π -bond character of the bonds to oxygen is

Table XXII. Interatomic distances (Å) and angles (degrees) in $\underline{\text{MPO}}_2\text{F}_2$.

<u>M</u>	K	Cs
Ionic radius of <u>M</u> ⁺	1.33	1.69
P-F(3)	1.552	1.59
P-F(4)	1.552	1.53
Mean P-F	1.552(1.575*)	1.56 (1.58*)
P-O(5)	1.457(1.470*)	1.47 (1.48*)
F(3)-P-F(4)	97.1°	97.7°
O(5)-P-O(5')	122.4	122.6
F(3)-P-O(5)	108.3	107.9
F(4)-P-O(5)	108.9	108.9
Mean F-P-O	108.6	108.4
<u>M</u> -O (2x)	2.76	3.07
<u>M</u> -F	2.83	3.26
<u>M</u> -O (2x)	2.93	3.16
<u>M</u> -O (2x)	3.08	3.29
<u>M</u> -F	3.14	3.42
<u>M</u> -F (2x)	3.34	3.61
<u>M</u> -F	3.62	3.62
<u>M</u> -F	3.68	3.60
<u>M</u> -F (2x)	3.88	4.28
σ (P-F)	0.007	0.03
σ (P-O)	0.005	0.02
σ (F,O-P-F,O)	0.4	1.7°

* corrected for rotational oscillation

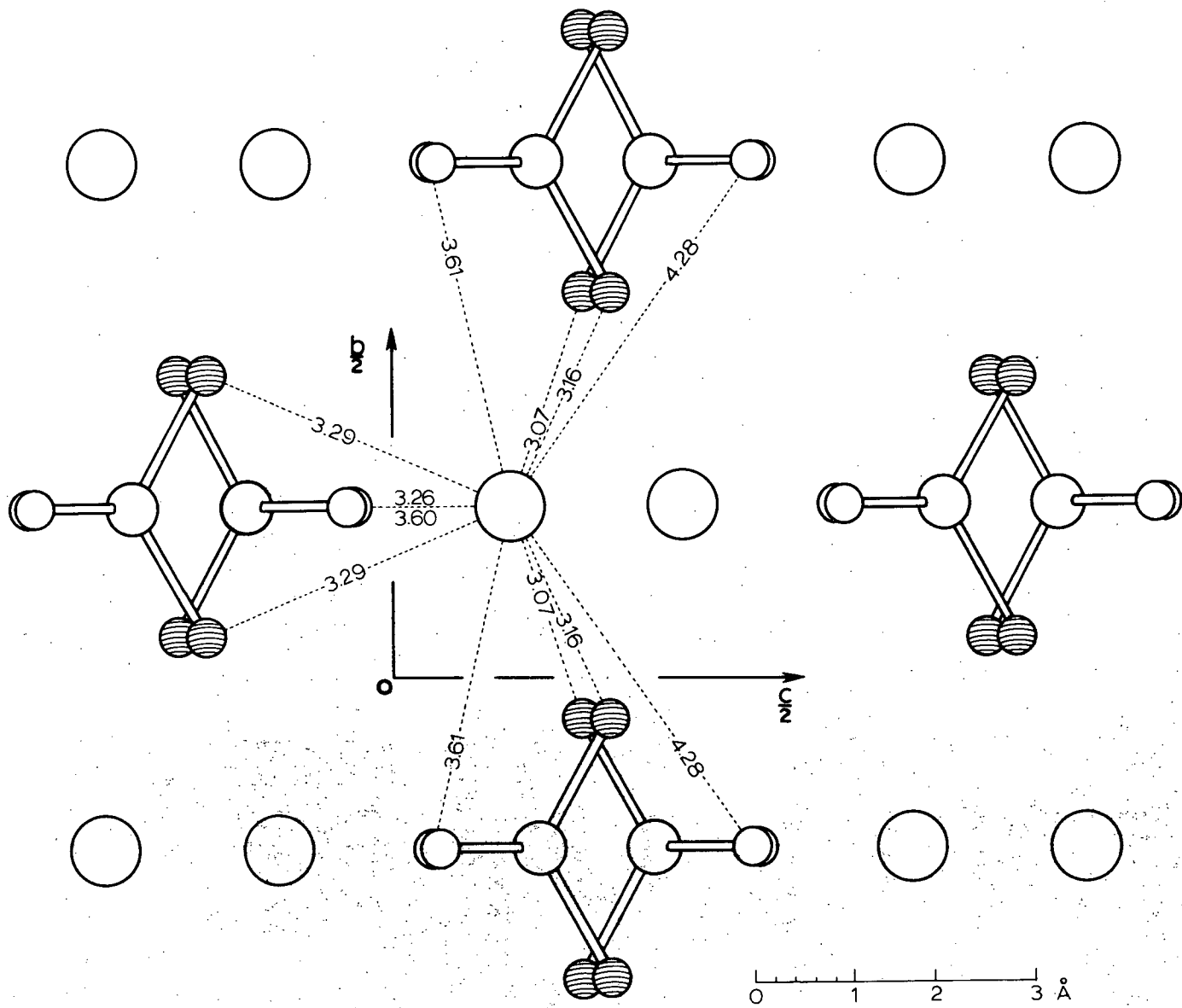


Figure 15. The structure viewed along the a -axis. The oxygen atoms are shaded.

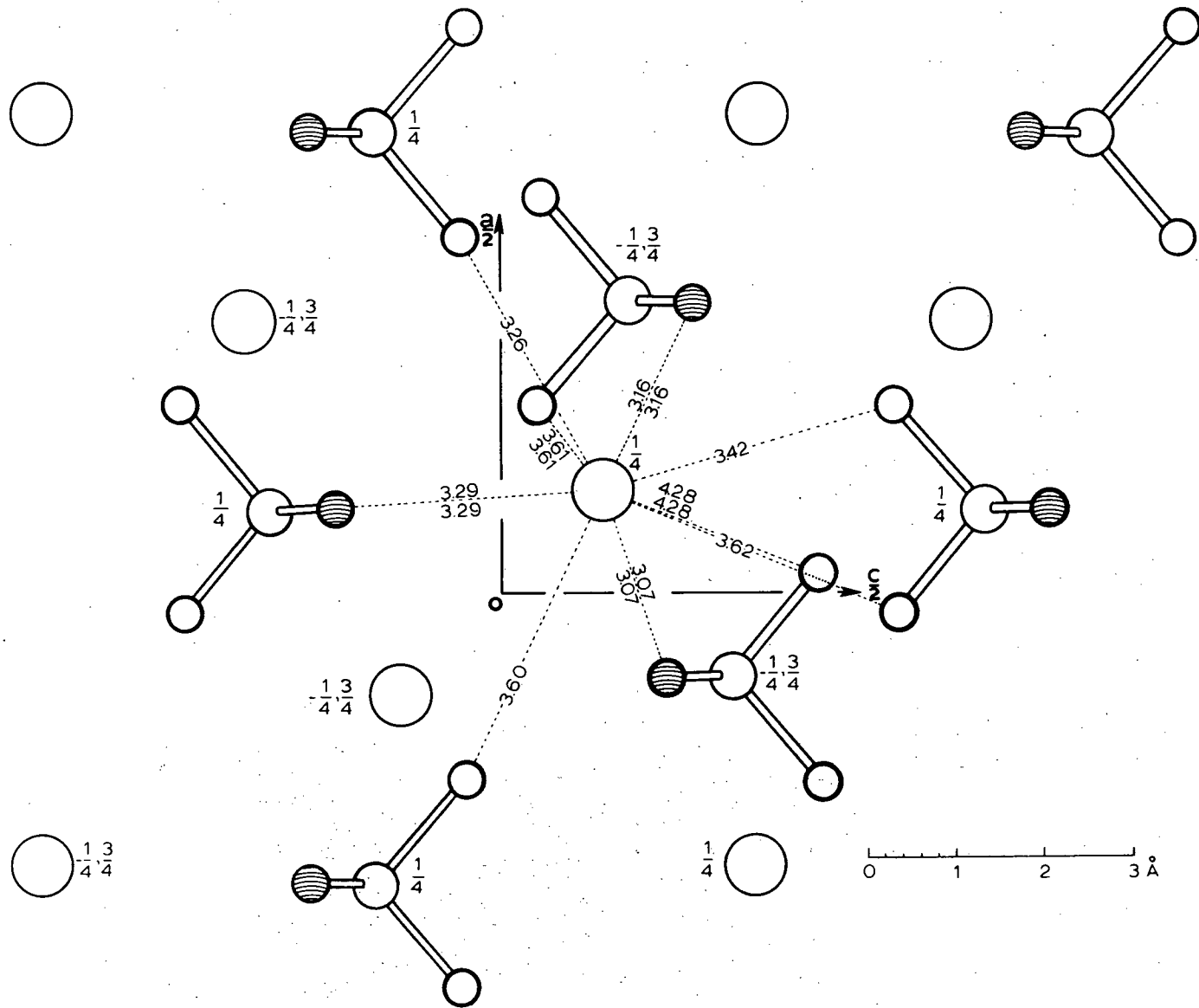


Figure 16. The structure viewed along the b -axis. The oxygen atoms are shaded.

also shown by a comparison of the O-P-O and F-P-F angles which are distorted from the tetrahedral values. The angles are 122.6° and 97.7° respectively because the P-O bonds having the greater electron density repel each other more than do the P-F bonds.

The crystal structure of caesium difluorophosphate is similar to that of the potassium salt. All of the shorter $\text{M}\dots\text{O}$ distances are increased in the caesium compound in accord with the larger ionic radius of Cs^+ (Table XXII). Some of the longer $\text{M}\dots\text{O}$ distances, which are more influenced by anion-anion contacts, have rather similar values in the two structures. The isomorphism of the potassium, rubidium and caesium difluorophosphates is evident from the lattice parameters, which show a steady increase with ionic radius. The interionic distances in the rubidium salt could be estimated approximately by interpolation between the values for the potassium and caesium compounds.

APPENDIX

THE COMPUTER PROGRAMS

COFSYM AND CELDIM

A. COFSYM PROGRAM FOR INDICATING CENTRE OF SYMMETRY

In the structure analysis of $[\text{NP}(\text{OMe})_2]_8$ statistical tests were used to determine the space group and molecular symmetry. A résumé of the theory is presented here, together with the input requirements for the program and a Fortran listing. Good summaries of the method are given in several of the standard references mentioned in the General Introduction at the beginning of the thesis.

For a crystal belonging to the triclinic system, two space groups are possible, $P1$ and $P\bar{1}$. Since a centre of symmetry gives rise to no special absences, the two space groups cannot be distinguished on the basis of systematically missing reflexions. However, Wilson⁷⁹ has shown that the intensity distribution itself is characteristic of the symmetry of the unit cell. Thus if the intensity distribution can be recognized, the proper space group can be inferred.

The distribution of function for a non-centrosymmetric space group can be predicted from the Gaussian equation for a two-dimensional random walk. The resulting expression is

$$P(I)dI = S^{-1} \exp(-I/S)dI$$

where $P(I)dI$ is the proportion of intensities having a value between I and $I+dI$, and S is a distribution parameter equal to the sum of the squares of the atomic scattering factors. It can be identified with $\langle I \rangle$ which is the local average intensity.

For a centrosymmetric space group the structure factors are all real and there are no imaginary terms on an Argand diagram of

structure factors. This simplified distribution can be represented by an equation derived from the expression for a one-dimensional random walk,

$$\frac{1}{I} P(I) dI = (2\pi SI)^{-1/2} \exp(-I/2S) dI$$

The difference between these distributions is usually detectable. Wilson⁸⁰ considered the fraction

$$\rho = \langle |F|^2 \rangle / \langle I \rangle$$

and showed that the ratio of the square of the mean structure amplitude to the local mean intensity should be 0.785 for a non-centrosymmetric distribution, 0.637 for a centric one.

Howells, Phillips and Rogers⁸¹ proposed the $N(Z)$ test in which the choice between distributions is based upon a comparison of a number of points. For this method each intensity is expressed in terms of its local average

$$Z = I / \langle I \rangle$$

Then the fraction $N(Z)$ of reflexions whose intensities are equal to or less than a fraction Z of the local average are given as

$$\frac{1}{I} N(Z) = 1 - \exp(-Z)$$

and

$$\frac{1}{I} N(Z) = \operatorname{erf} \left(\frac{1}{2} Z \right)^{1/2}$$

for the acentric and centric distributions respectively. Here erf is the statistical error function. A comparison of the two theoretical curves

with the experimental one should indicate the appropriate distribution and permit the correct space group to be chosen.

Input for the computer program to carry out these tests consists simply of a starting value of $\sin\theta/\lambda$, the range increment, and the input tape and file number of the data tape. The tape is read twice: the first time to sort the reflexions into ranges and to calculate the averages, and then to determine what fraction each intensity is of its local mean intensity. The intensity distribution is output as well as the Wilson Ratio for each range. The weighted averages can then be compared with the theoretical values in order to determine which is the most likely distribution.

A listing of the program follows. The program is fairly direct and largely self-explanatory. The subroutine POSN is used to locate the correct file on the input tape.

SIBFTC COFSYM

C
C PROGRAM FOR STATISTICAL TEST OF INTENSITY DATA FOR CENTRE OF SYMMETRY
C IN TRICLINIC CRYSTALS

C
DIMENSION SN(10),SUMF2(10),AMEAN(10,10),DIST(10,10),WAVG(10),F(8)
DIMENSION TSUMF(10), RATIO(10)
ARATIO = 0.0
DO 175 K = 1,10
SN(K) = 0.0
SUMF2(K) = 0.0
TSUMF(K) = 0.0
DO 275 I = 1,10
WAVG(I) = 0.0
275 DIST(K,I) = 0.0
175 CONTINUE
READ 5, SOLST, SINCR, INPUT, IFILE
5 FORMAT(2F10.0,2I2)
CALL POSN (INPUT, IFILE)
252 READ(INPUT)II,IGPEN,SSOLS,FH,FK,FL,FOBS,FOBS2,(F(I),I = 1,8)
SOL = SQRT(SSOLS)
IF(IGPEN .NE. 0) GO TO 1
C SORT DATA INTO RANGES AND COUNT
K = 1
SOLLIM = SOLST
100 IF (SOL .LE. SOLLIM) GO TO 101
SOLLIM = SOLLIM + SINCR
IF(K .GE. 10) GO TO 4
K = K + 1
GO TO 100
101 SN(K) = SN(K) + 1.0
SUMF2(K) = SUMF2(K) + FOBS2
TSUMF(K) = TSUMF(K) + ABS(FOBS)
GO TO 252
4 PRINT 15, K, SOL, SOLLIM
15 FORMAT (3X, I4, 2(F10.5, 3X), 40H SOL TOO LARGE - MAKE INCREMENT
1 LARGER)
GO TO 999
1 CONTINUE
C WILSON RATIO TEST

```

      DO 8 K = 1,10
8     RATIO(K) = TSMF(K)**2/(SN(K)* SUMF2(K))
C    CALCULATE MEANS FOR EACH RANGE
      DO 150 K = 1,10
      I = 1
      AMEAN(K,I) = SUMF2(K)/SN(K) * 0.1
      DO 250 I = 2,10
      AI = I
250   AMEAN(K,I) = AMEAN(K,1) * AI
150   CONTINUE
      REWIND INPUT
      CALL POSN (INPUT, IFILE)
253   READ(INPUT) I1,IGPEN,SSOLS,FH,FK,FL,FOBS,FOBS2,(F(I),I = 1,8)
      SOL = SQRT(SSOLS)
      IF(IGPEN .NE. 0) GO TO 11
22    K = 1
      SOLLIM = SOLST
200   IF (SOL .LE. SOLLIM) GO TO 201
      SOLLIM = SOLLIM + SINCR
      K = K + 1
      GO TO 200
C    COMPARE DATA WITH MEANS OF APPROPRIATE RANGE
201   I = 1
300   IF(FOBS2 - AMEAN(K,I))301,301,302
301   DIST(K,I) = DIST(K,I) + 1.0
302   I = I + 1
      IF (I .GT. 10) GO TO 253
      GO TO 300
11    PRINT 55
55    FORMAT(4X, 5HRATIO 6X,11HINTENSITIES 20X,36HINTENSITY DISTRIBUTION
1     N(4) TEST /)
      DO 350 K = 1,10
      DO 450 I = 1,10
450   DIST(K,I) = DIST(K,I)/SN(K)
350   PRINT 65, RATIO(K), SN(K), (DIST(K,I), I = 1,10)
65    FORMAT(1X,F9.4,5X, F9.1, 5X, 10(F9.4))
C    CALCULATE WEIGHTED AVERAGE
      TOT = 0.0
      DO 550 K = 2,9
      ARATIO = ARATIO + RATIO(K) * SN(K)

```

```

550  TOT = TOT + SN(K)
      DO 650 I = 1,10
      DO 750 K = 2,9
750  WAVG(I) = WAVG(I) + SN(K) * DIST(K,I)
      WAVG(I) = WAVG(I)/TOT
650  CONTINUE
      ARATIO = ARATIO/TOT
      PRINT 75, ARATIO, TOT, (WAVG(I), I = 1,10)
75   FORMAT (// 30X, 53HWEIGHTED AVERAGE (OMMITTING FIRST AND LAST
IRANGES) , / 1X, F9.4, 5X, F9.1, 5X, 10(F9.4))
      PRINT 95
95   FORMAT(// 1X, 123HTHE RATIO SHOULD BE COMPARED WITH THE THEORETICA
1L VALUES, 0.637 FOR A CENTRIC DISTRIBUTION, OR 0.785 FOR AN ACENTR
2IC ONE. // 1X, 80HTHE N(Z) DISTRIBUTION SHOULD BE COMPARED WITH T
3HE FOLLOWING THEORETICAL CURVES, /5X, 15HCENTROSYMMETRIC 9X, 90H
4   .2481   .3453   .4187   .4738   .5205   .5614   .5972
5   .6289   .6572   .6833   /5X, 19HNON-CENTROSYMMETRIC 5X, 90H
6   .0952   .1813   .2592   .3297   .3935   .4512   .5034   .5
7507   .5934   .6321   )
999  CALL RUN (INPUT)
      STOP
      END

```

B. CELDIM PROGRAM FOR CELL DIMENSION REFINEMENT

This program is designed to give accurate unit cell parameters by means of a least-squares refinement. The most probable lattice dimensions are found by minimizing the sums of the squares of the deviations between measured and calculated values of sine theta over lambda.

Although the principle of the method is well known,^{2,82-84} a summary of the theory is presented here. In the discussion let there be p parameters and n reflexions. The i th reflexion and j th parameter will be considered as typical.

The general equation relating reciprocal lattice parameters to the Bragg angle is given by

$$h^2 a^{*2} + k^2 b^{*2} + l^2 c^{*2} + 2k l b^* c^* \cos \alpha^* + 2l h c^* a^* \cos \beta^* + 2h k a^* b^* \cos \gamma^* = 4 \frac{\sin^2 \theta}{\lambda^2} = S^2$$

where θ can be measured either on film or by diffractometer. The best values of the parameters are those which make the sum of the squares of the deviations, R,

$$R = \sum_{i=1}^n W_i (|S| - |S_c|)_i^2 = \sum W_i \Delta_i^2$$

a minimum. This will occur for each variable when

$$\frac{\partial R}{\partial p_j} = \sum_{i=1}^n W_i \Delta_i \frac{\partial S_c}{\partial p_j} = 0$$

where p_j is one of the parameters, W_i the weight, S and S_c are measured and calculated values of $\sin\theta/\lambda$, and Δ is their difference.

Although these equations are not linear and hence there may be several minima, a set of equations can be written to give corrections to the parameters by expanding $p_j = (p_j + \Delta p_j)$ as a Taylor series. Since Δp_j is assumed to be a small increment, cross terms such as $\Delta p_j \Delta p_k$ will be very small and derivatives higher than the first can be omitted. This leads to a set of normal equations of the form

$$\sum_{j=1}^p \left\{ \sum_{i=1}^n W_i \frac{\partial S_c}{\partial p_i} \frac{\partial S_c}{\partial p_j} \right\} \Delta p_j = \sum_{j=1}^p \sum_{i=1}^n W_i \Delta_i \frac{\partial S_c}{\partial p_j}$$

which can be solved for the corrections, Δp_j , to the lattice parameters.

In the present application, initial reciprocal dimensions are first calculated from the given direct cell lengths and angles. Then the matrix $\underline{A}(I,J)$ is formed. The element $a_{ij} = \sqrt{W_i} \frac{\partial S_c}{\partial p_{ij}}$ is the derivative of the general equation with respect to the p_{ij} j th parameter for the i th reflexion multiplied by the square root of the weight appropriate for that reflexion. The matrix $\underline{G}(I,1)$ is formed by using the initial parameters to calculate a value of S_c . The differences between the observed and calculated values of $\sin\theta/\lambda$ are multiplied by the observed value and the square root of the weight to give the general element $g_i = \sqrt{W_i} \Delta_i S_i$. The weighted observational equations are then given by $\underline{A}\underline{P} = \underline{G}$ where \underline{P} is a column matrix with the element $p_j = \Delta p_j$. To obtain the p normal equations which determine the p unknowns it is only necessary to multiply each side of the matrix equation above by \underline{A}^t the transpose of

\underline{A} (formed by replacing each element a_{ij} by a_{ji}). In the program,

$\underline{B} = \underline{A}^t \underline{A}$ and $\underline{E} = \underline{A}^t \underline{G}$. The normal equations are written as $\underline{B}\underline{P} = \underline{E}$

$$\text{or } e_j = \sum_k b_{jk} p_k \quad \text{where } b_{ij} = \sum_k a_{ki} a_{kj}.$$

The corrections to the parameters are then given by $\underline{P} = \underline{B}^{-1} \underline{E}$ where \underline{B}^{-1} is the inverse of the matrix \underline{B} .

The variance, σ^2 , is estimated from the residuals

$$\sigma^2 = \frac{\sum_{i=1}^n W_i \Delta_i^2}{(n-p)}$$

and the standard deviation of the j th parameter is then given by

$$\sigma(p_j) = \sqrt{b_{jj}^{-1} \sigma^2}$$

where b_{jj}^{-1} is the corresponding diagonal element of the inverse matrix \underline{B}^{-1} . The corrections to the parameters are applied and the cycle is repeated with the new values until the change in variance is less than 10% between cycles. In practice, rarely more than three cycles are required for convergence. After the final cycle, real parameters are calculated and output together with their standard deviations.

During the formation of the derivatives, lattice restrictions are observed. For example, in the monoclinic system, α and γ are held at 90.0° by setting $\partial\alpha^* = \partial\gamma^* = 0$. This can be overruled, however. If it is desirable, all parameters can be refined merely by treating the crystal as triclinic. Alternatively, if β were known very accurately and was not to be refined, a monoclinic crystal could be treated as an

orthorhombic one in which case only the axial lengths would be refined. In addition a FUDGE(J) factor can be controlled so as to apply any fraction of the calculated correction to a parameter.

Various weighting schemes are incorporated in the program including several functions of theta and a form of the Nelson Riley function. In general, however, for theta values less than 20° these weighting schemes lead to very similar results and a weight of one is usually used for each reflexion. Reflexions of exceptional reliability can be weighted individually.

The program is primarily intended to refine cell dimensions from diffractometer measurements prior to calculating final angular settings. It may also be used to give cell dimensions from zero-layer Weissenberg photographs. It is particularly useful here when there are few axial spots since general spots on the layer may also be measured. The program may be used with data obtained from a back-reflexion camera. Here, the positions of the front- and back-reflected spots are used to accurately determine the effective radius of the film cassette. Values of theta are then derived from the film measurements and the data are refined as before.

The subroutines used in this program are standard library programs of the U.B.C. Computing Centre. The purpose and result of each subroutine call is fairly straight-forward. Programming details can be found in the UBCMATR subroutine package for square matrices.⁸⁵

On the following pages are a description of the input requirements for the program and a source deck listing.

CELDIM CELL DIMENSION REFINEMENT BY LEAST SQUARES

The program is designed to refine unit cell parameters and will accept θ , 2θ , or back reflexion data for general HKL reflexions.

- Notes :
1. No decimals to be punched.
 2. Limit of reflexions is 30.
 3. Bracketed columns need not be punched.

Input Requirements

<u>Column</u>		<u>Description</u>
<u>Card 1</u>	-	Identification
2-80		Anything for identification
<u>Card 2</u>	-	Initial cell parameters
1-5	xx.xxx	a .xxxxx a*
6-10	xx.xxx	b .xxxxx b*
11-15	xx.xxx	c .xxxxx c*
16-21	(xxx.xxx)	α (xxx.xxx) α^*
22-27	(xxx.xxx)	β (xxx.xxx) β^*
28-33	(xxx.xxx)	γ (xxx.xxx) γ^*
		90° assumed if angles left blank
34	(x)	1 if RECIPROCAL DIMENSIONS
35-36	xx	CRYSTAL SYSTEM: 1 = triclinic, 2 = monoclinic, 3 = orthorhombic, 4 = tetragonal, 5 = cubic, 6 = hexagonal, 7 = rhombohedral
40-41	xx	RADIATION: 1 = Mo-K α , 2 = Cu-K α
42-43	(xx)	METHOD: 0 = read in θ , 1 = read in 2θ , 2 = back reflexion, read in separation (mm.)
44-45	(xx)	WEIGHTING SCHEME: 0 = 1, 1 = $\sin\theta$, 2 = $\tan\theta$, 3 = $\sin^2\theta$, 4 = $\sin^22\theta$, 5 = form of Nelson- Riley function
50-51	xx	NUMBER OF REFLEXIONS
52-53	(xx)	NUMBER OF CYCLES: usually = 0, program will run until convergence

...../continued

Card 3 - Data cards - one card per reflexion

1-3	±xx	H
4-6	±xx	K
7-9	±xx	L
15-20	xxx.xxx	POSITION: θ , 2θ , or position of front reflexion (mm.) depending on METHOD
22-23	(xx)	WAVELENGTH: if different from initial radiation, 1 = Mo-K α , 2 = Cu-K α , 3 = Mo-K α , 4 = Mo-K α , 5 = Mo-K β , 6 = Cu-K α , 7 = Cu-K α , 8 = Cu-K β , 9 = special
25-30	(xxx.xxx)	POSITION OF FRONT REFLEXION: (mm.)
35-40	(xxx.xxx)	POSITION OF BACKREFLEXION: (mm.)
45-50	(xxx.xxx)	POSITION OF BACK REFLEXION: (mm.)
55-60	(x.xxxxx)	SPECIAL RADIATION: (only if 9 in 23)
61-66	(xx.xxxx)	SPECIAL WEIGHT

\$IBFTC CELDIM

```
C REFINEMENT OF CELL PARAMETERS BY LEAST SQUARES MARCH 1968
DIMENSION A(30,30), ATRAN(30,30), P(6,6)
DIMENSION ZH(30), ZK(30), ZL(30), THETA(30)
DIMENSION G(30,30), NEWLAM(30), WAIT(30)
DIMENSION B(30,30), E(30,30), B6U6,6), E6(6,6)
DIMENSION WAV(9), FUDGE(6), NSTORE(30)
DIMENSION SYSTEM(14)
DIMENSION ICOL(6), TEMP(6), ATEMP(30,30)
DIMENSION SIG6(6,6), SIGREP(6,6), REALSG(6,6)
DIMENSION VIANCE(10), LABRL(12), LABREP(12)
DATA WAV/54HMOA CUA MOA1 MOA2 MOB1 CUA1 CUA2 CUB SPEC
1 /
DATA SYSTEM/ 84TRICLINIC MONOCLINIC ORTHORHOMBICTETRAGONAL CU
1BIC HEXAGONAL RHOMBOHEDRAL /
DATA LABRL/72HA AXIS = B AXIS = C AXIS = ALPHA = BETA
1 = GAMMA = /
DATA LABREP/72H A AXIS * B AXIS * C AXIS * ALPHA * BE
1TA * GAMMA * /
IEND = 0
IRANK = 0
ICOLS = 0
IRECIP = 0
NLOW = 0
NHIGH = 0
SENT = 0.0
SEXIT = 0.0
DSTH1 = 0.0
DSTH2 = 0.0
DISTL2 = 0.0
MCYCLE = 1
DO 51 J = 1, 6
TEMP(J) = 0.0
FUDGE(J) = 1.0
51 ICOL(J) = 0
C TO HOLD A PARTICULAR LENGTH OR ANGLE CONSTANT SET FUDGE(J) = 0
C FOR THAT VARIABLE
DO 52 I = 1, 30
NEWLAM(I) = 0
NSTORE(I) = 0
```

```

DO 53 J = 1, 30
ATEMP(I,J) = 0.0
53 A(I,J) = 0.0
52 CONTINUE
DO 111 I = 1, 6
DO 112 J = 1, 6
SIGREP(I,J) = 0.0
REALSG(I,J) = 0.0
112 SIG6(I,J) = 0.0
111 CONTINUE
PRINT 22
22 FORMAT(1H0, 23HUNIT CELL LEAST SQUARES / )
READ 4
4 FORMAT (1X, 79H
1
PRINT 4
READ 1, AAXIS, BAXIS, CAXIS, ALPHA, BETA, GAMMA, IRECIP, ITYPE,
1 I WAVE, METHOD, IWAIT, NDATA, NCYCLE
1 FORMAT (3F5.3, 3F6.3, I1, I2, 3X, 3I2, 4X, 2I2 )
PRINT 23, NDATA, SYSTEM(2*ITYPE-1), SYSTEM(2*ITYPE)
23 FORMAT (5X, I3, 8H PLANES, 10X, 2A6 )
DATA = NDATA
IF(AAXIS .EQ. 0.0 .OR. BAXIS .EQ. 0.0 .OR. CAXIS .EQ. 0.0)PRINT 25
25 FORMAT(1H0, 44HTHE PROGRAM REQUIRES ALL THREE AXIAL LENGTHS )
IF(AAXIS .EQ. 0.0 .OR. BAXIS .EQ. 0.0 .OR. CAXIS .EQ. 0.0)GOTO 999
IF(ALPHA .EQ. 0.0) ALPHA = 90.0
IF(BETA .EQ. 0.0) BETA = 90.0
IF(GAMMA .EQ. 0.0) GAMMA = 90.0
IF (IRECIP .EQ. 1) GO TO 8
PRINT 3, LABRL(1),LABRL(2),AAXIS,LABRL(3),LABRL(4),BAXIS,LABRL(5),
1LABRL(6),CAXIS,LABRL(7),LABRL(8),ALPHA,LABRL(9),LABRL(10),BETA,
2 LABRL(11),LABRL(12),GAMMA
3 FORMAT(1H0, 9X, 24HORIGINAL REAL PARAMETERS // (12X,A6,A4,F10.3))
GO TO 10
8 AAXIS = AAXIS/100.0
BAXIS = BAXIS/100.0
CAXIS = CAXIS/100.0
PRINT 9,LABREP(1),LABREP(2), AAXIS,LABREP(3),LABREP(4),BAXIS,
1 LABREP(5), LABREP(6), CAXIS
9 FORMAT(1H0,9X, 30HORIGINAL RECIPROCAL PARAMETERS // (14X,A6,A4,

```

```

1 3H= , F10.5))
  PRINT 7,LABREP(7),LABREP(8),ALPHA,LABREP(9),LABREP(10),BETA,
1 LABREP(11),LABREP(12),GAMMA
7  FORMAT (14X,A6,A4,1H=,F10.3)
10  ALPHA = ALPHA/57.295779
    BETA  = BETA/57.295779
    GAMMA = GAMMA/57.295779
    IF (IWAVE .EQ. 1) WAVE = 0.71069
    IF (IWAVE .EQ. 2) WAVE = 1.54178
    ORIG = WAVE
    IF (METHOD .EQ. 2) PRINT 36
36  FORMAT(1H1, 10X, 19HBACK REFLEXION DATA // 77H PLANE H K
1    L LOW ANGLE POSITION HIGH ANGLE POSITION /)
    IF (IRECIP .EQ. 1) GO TO 49
500 VOL = AAXIS*BAXIS*CAXIS*SQRT(1.0+2.0*COS(ALPHA)*COS(BETA)*COS(
1 GAMMA)-COS(ALPHA)**2 -COS(BETA)**2 -COS(GAMMA)**2)
    ASTAR = BAXIS*CAXIS*SIN(ALPHA)/VOL
    BSTAR = CAXIS*AAXIS*SIN(BETA)/VOL
    CSTAR = AAXIS*BAXIS*SIN(GAMMA)/VOL
    CALSTR = (COS(BETA)*COS(GAMMA)-COS(ALPHA))/(SIN(BETA)*SIN(GAMMA))
    CBESTR = (COS(GAMMA)*COS(ALPHA)-COS(BETA))/(SIN(GAMMA)*SIN(ALPHA))
    CGASTR = (COS(ALPHA)*COS(BETA)-COS(GAMMA))/(SIN(ALPHA)*SIN(BETA))
    ALSTR = ARCOS(CALSTR)
    BESTR = ARCOS(CBESTR)
    GASTR = ARCOS(CGASTR)
    IF(IEND)50, 50, 300
49  ASTAR = AAXIS
    BSTAR = BAXIS
    CSTAR = CAXIS
    ALSTR = ALPHA
    BESTR = BETA
    GASTR = GAMMA
50  DO 100 I = 1, NDATA
    READ 2, IH, IK, IL, THETA(I), NEWLAM(I), DISTL2, DISTH1, DISTH2,
1 SPWAVE, SPECWT
2  FORMAT(3I3, 5X, F6.3, 1X, I2, 1X, 3(F6.3,4X), F6.5, F6.4)
    ZH(I) = IH
    ZK(I) = IK
    ZL(I) = IL
    IF(METHOD .NE. 2) GO TO 71

```

```

C      CALCULATION OF THETA FROM BACK REFLEXION DATA
      IF(THETA(I) .NE. 0.0 .OR. DISTL2 .NE. 0.0) PRINT 37, I, IH, IK,
1 IL, THETA(I), DISTL2
37     FORMAT(5X, I3, 4X, 3(I3,2X), 2(2X, F8.2))
      IF(THETA(I) .EQ. 0.0 .AND. DISTL2 .EQ. 0.0) PRINT 38, I, IH, IK,
1 IL, DISTH1, DISTH2
38     FORMAT(5X, I3, 4X, 3(I3,2X), 28X, 2(2X, F8.2))
      IF(THETA(I) .EQ. 0.0 .OR. DISTL2 .EQ. 0.0) GO TO 75
      EXIT = (THETA(I) + DISTL2)/2.0
      THETA(I) = ABS(THETA(I) - DISTL2)
      NLOW = NLOW + 1
      SEXIT = SEXIT + EXIT
      GO TO 100
75     IF(THETA(I) .EQ. 0.0 .AND. DISTL2 .EQ. 0.0) GO TO 76
      THETA(I) = ABS(THETA(I) - DISTL2)
      NSTORE(I) = 1
      GO TO 100
76     IF(DISTH1 .EQ. 0.0 .OR. DISTH2 .EQ. 0.0) GO TO 77
      ENTRY = (DISTH1 + DISTH2)/2.0
      THETA(I) = ABS(DISTH1 - DISTH2)
      NHIGH = NHIGH + 1
      SENT = SENT + ENTRY
      NSTORE(I) = 2
      GO TO 100
77     THETA(I) = ABS(DISTH1 - DISTH2)
      NSTORE(I) = 3
      GO TO 100
71     THETA(I) = THETA(I)/57.295779
      IF (METHOD .EQ. 1) THETA(I) = THETA(I)/2.0
100    CONTINUE
      IF(METHOD .NE. 2) GO TO 60
      CTHIGH = NHIGH
      CTLOW = NLOW
      AVENT = SENT/CTHIGH
      AVEXIT = SEXIT/CTLOW
      HFCIR = ABS(AVENT - AVEXIT)
      RADIUS = HFCIR/3.1415927
      PRINT 80, RADIUS
80     FORMAT(1H0, 43EFFECTIVE RADIUS OF BACK REFLEXION CAMERA = ,F10.5,
1 6H M.M. )

```

```

DO 81 I = 1, NDATA
IF(NSTORE(I) .GT. 1) GO TO 85
IF(NSTORE(I) .EQ. 1) GO TO 84
ANG = (THETA(I)/(4.0*RADIUS))
THETA(I) = ANG
GO TO 81
84  FDIST = ABS(THETA(I) - AVEXIT)* 2.0
    ANG = FDIST/(4.0*RADIUS)
    THETA(I) = ANG
    GO TO 81
85  IF(NSTORE(I) .EQ. 3) GO TO 86
    ANG = 3.1415927/2.0 - THETA(I) / (4.0*RADIUS)
    THETA(I) = ANG
    GO TO 81
86  BDIST = ABS(THETA(I) - AVENT) * 2.0
    ANG = 3.1415927/2.0 - BDIST / (4.0*RADIUS)
    THETA(I) = ANG
81  CONTINUE
60  PRINT 35
35  FORMAT(1H1, 95H      PLANE      H      K      L      THETA OBS      THETA CA
1L   DIFF      WT      RAD@N      MINIMIZE /)
    SDEL = 0
    DO 200 I = 1, NDATA
70  IF (IWAIT .EQ. 0) WAIT(I) = 1.0
    IF (IWAIT .EQ. 1) WAIT(I) = SIN(THETA(I))
    IF (IWAIT .EQ. 2) WAIT(I) = TAN(THETA(I))
    IF (IWAIT .EQ. 3) WAIT(I) = SIN(THETA(I))**2
    IF (IWAIT .EQ. 4) WAIT(I) = SIN(THETA(I)*2.0)**2
    IF (IWAIT .EQ. 5) WAIT(I) = 1.0/(2.0*(COS(THETA(I))**2/SIN(THETA(I))
1 + COS(THETA(I))**2/THETA(I)))
C   OTHER WEIGHTING SCHEMES MAY BE INCLUDED HERE
    IF (SPECWT .NE. 0.0) WAIT(I) = SPECWT
    ROOTWT = SQRT(WAIT(I))
    GO TO (400,400,400,401,402,403,404), ITYPE
C   PREPARATION OF MATRIX OF DERIVATIVES (OBSERVATION EQUATIONS)
401  A(I,1) = ((ZH(I)**2 + ZK(I)**2)*AS1AR)*ROOTWI
    A(I,3) = (ZL(I)**2*CS1AR)*ROOTWI
    GO TO 61
402  A(I,1) = ((ZH(I)**2 + ZK(I)**2 + ZL(I)**2)*AS1AR)*ROOTWI
    GO TO 61

```

```

403  A(I,1) = ((ZH(I)**2 + ZK(I)**2 + 2.0*ZH(I)*ZK(I)*COS(GASIR))
1  *ASTAR)*ROOTWT
      A(I,3) = (ZL(I)**2*CSTAR)*ROOTWT
      GO TO 61
404  A(I,1) = ((ZH(I)**2 + ZK(I)**2 + ZL(I)**2)*ASIR + 2.0*COS(ALSIR)
1  *(ZK(I)*ZL(I) + ZL(I)*ZH(I) + ZH(I)*ZK(I))*ASTAR)*ROOTWT
      A(I,4) = (-SIN(ALSTR)*ASTAR**2*(ZK(I)*ZL(I) + ZL(I)*ZH(I) + ZH(I)
1  *ZK(I)))*ROOTWT
      GO TO 61
400  A(I,1) = ROOTWT*(ZH(I)**2*ASTAR + ZH(I)*ZL(I)*CSIR*COS(BESIR)
1  + ZH(I)*ZK(I)*BSTAR*COS(GASTR))
      A(I,2) = ROOTWT*(ZK(I)**2*BSIR + ZK(I)*ZH(I)*ASIR*COS(GASIR)
1  + ZK(I)*ZL(I)*CSTAR*COS(ALSTR))
      A(I,3) = ROOTWT*(ZL(I)**2*CSTAR + ZL(I)*ZK(I)*BSIR*COS(ALSTR)
1  + ZL(I)*ZH(I)*ASTAR*COS(BESTR))
      IF (ITYPE .GE. 3 .AND. ITYPE .LE. 6) GO TO 61
      IF (ITYPE .EQ. 2) GO TO 62
      A(I,4) = ROOTWT*(-ZK(I)*ZL(I)*BSTAR*CSTAR*SIN(ALSIR))
      A(I,6) = ROOTWT*(-ZH(I)*ZK(I)*ASTAR*BSTAR*SIN(GASIR))
62  A(I,5) = ROOTWT*(-ZL(I)*ZH(I)*CSIR*ASIR*SIN(BESIR))
61  GCALC = SQRT(ZH(I)**2*ASTAR**2 + ZK(I)**2*BSTAR**2
1  + ZL(I)**2*CSTAR**2
2  + 2.0*ZK(I)*ZL(I)*BSTAR*CSIR*COS(ALSIR)
3  + 2.0*ZL(I)*ZH(I)*CSIR*ASIR*COS(BESIR)
4  + 2.0*ZH(I)*ZK(I)*ASIR*BSIR*COS(GASIR))
      IF (NEWLAM(I))32,32,33
33  IF (NEWLAM(I) .EQ. 1) WAVE = 0.71069
      IF (NEWLAM(I) .EQ. 2) WAVE = 1.54178
      IF (NEWLAM(I) .EQ. 3) WAVE = 0.70926
      IF (NEWLAM(I) .EQ. 4) WAVE = 0.71354
      IF (NEWLAM(I) .EQ. 5) WAVE = 0.632253
      IF (NEWLAM(I) .EQ. 6) WAVE = 1.54051
      IF (NEWLAM(I) .EQ. 7) WAVE = 1.54433
      IF (NEWLAM(I) .EQ. 8) WAVE = 1.39217
      IF (NEWLAM(I) .EQ. 9) WAVE = SPWAVE
32  GMEAS = 2.0*SIN(THETA(I))/WAVE
      DEL = GMEAS - GCALC
      SDEL = SDEL + ABS(DEL)
      THCALC = ARSIN(GCALC*WAVE/2.0)*57.295779
      THOBS = THETA(I)*57.295779

```

```

DIFTH = THOBS - THCALC
J = IWAVE
IF (NEWLAM(I) .NE. 0) J = NEWLAM(I)
IH = ZH(I)
IK = ZK(I)
IL = ZL(I)
PRINT 34, I, IH, IK, IL, THOBS, THCALC, DIFTH, WAI(I), WAV(J), DEL
34  FORMAT(5X, I3, 5X, 3(I3, 2X), 2(3X, F9.5), 3X, F8.5, 4X, F6.2, 5X, A4, 5X, F9.5)
G(I, 1) = ROOTWT*DEL*GMEAS
WAVE = ORIG
200 CONTINUE
C DETERMINATION OF RANK AND REMOVAL OF ZERO ROWS
IF(IRANK .EQ. 6) GO TO 275
IF(MCYCLE .GT. 1) GO TO 256
DO 251 J = 1, 6
DO 252 I = 1, NDATA
IF(A(I, J) .NE. 0.0) GO TO 251
IF(I .EQ. NDATA) ICOL(J) = 1
252 CONTINUE
251 CONTINUE
DO 255 J = 1, 6
255 ICOLS = ICOLS + ICOL(J)
IRANK = 6 - ICOLS
IF(IRANK .EQ. 6) GO TO 275
256 NCOL = 0
DO 260 J = 1, 6
L = J - NCOL
IF (ICOL(J) .NE. 1) GO TO 263
NCOL = NCOL + 1
GO TO 260
263 DO 261 I = 1, NDATA
ATEMP(I, L) = A(I, J)
261 CONTINUE
260 CONTINUE
DO 265 J = 1, 6
DO 266 I = 1, NDATA
266 A(I, J) = ATEMP(I, J)
265 CONTINUE
275 CONTINUE
DEVN = SDEL/DATA

```

```

PRINT 103, IRANK, DEVN
103  FORMAT (1H0, 6HRANK = , I5, 58X, 17HMEAN DEVIATION = , F9.5)
      CALL TRANSP(A, ATRAN, NDATA, 30)
      CALL MULT(ATRAN, A, B, NDATA, 30)
      DO 109 I = 1, IRANK
      DO 109 J = 1, IRANK
109   B6(I,J) = B(I,J)
      CALL MULT(ATRAN, G, E, NDATA, 30)
      DO 110 I = 1, IRANK
      DO 110 J = 1, IRANK
110   E6(I,J) = E(I,J)
      CALL INVERT(B6, IRANK, 6, DET, CONDNO)
      PRINT 39, DET
39   FORMAT (1X, 14HDETERMINANT = , 1PE16.5 /)
      IF (DET .EQ. 0.0) GO TO 999
      CALL MULT(B6, E6, P, IRANK, 6)
      RANK = IRANK
      SIGSQD = 0.0
      DO 180 I = 1, NDATA
180   SIGSQD = SIGSQD + G(I,1)**2
      SIGSQD = SIGSQD/(DATA - RANK)
      VIANCE(MCYCLE) = SIGSQD
      IF (IRANK .EQ. 6) GO TO 276
C    ADJUSTMENT OF MAIRICES TO ALLOW FOR ZERO ROWS
      J = 0
      DO 281 I = 1,6
      J = J + 1
      IF(ICOL(I) .NE. 1) GO TO 282
      GO TO 283
282   TEMP(I) = P(J,1)
      GO TO 281
283   TEMP(I) = 0.0
      J = J - 1
281   CONTINUE
      DO 284 I = 1,6
      P(I,1) = TEMP(I)
284   TEMP(I) = 0.0
      J = 0
      DO 291 I = 1,6
      J = J + 1

```

```

IF(ICOL(I) .NE. 1) GO TO 292
GO TO 293
292 TEMP(I) = B6(J,J)
GO TO 291
293 TEMP(I) = 0.0
J = J - 1
291 CONTINUE
DO 294 I = 1,6
B6(I,I) = TEMP(I)
294 TEMP(I) = 0.0
276 SIGA = SQRT(B6(1,1)*SIGSQD)
SIGB = SQRT(B6(2,2)*SIGSQD)
SIGC = SQRT(B6(3,3)*SIGSQD)
SIGAL= SQRT(B6(4,4)*SIGSQD)
SIGBE= SQRT(B6(5,5)*SIGSQD)
SIGGA= SQRT(B6(6,6)*SIGSQD)
ANEW = ASTAR + P(1,1) * FUDGE(1)
BNEW = BSTAR + P(2,1) * FUDGE(2)
CNEW = CSTAR + P(3,1) * FUDGE(3)
ALNEW= ALSTR + P(4,1) * FUDGE(4)
BENEW= BESTR + P(5,1) * FUDGE(5)
GANEW= GASTR + P(6,1) * FUDGE(6)
IF(ITYPE .GE. 4) BNEW = ANEW
IF(ITYPE .EQ. 5 .OR. ITYPE .EQ. 7) CNEW = ANEW
IF(ITYPE .EQ. 7) BENEW = ALNEW
IF(ITYPE .EQ. 7)CNEW = ALNEW
ALSDEG = ALNEW*57.295779
BESDEG = BENEW*57.295779
GASDEG = GANEW*57.295779
PRINT 181
181 FORMAT(10X, 22HRECIPROCAL DIMENSIONS //14X, 95HPREVIOUS VALUE
1 SHIFT NEW PARAMETER SIGMA D
2EGREES /)
182 FORMAT(A6,A4, 3(5X,F10.6), 10X,F10.6,15X,F15.5)
PRINT 182,LABREP(1),LABREP(2),AS,AR,P(1,1),ANEW,SIGA
PRINT 182,LABREP(3),LABREP(4),BS,AR,P(2,1),BNEW,SIGB
PRINT 182,LABREP(5),LABREP(6),CS,AR,P(3,1),CNEW,SIGC
PRINT 182,LABREP(7),LABREP(8),ALS,IR,P(4,1),ALNEW,SIGAL,ALSDEG
PRINT 182,LABREP(9),LABREP(10),BES,IR,P(5,1),BENEW,SIGBE,BESDEG
PRINT 182,LABREP(11),LABREP(12),GAS,IR,P(6,1),GANEW,SIGGA,GASDEG

```

```

PRINT 183, MNCYCLE, SIGSQD
183  FORMAT(5X, 13HEND OF CYCLE ,I3,5A,15HSIGMA SQUARED = ,1PE16.6, /)
      IF(NCYCLE - 1) 189,190, 191
189  IF(MNCYCLE .EQ. 1) GO TO 191
      IF(VIANCE(MNCYCLE-1) - VIANCE(MNCYCLE) .LT. 0.1 *VIANCE(MNCYCLE)
1  .OR. MNCYCLE .GE. 10) GO TO 190
191  NCYCLE = NCYCLE - 1
      MNCYCLE = MNCYCLE + 1
      ASTAR = ANEW
      BSTAR = BNEW
      CSTAR = CNEW
      ALSTR = ALNEW
      BESTR = BENEW
      GASTR = GANEW
C    HAVE RESET RECIPROCAL DEMENSIONS
      GO TO 60
190  IEND = 1
      AAXIS = ANEW
      BAXIS = BNEW
      CAXIS = CNEW
      ALPHA = ALNEW
      BETA = BENEW
      GAMMA = GANEW
C    ALL THESE ARE RECIPROCAL DIMENSIONS
      GO TO 500
300  AFINL = ASTAR
      BFINL = BSTAR
      CFINL = CSTAR
      ALFINL = ALSTR
      BEFINL = BESTR
      GAFINL = GASTR
C    THESE @FINL@ VALUES ARE FINAL REAL VARIABLES
      ALFDEG = ALFINL * 57.295779
      BEFDEG = BEFINL * 57.295779
      GAFDEG = GAFINL * 57.295779
C    DERIVATIVES OF REAL PARAMETERS wCR.T. RECIPROCAL ONES
      SIG6(1,1) = -AFINL/ANEW
      SIG6(1,5) = -AFINL*COTAN(BENEW)
      SIG6(1,6) = -AFINL*COTAN(GANEW)
      SIG6(2,2) = -BFINL/BNEW

```

```

SIG6(2,4) = -BFINL*COTAN(ALNEW)
SIG6(2,6) = -BFINL*COTAN(GANEW)
SIG6(3,3) = -CFINL/CNEW
SIG6(3,4) = -CFINL*COTAN(ALNEW)
SIG6(3,5) = -CFINL*COTAN(BENEW)
SIG6(4,4) = -SIN(ALNEW)/(SIN(ALFINL)*SIN(BENEW)*SIN(GANEW))
SIG6(4,5) = (COS(ALFINL)*COTAN(BENEW) + COTAN(GANEW))/SIN(ALFINL)
SIG6(4,6) = (COS(ALFINL)*COTAN(GANEW) + COTAN(BENEW))/SIN(ALFINL)
SIG6(5,4) = (COS(BEFINL)*COTAN(ALNEW) + COTAN(GANEW))/SIN(BEFINL)
SIG6(5,5) = -SIN(BENEW)/(SIN(BEFINL)*SIN(ALNEW)*SIN(GANEW))
SIG6(5,6) = (COS(BEFINL)*COTAN(GANEW) + COTAN(ALNEW))/SIN(BEFINL)
SIG6(6,4) = (COS(GAFINL)*COTAN(ALNEW) + COTAN(BENEW))/SIN(GAFINL)
SIG6(6,5) = (COS(GAFINL)*COTAN(BENEW) + COTAN(ALNEW))/SIN(GAFINL)
SIG6(6,6) = -SIN(GANEW)/(SIN(GAFINL)*SIN(ALNEW)*SIN(BENEW))
DO 315 I = 1,6
DO 315 J = 1,6
315 SIG6(I,J) = SIG6(I,J)**2
SIGREP(1,1) = SIGA **2
SIGREP(2,1) = SIGB **2
SIGREP(3,1) = SIGC **2
SIGREP(4,1) = SIGAL **2
SIGREP(5,1) = SIGBE **2
SIGREP(6,1) = SIGGA **2
CALL MULT(SIG6, SIGREP, REALSG, 6, 6)
SIGRA = Sqrt(REALSG(1,1))
SIGRB = Sqrt(REALSG(2,1))
SIGRC = Sqrt(REALSG(3,1))
SIGRAL = Sqrt(REALSG(4,1) * 57.2957779)
SIGRBE = Sqrt(REALSG(5,1) * 57.2957779)
SIGRGA = Sqrt(REALSG(6,1) * 57.2957779)
IF(I TYPE .EQ. 1) GO TO 304
IF(I TYPE .GE. 4) SIGRB = SIGRA
IF(I TYPE .EQ. 5 .OR. I TYPE .EQ. 7) SIGRC = SIGRA
IF(I TYPE .EQ. 7) SIGRBE = SIGRAL
IF(I TYPE .EQ. 7) SIGRGA = SIGRAL
IF(I TYPE .EQ. 7) GO TO 304
SIGRAL = 0.0
IF(I TYPE .NE. 2) SIGRBE = 0.0
SIGRGA = 0.0
304 PRINT 301
301 FORMAT (1H1, 9X, 21HFINAL REAL PARAMETERS // 16X, 33HPARAMETER
      1 SIGMA /)
PRINT 302, LABRL(1), LABRL(2), AFINL, SIGRA, LABRL(3), LABRL(4), BFINL,
1 SIGRB, LABRL(5), LABRL(6), CFINL, SIGRC, LABRL(7), LABRL(8), ALFDEG,

```

```
2  SIGRAL,LABRL(9),LABRL(10),BEFDEG,SIGRBE,LABRL(11),LABRL(12),
3  GAFDEG, SIGRGA
302  FORMAT(10X,A6,A4,F10.5,10X,F10.5)
      RVOL = 1.0/VOL
      PRINT 303, RVOL
303  FORMAT(1H0, 18HUNIT CELL VOLUME = , F15.4)
999  STOP
      END
```

REFERENCES

1. W.L. Bragg, Proc. Cambridge Phil. Soc. 17, 43 (1913).
2. H. Lipson and W. Cochran, "The Crystalline State. Vol. III: The Determination of Crystal Structures," 3rd. ed., G. Bell and Sons Ltd., London, 1966.
3. G.H. Stout and L.H. Jensen, "X-ray Structure Determination," The Macmillan Company, New York, 1968.
4. M.J. Buerger, "Vector Space," J. Wiley and Sons Inc., New York, 1959.
5. M.J. Buerger, "Crystal Structure Analysis," J. Wiley and Sons Inc., New York, 1960.
6. "International Tables for X-ray Crystallography," Vol. I, 1952, Vol. II, 1959, Vol. III, 1962, Kynoch Press, Birmingham.
7. H. Rose, Ann. 11, 131 (1834).
8. J. Liebig and F. Wöhler, Ann. 11, 139 (1834).
9. H.N. Stokes, J. Am. Chem. Soc. 18, 629 (1896).
10. L.E. Audrieth, R. Steinman and A.D. Toy, Chem. Rev. 32, 109 (1943).
11. N.L. Paddock and H.T. Searle, "Advances in Inorganic Chemistry and Radiochemistry," Vol. I, H.J. Emeleus and A.G. Sharpe, eds., Academic Press Inc., New York, 1959, p. 347.
12. N.L. Paddock, Endeavour 19, 134 (1960).
13. I.A. Gribova and U. Ban-Yuan, Russ. Chem. Rev. 30, 1 (1961).
14. N.L. Paddock, Roy. Inst. Chem. Lecture Series No. 2 (1962).
15. C.D. Schmulbach, "Progress in Inorganic Chemistry," Vol. IV, F.A. Cotton ed., Interscience Publishers, London, 1962, p. 275.

16. R.A. Shaw, B.W. Fitzsimmons and B.C. Smith, Chem. Rev. 62, 247 (1962).
17. N.L. Paddock, Quart. Rev. 18, 168 (1964).
18. R.A. Shaw, R. Keat and C. Hewlett, "Preparative Inorganic Reactions," Vol. II, W.L. Jolly ed., Interscience Publishers, London, 1965, p. 1.
19. D.E.C. Corbridge, "Topics in Phosphorus Chemistry," Vol. III, E.J. Griffith and M. Grayson eds., Interscience Publishers, New York, 1966, p. 57.
20. D.P. Craig and N.L. Paddock, Nature 181, 1052 (1958).
21. D.P. Craig, J. Chem. Soc. 997 (1959).
22. D.P. Craig and N.L. Paddock, ibid. 4118 (1962).
23. D.P. Craig, A. Maccoll, R.S. Nyholm, L.E. Orgel and L.E. Sutton, ibid. 332 (1954).
24. M.J.S. Dewar, E.A.C. Lucken and M.A. Whitehead, ibid. 2423 (1960).
25. A. Wilson and D.F. Carroll, ibid. 2548 (1960).
26. E. Cipollini, F. Pompa and A. Ripamonti, Ric. Sci. 28, 2055 (1958).
27. F. Pompa and A. Ripamonti, ibid. 29, 1516 (1959).
28. E. Giglio, ibid. 30, 721 (1960).
29. P. de Santis, E. Giglio and A. Ripamonti, J. Inorg. Nucl. Chem. 24, 469 (1962).
30. H. Bode, Struct. Repts. 12, 227 (1949).
31. M.W. Dougill, J. Chem. Soc. 3211 (1963).

32. H. Jagodzinski and I. Oppermann, Z. Krist. 113, 241 (1960).
33. N.V. Mani, F.R. Ahmed and W.H. Barnes, Acta Cryst. 19, 693 (1965).
34. N.V. Mani, F.R. Ahmed and W.H. Barnes, ibid. 21, 375 (1966).
35. N.V. Mani and A.J. Wagner, Chem. Comm. 658 (1968).
36. R. Hazekamp, T. Migchelsen and A. Vos, Acta Cryst. 15, 539 (1962).
37. J.A. Ketelaar and T.A. de Vries, Rec. Trav. Chim. 58, 1081 (1939).
38. A.J. Wagner and A. Vos, Acta Cryst. B24, 707 (1968).
39. H. McD. McGeachin and F.R. Tromans, J. Chem. Soc. 4777 (1961).
40. M.W. Dougill, ibid. 5471 (1961).
41. G.J. Bullen, ibid. 3193 (1962).
42. G.B. Ansell and G.J. Bullen, Chem. Comm. 430 (1966).
43. M.R. Churchill and R. Mason, Proc. Roy. Soc. A279, 191 (1964).
44. J. Dyson, Ph.D. Thesis, Victoria University of Manchester, 1964.
45. E. Hobbs, D.E.C. Corbridge and B. Raistrick, Acta Cryst. 6, 621 (1953).
46. D.W.J. Cruickshank, ibid. 17, 671 (1964).
47. T. Migchelsen, R. Olthof and A. Vos, ibid. 19, 596 (1965).
48. T. Migchelsen, R. Olthof and A. Vos, ibid. 19, 603 (1965).
49. O. Bastiansen, L. Hedberg and K. Hedberg, J. Chem. Phys. 27, 1311 (1957).
50. L. Helmholz and R.F. Kruh, J. Am. Chem. Soc. 74, 1176 (1952).
51. B. Morosin and E.C. Lingafelter, J. Phys. Chem. 65, 50 (1961).

52. L.E. Orgel, "An Introduction to Transition-Metal Chemistry," Methuen and Co. Ltd., London, 1960, p. 65.
53. G.Felsenfeld, Proc. Roy. Soc. A236, 506 (1956).
54. D.S. Brown, J.D. Lee, B.G.A. Melsom, Chem. Comm. 852 (1968).
55. R.D. Willett, J. Chem. Phys. 41, 2243 (1964).
56. J. Donohue, J. Phys. Chem. 56, 502 (1952).
57. A.W. Hanson, Acta Cryst. B24, 1084 (1968).
58. G.H. Stout and L.H. Jensen, "X-ray Structure Determination," The Macmillan Company, New York, 1968, p. 456.
59. A.J. Wagner and A. Vos, Acta Cryst. B24, 1423 (1968).
60. N.L. Paddock, personal communication.
61. G.C. Pimentel and A.L. McClellan, "The Hydrogen Bond," W.H. Freeman and Co., London, 1960, p. 290.
62. A.W. Schleuter and R.A. Jacobson, J. Chem. Soc. (A) 2317 (1968).
63. G. Allen, D.J. Oldfield, N.L. Paddock, F. Rallo, J. Serreqi and S.M. Todd, Chem. Ind. 1032 (1965).
64. M.J. Buerger, Z. Krist. 109, 42 (1957).
65. J.D. Dunitz and J.S. Rollett, Acta Cryst. 9, 327 (1956).
66. A.D. Booth and F.J. Liewellyn, J. Chem. Soc. 837 (1947).
67. D. Crowfoot Hodgkin, J. Pickworth, J.H. Robertson, A.J. Prosen, R.A. Sparks and K.N. Trueblood, Proc. Roy. Soc. A242, 228 (1957).
68. M. Calleri and J.C. Speakman, Acta Cryst. 17, 1097 (1964).
69. V. Schomaker and D.P. Stevenson, J. Am. Chem. Soc. 63, 37 (1941).
70. S. Geller and J.H. Durand, Acta Cryst. 13, 325 (1960).

71. Q. Williams, J. Sheridan and W. Gordy, J. Chem. Phys. 20, 164 (1952).
72. N.J. Hawkins and V.W. Cohen, ibid. 20, 528 (1952).
73. D.W.J. Cruickshank, J. Chem. Soc. 5486 (1961).
74. W. Reed, M.Sc. Thesis, University of British Columbia, 1965.
75. R.W. Harrison, R.C. Thompson and J. Trotter, J. Chem. Soc. (A) 1775 (1966).
76. R.W.G. Wyckoff, "Crystal Structures," Vol. III, 2nd. ed., Interscience Publishers, New York, 1965, p. 45.
77. M.C.M. Farquhar and H. Lipson, Proc. Phys. Soc. 58, 200 (1946).
78. P.R. Pinnock, C.A. Taylor and H. Lipson, Acta Cryst. 9, 173 (1956).
79. A.J.C. Wilson, Nature 150, 152 (1942).
80. A.J.C. Wilson, Acta Cryst. 2, 318 (1949).
81. E.R. Howells, D.C. Phillips and D. Rogers, ibid. 3, 210 (1950).
82. P. Main and M.M. Woolfson, ibid. 16, 731 (1963).
83. J.S. Rollett, "Computing Methods in Crystallography," Pergamon Press, Oxford, 1966, p. 32.
84. H.D. Young, "Statistical Treatment of Experimental Data," McGraw-Hill Book Company, Inc., Toronto, 1962, p. 100.
85. J.L. Allard, K. Teng, S. Gray and R. Hogan, "Subroutine Package for Square Matrices," U.B.C. Computing Centre, 1965.